Master Thesis in Chemistry

Polar Components in Crude Oils and Their Correlation to Physiochemical Properties.

By

Inger Gine Sørbø

June 2016

Faculty of Mathematics and Natural Sciences

Department of Chemistry

University of Bergen

Abstract

The composition and properties of crude oils have been subjected to much scrutinization over the past decades due to the decreasing oil quality and thus increasingly difficult oil recovery. The physical properties of crude oils are found to be very dependent on the chemical composition. This complex relationship is important to understand in order to predict what EOR method is best suited for one specific oil type.

The aim of this work has been to improve the understanding of how polar components in a crude oil will affect physiochemical properties such as interfacial tension, contact angle and zeta potential. These physiochemical properties measurements are important factors in reservoir interactions.

Due to the complex nature of the crude oil composition, fractionation by chemical properties was used to simplify the characterization of polar compounds. The asphaltene fraction was recovered by precipitation with *n*-hexane. The maltene oil was fractionated into four increasingly polar fractions by SPE-LC. These fractions were further analyzed by FT-IR and ^{31}P NMR. The ^{31}P NMR analytical technique was utilized for the first time in the analysis of crude oils. It was found to have an interesting potential in the molecular characterization of polar compounds. In addition to chemical composition, the biodegradation ranks and TAN were found for each crude oil.

The physiochemical properties measured by Kolltveit, and the chemical component data obtained in this thesis, were analyzed by principal component analysis (PCA).

The analysis revealed that the heavier and more biodegraded oils consisted of more carboxylic acid functional groups, while the lighter, non-biodegraded contained more aliphatic alcohols and phenolic functional groups. The physiochemical properties were found to be less dependent on the amount of TAN and more dependent on the chemical composition of the acids present in the crude oils. The TAN was found to be independent of the asphaltenes, indicating that the acids are present in both the maltene and asphaltene fractions.

Acknowledgements

The success and final outcome of this thesis is due to a lot of guidance and assistance from many people whom I am extremely glad to have had in my corner. I would like to express my profound gratitude to both of my supervisors, Tanja Barth and Kristine Spildo, whom have been an unrelenting source of knowledge, advice and encouragement.

I would also like to express my gratitude towards everyone who has helped me in one way or another, especially Terje Lygre, Egil Nodland, Inger Johanne Fjellanger, Tore Skodvin, Jarl Underhaug and Olav-Audun Bjørklund. Thank you for your help in completion of my thesis and for the encouraging words along the way.

My thanks and appreciation also goes out to everyone in room 3009, especially for the many coffee breaks and great working environment. In addition, a special thanks is in order to Yvonne Kolltveit who has been a great friend and colleague. Thank you for always listening and helping when I have had doubts and questions.

I also wish to thank my wonderful and supporting family. Thanks for always helping me achieve my goals and pushing me to do my absolute best.

Last but not least, I would like to thank Tina and Jeanette from the bottom of my heart. You have been the greatest friends and supporters throughout the entire thesis. Thank you for reminding me that there is a life beyond school.

Thank you,

Inger Gine Sørbø

Abbreviations

ATR	Attenuated Total Reflectance
BDL	Below Detection Limit
CA	Contact Angle
CORB	Crude Oil, Rock, Brine
$Cr(acac)_3$	Chromium(III) acetylacetonate
DCM	Dichloromethane
EOR	Enhanced Oil Recovery
E_D	Microscopic Displacement Efficiency
E_R	Total Displacement Efficiency
E_V	Volumetric Displacement Efficiency
FID	Flame Ionization Detector
FT-IR	Fourier Transform – Infrared Spectroscopy
GC	Gas Chromatography
IFT	Interfacial Tension
IS	Internal Standard
KHP	Potassium Hydrogen Phthalate
KOH	Potassium Hydroxide
LC	Liquid Chromatography
MeOH	Methanol
MP	Mobile Phase
NIGOGA	Norwegian Industry Guide to Organic Geochemical Analysis
NMR	Nuclear Magnetic Resonance
NSO	Norwegian Standard Oil
PCA	Principal Component Analysis
PC	Principal Component
PTGC	Program Temperature Gas Chromatography

SARA	Saturates Aromatics Resins Asphaltenes
SP	Stationary Phase
SPE	Solid Phase Extraction
TAN	Total Acid Number
TMDP	2-chloro-4,4,5,5-tetramethyl-1,3,2-dioxsafosfolane
UCM	Unidentified Complex Mixture
WOGC	Whole Oil Gas Chromatography

Contents

Chapter 1

Introduction

1.1 Background

Petroleum has a complex chemical environment with intricate mixtures of hydrocarbons and small amounts of heteroatom compounds. To anticipate the behavior of any petroleum product, it is important to understand the chemical composition. Corrosion, density, emulsion stability, interfacial tension and viscosity are all important physiochemical properties that have impact on how crude oil acts and how it should be handled. Polar components have been found to be one of the most important factors in understanding the physical and chemical behavior of crude oils. Known polar compounds are carboxylic and phenolic acids, organic bases and metal complexes. Naphthenic acid is often used as a word in reference to all the organic acids (Barth *et al.*, 2004; Clemente *et al.*, 2005; Speight, 2006).

1.2 Formation of crude oil

Petroleum is a result of incomplete decay of organic matter. The starting material in marine sediments consist mostly of aquatic plants and animals, such as algae and plankton. Over a long geological timespan, this sediment is subjected to increasing temperatures and pressure. Figure 1.2.1 is a simplified illustration of the petroleum production process, where the depth of burial is measured in temperature (°C).

Diagenesis is the first phase of transformation and refers to the biological, chemical and physical alteration of the organic material. Here, heat is not yet significant and hydrolysis is the main chemical reaction. The end result is a complex, high molecular weight polymer termed kerogen, which represents the halfway point in formation of petroleum products. As the sediment is increasingly buried, temperature rises and at a depth corresponding to 60℃, catagenesis starts. Also called the opening of the oil window, the large kerogen structures are reduced by thermal cracking, where homolytic bond cleavage dominates. The large amount of possible products in petroleum is made possible by the production of radicals and their propagation reactions. The oil window is closed at a depth corresponding to 170℃, and gas is the only product produced to a

depth corresponding to 225 ℃. At this depth, metagenesis starts and represents the final carbonaceous product graphite (Schobert, 2013).

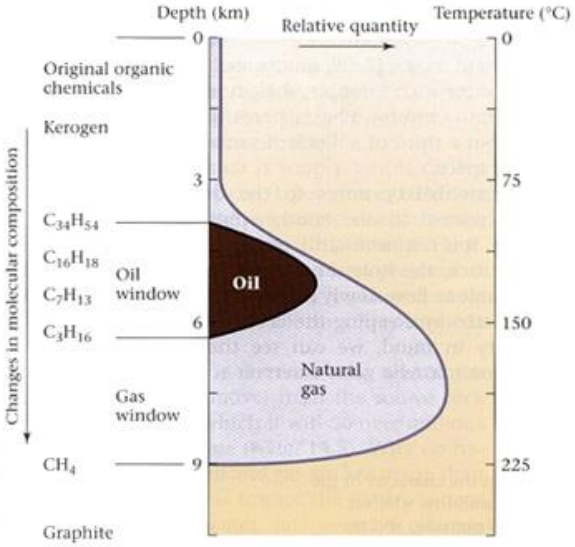

Figure 1.2.1: Simplified picture of the oil window (UC San Diego, 2012).

1.3 Petroleum recovery

Crude oil recovery in petroleum reservoirs can be divided into three distinct phases; primary, secondary and tertiary recovery. The primary recovery method involves the natural pressure present in the reservoir, which drives the oil to the production well. This method however, is only able to produce approximately 5-10% of the oil present before the decrease in pressure is no longer a sufficient driving force. In the secondary recovery method, an external energy source such as water or gas is applied. Water flooding is the most common method where the water replaces oil and maintains the initial pressure. The efficiency of this method is dependent on other factors such as the reservoir rock characteristics, oil viscosity and other physiochemical properties of the oil. Even with additional force, only 25-30% of the oil present in the reservoir is recovered. The tertiary recovery method is often referred to as enhanced oil recovery (EOR) and involves a higher operation cost and a more scientific approach. Examples of such methods are “fire-flooding”, steam injection and the use of surfactants. After the three recovery methods have been utilized, roughly 60% of the oil present in the reservoir has been recovered (Speight, 2006; Sheng,2010).

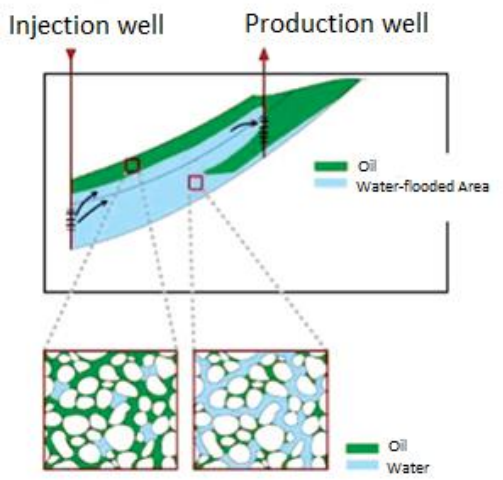

Figure 1.3.1: Illustration of water-flooding (Norwegian Petroleum Directorate, 2009).

Figure 1.3.1 depicts water-flooding of a reservoir. The total(E_R) displacement efficiency in the reservoir is dependent on the volumetric(E_V)- and microscopic(E_D)- displacement efficiency. The volumetric displacement efficiency is expressed by how big of a proportion of the total volume is in contact with the injected water. E_D indicates the displacement efficiency in the water-flooded area. To increase oil recovery, either E_V and/or E_D has to be increased. E_D is directly related to the capillary forces, and if E_D is to be increased, these forces need to be decreased. Therefore, it is necessary to know what influences these capillary forces (Sheng, 2010).

1.4 Composition of crude oil

Regarding the elemental composition of different crude oils, it has been determined that there are no profound differences between samples. For liquid petroleum products the elemental composition is usually in the range of 82-87% carbon, 11-15% hydrogen and the remaining balance occupied by the heteroatoms oxygen, nitrogen and sulfur and very small amounts of coordination series metals. Even though the variation is small, no two samples are identical in their physical appearance or behavior. To determine this, a look into the molecular composition is necessary. The controlling factors for a crude oil's chemical composition lies in its degree of catagenesis, which is dependent on residence time and temperature exposure. Samples are so

complex that the exact number of single components present in a crude oil is unknown (Speight,2006; Schobert, 2013).

Due to the complex composition, characterization of individual components is impossible and elemental analysis provides little to no additional structural and/or physical information. The established solution is therefore to fractionate the crude oil either by boiling point range, as they do in refineries, or by polarity. Fractionation by solubility in low-weight paraffinic hydrocarbons combined with adsorption chromatography is referred to as SARA separation, which divides the crude oil into four chemical classes; saturates(S), aromatics(A), resins(R) and asphaltenes(A).

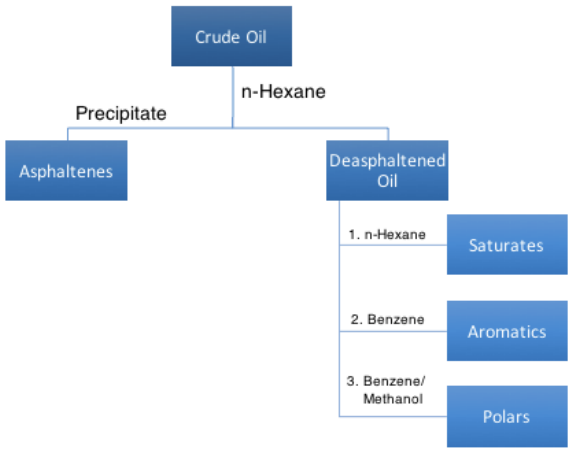

Figure 1.4.1: SARA fractionation process (Speight, 2006).

Figure 1.4.1 shows a simplified procedure of how the maltene fraction can be further divided into the three chemical classes by adsorption chromatography.

Saturates are non-polar hydrocarbons and occur as straight-chain, branched or cyclic structures. The proportion of saturates decreases with increasing molecular weight and is therefore most commonly found in the lighter distillate fractions. This fraction can make up as much as 40-60 weight% of the crude oil (Speight, 2006).

The aromatic fraction refers to benzene and structural derivatives such as toluene, naphthalene and anthracene. The single ring molecules occur mostly in the lighter fractions, while the more extensive ring systems can be found in the heavier fractions. The ring number is directly related to density, where more substitution gives higher densities. The content of aromatics can range from 10% to over 50%, depending on the quality of the crude oil (Schobert, 2013).

Resins are defined as polar-compounds that are soluble in n-pentane, n-hexane or n-heptane. Being a solubility class, some overlap between the aromatic and asphaltene fractions is expected. This fraction contains polar molecules with heteroatoms such as nitrogen, oxygen and sulfur (Mitchell *et al.*, 1973).

Asphaltenes are defined as the insoluble components in the small liquid hydrocarbons. It is a group of high molecular weight components, with approx. 85% carbon. Due to their large size, molecular structures are presumed to contain large polycyclic aromatic and naphthenic sheets. This fraction also contains the highest amount of heteroatom and organometallic constituents. Due to their high amount of polar components and large, complex molecular structure, asphaltenes are considered the cause of numerous problems with production, transportation and processing (Auflem *et al.*, 2002).

1.5 Surface active compounds

In order to predict physiochemical properties such as emulsion stability, wetting properties, interfacial tension and viscosity it is important to understand the role surface active components play in the crude oil. These surface active species are the polar components present in the crude oil, where the carboxylic acids have been found especially important. The polar components stem from the heteroatoms present in the heavier fractions (Seifert *et al.*, 1969; Speight, 2006).

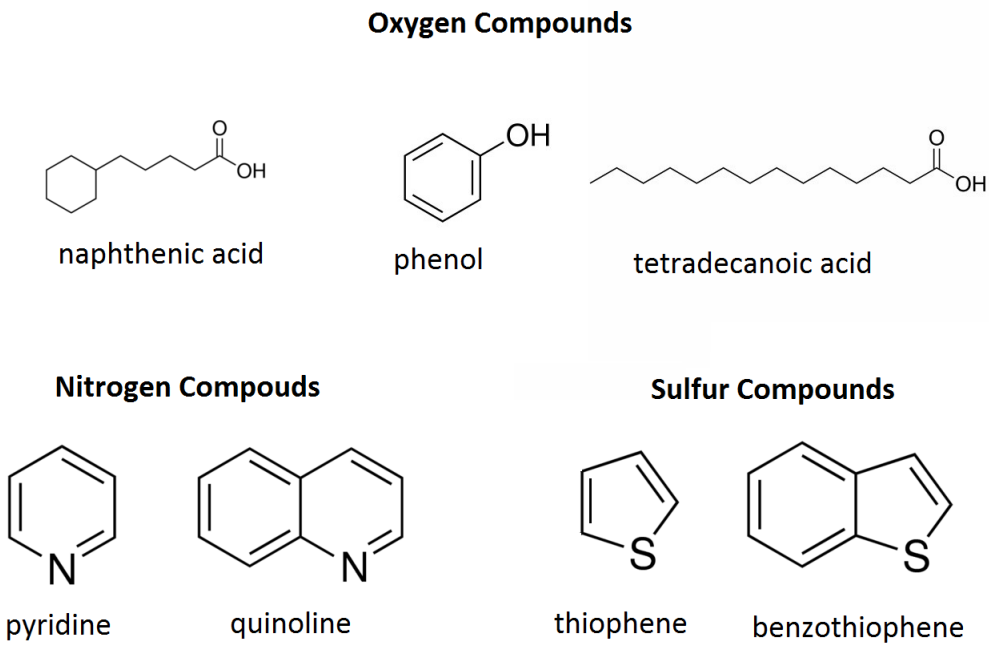

Figure 1.5.1: Examples of polar components present in the crude oil (Speight, 2006).

Compounds that contain oxygen are most commonly alcohols, phenols, carboxylic acids, ketones, esters and ethers. These are often acidic in nature and the collective term naphthenic acid is often used in reference to them. These acids are often considered the problem behind corrosion of production and transportation equipment (Paukku *et al.*, 1981; Clemente *et al.*, 2005). Nitrogen and sulfur are both troublesome elements as oxides of both contribute to production of acid rain. Common basic nitrogen containing compounds are pyridine and quinolone, non-basic compounds are typically pyrrole, indole and carbazole and their derivatives. Sulfur compounds commonly found in crude oils are thioalkanes and heterocyclic compounds derived from thiophene. Examples of these compounds can be found in Figure 1.5.1 (Schobert, 2013).

1.6 Petroleum acids

Acids occurring in petroleum have been analyzed, extracted and tested on many occasions and found to be important due to their interfacial activity (Meredith *et al.*, 2000; Barth *et al.*, 2004; Negash, 2004).

There are several factors controlling the amount of acidic components present in petroleum products. Important factors such as the type of sediment the petroleum stems from, how long it has been buried and most importantly how deep it was buried control the outcome. The depth of burial relates directly to the temperature conditions and catagenesis. Other processes such as biodegradation can alter the composition and increase the concentration of the acidic components (Schobert, 2013).

1.7 Biodegradation of crude oil

Biodegradation comprises of a consumption of organic matter by bacteria, either aerobically or anaerobically as in an oil reservoir. Bacteria have a preference for the straight chain saturates, followed by branched saturates, cyclic saturates and finally aromatic hydrocarbons. The degradation of the lighter components causes an increase in the concentration of the more polar and heavy compounds (Peters *et al.*, 1991). Biodegradation occurs generally in reservoirs that are shallow, with temperatures under 80°C (Larter *et al.*, 2006). By using whole oil gas chromatography (WOGC) biodegradation levels can be determined. Assessing if a crude oil is biodegraded has become an important factor for the oil industry due to the decreased recovery efficiency, decreased product quality and increased problems under production and handling (Wenger *et al.*, 2002).

The level of biodegradation can be classified by using Peters and Moldovans (1993) table of biodegradation. The scale goes from 1 to 10, where 1 represents oils that have experienced little to no biodegradation and 10 is given to strongly biodegraded samples. In this thesis 0 is given to the non-biodegraded samples. Another method of ranking less biodegraded samples was developed by Wegner et al. (2002) where the carbon isotopic ratio was used. Also the author used three occurring trends in WOGC to determine the degradation. The first trend was to observe if all the n-alkanes, from n-C8 to n-C15, were intact. The second, was to determine the pristane/C17

and pristane/phytane ratio, where a large ratio between pristane/C17 and phytane/C18 indicated an increasingly biodegraded sample. The third observation was to look for the unresolved complex mixture(UCM) hump. A non-biodegraded oil would have all its n-alkanes intact, a small pristane/C17 ratio, no UCM hump and be given the value zero in Peters and Moldovans ranking (Wenger *et al.*, 2002).

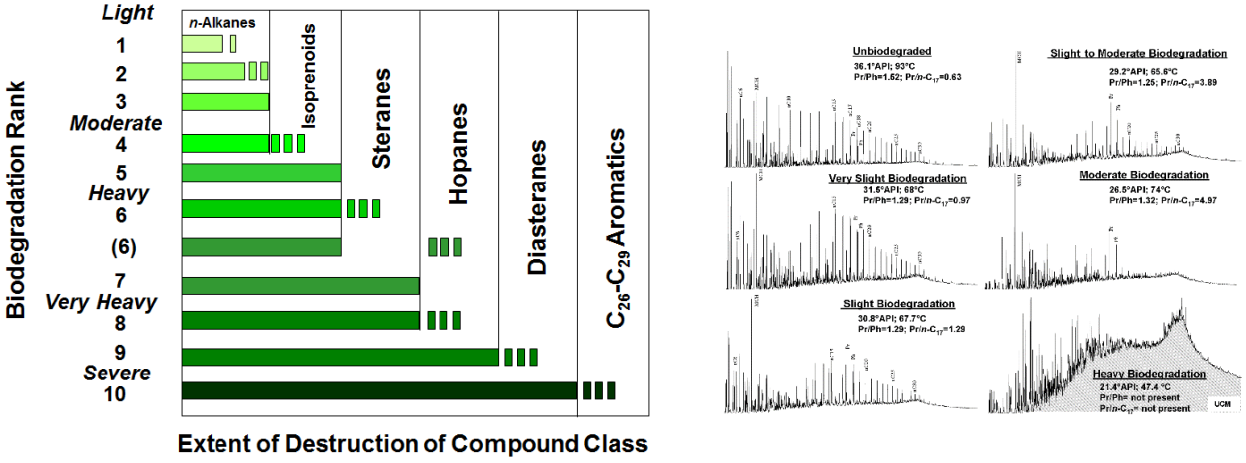

Figure 1.7.1: Peter and Moldowan Biodegradation ranking and example from Wenger *et al.* of increasingly biodegraded samples (Peters *et al.*, 1993; Wenger *et al.*, 2002).

1.8 Biomarkers

Biomarkers are complex molecules which stem from once living organisms. Biomarkers found in crude oils, rocks and sediments are very resistant to alteration and therefore show little to no change in structure from their biogenic precursors. They therefore carry valuable information about the origin, geological and thermal history of the petroleum products. With this information, producers have been able find the original source material, approximate a geological age (and thus maturity) and have also been able to see if samples where biodegraded or not (Wang *et al.*, 2006; Schobert, 2013).

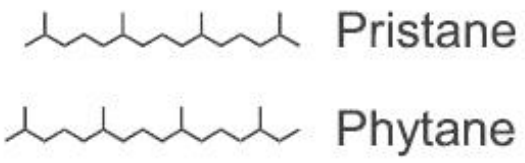

Figure 1.8.1: Molecular structure of the two biomarkers pristane and phytane (Peters *et al.*, 1993).

In crude oil pristane and phytane are common biomarker used in biodegradation analysis. They stem from the original organic matter. Since pristane and phytane are isoprenoids, they are more resistant to bacterial attack, which degrades the n-alkanes first. However, these biomarker ratios should be used with caution as pristane/C17 and phytane/C18 ratios decrease with thermal maturity, while biodegradation increases the ratio. Peters *et al* (1993) also found that the pristane/phytane ratio increased with thermal maturity.

1.9 Objective of this work

An occurring problem in enhanced oil recovery (EOR), is the inability to generalize the effects on wettability in a crude oil/rock/brine (CORB) system due to the interrelated effects of physiochemical properties in the system and the chemical composition of the components.

Even though crude oils consist mostly of hydrocarbons, it is often the other elements that play important parts for many of the physical and chemical properties. These polar compounds, containing one or more heteroatoms are crucial for parameters such as viscosity, interfacial activity, emulsion and chemical stability.

To better understand many of the physiochemical properties of crude oil, it is important to study the polar and surface active components present. The aim of this study is to connect the organic analysis of the polar components in the crude oils to their physiochemical properties and to explore the relationship between them.

Chapter 2

Experimental Theory

2.1 Whole oil gas chromatography

Chromatography is an analytical laboratory technique where mixtures are separated and analyzed. One phase is held in place, the stationary phase (SP), while the other moves past it, the mobile phase (MP). The nature of the SP causes the different components of the mixture to move with various speeds throughout the column, generating separation (Miller, 2009).

Gas chromatography (GC) is a type of chromatography where the MP is a gas and the analyte can be vaporized without being decomposed.

Whole oil gas chromatography (WOGC) is a method of analysis in GC. In this case oil is analyzed without any other solvents present. The separation is usually preformed on a column with a length in the range of 15-60m, made of silica (SiO_2) and coated with polyimide for support and protection from atmospheric moisture (Harris, 2010).

A gas chromatogram is commonly described with three main parts, the injector port, the column and the detector and Figure 2.2.1 shows a simplified picture.

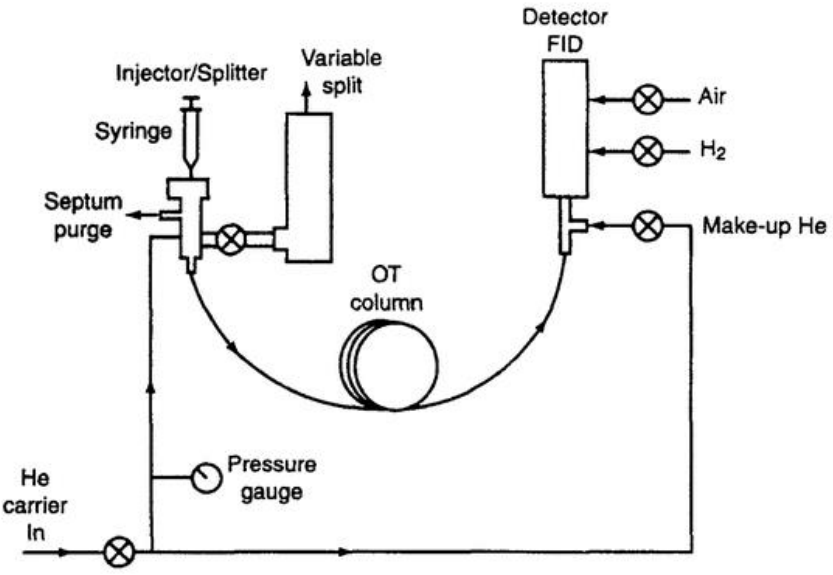

Figure 2.1.1: Simplified picture of the interior of a GC (Miller, 2009).

A volatile liquid or a gaseous sample is injected through a self-sealing rubber septum into a heated chamber. This injection chamber vaporizes the sample, which can either enter the column in its entirety or be split into smaller ratios. If the sample exceeds 0.1% of the mixture that is carried through the column, a split injection is recommended because overloading the column results in poor chromatograms. If the split ratio is 100:1, then for every 100 parts only 1 part of the analyte is let through to the column.

The vapor is pushed through to the column by the carrier gas, which is typically H_2, He or N_2, where helium is used in this thesis. The gases are selected due to their inertness, as they are a carrier gas and should not react with the analyte under investigation. Helium is a popular carrier gas due to the high optimal velocity (20-30 cm/s) and the small loss of efficiency if the optimal velocity is exceeded. The column is a long and extremely thin capillary, where the inside is coated with SP. A constant sorption-desorption process occurs and depending on the affinity the different parts of the mixture have for the SP, either equilibrate or partition between the two phases, resulting in different retention times. The column is placed inside an oven and to ensure that all the eluent is eluted from the column a program temperature GC (PTGC) can be run. This is the process of increasing the temperature of the column continuously throughout a run. The increase in temperature causes the partition coefficients to decrease and therefore move faster, which results in decreased retention times and constant peak widths and shapes.

After the column, the separated analytes need to be detected and identified. The most common detector for GC is the flame ionization detector (FID), which is also one of the more popular detectors because of its high sensitivity. Crude oil is a mixture of complex organic compounds, and the FID can detect all organic compounds, making it a perfect fit. The analyte is introduced to a small flame consisting of H_2 and air, where carbon containing compounds are burnt producing CHO^+ ions. The ions collected create a small current. The current is magnified and sent to a data system that makes a chromatogram (Miller, 2009).

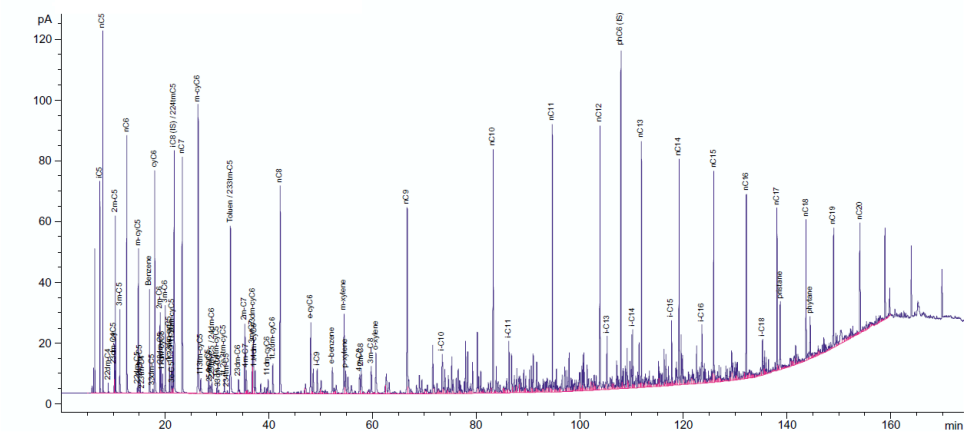

Figure 2.1.2: A chromatogram of a Norwegian standard oil (Weiss *et al.*, 2000).

The chromatogram in Figure 2.1.2 displays the peaks of the signals detected as a function of time, at their individual retention times. Quantitative analysis is possible by integration of each peak because the area of the peak is proportional with the quantity of that component in the mixture. Internal standards with known concentrations can be used to compare the integrated peaks and find the concentration of the unknowns.

The purpose of WOGC is to obtain information about the hydrocarbons in the gasoline-range (nC4 – nC20) and to see if the samples are biodegraded or not (Weiss *et al.*, 2000).

2.2 Determination of asphaltenes

In this thesis, asphaltenes are defined as insoluble in *n*-hexane.

Solvent treatment of crude oil is one of the most common methods of removing the asphaltene fraction. By careful selection of solvent type, separation of the fraction is achieved according to the molecular weight and aromaticity of the components. The separation is most commonly accomplished by addition of low-molecular weight paraffinic hydrocarbons such as *n*-pentane, *n*-hexane and *n*-heptane in a 40:1 solvent to oil volume ratio (Mitchell *et al.*, 1973; Speight, 2006).

2.3 Solid phase extraction – maltene fractionation

Liquid Chromatography (LC) is based on the same principles as GC, where the ultimate goal is to separate compounds in a solution based on their chemical composition, size or polarity. As the name implies, liquid is used as the MP, and the SP can be either packed, monolithic or open tubular. Packed columns are used in this thesis and consists of silica column modified with cyanopropyl groups (Borgund *et al*., 2007; Miller, 2009).

The important characteristics in a packed column are the particle size and distribution, pore size, surface area and shape. In general, spherical shaped beads are most wanted due to their ability for tighter packing and uniformity. An important note to make is that in LC, both the SP and the MP affects the separation, unlike in GC where only the SP has an effect (Miller, 2009).

Solid phase extraction (SPE) is a method of LC used to reduce the possibility of incomplete phase separations and most commonly used to clean samples and sample extraction. Figure 2.3.1 shows a simple setup for SPE. The basic principle behind SPE is that the various fractions of a solvent have different affinities for the SP. Using a cyano column, an increase in the polarity of the MP will elute the fractions gradually, where the least polar eluates first and the most polar last (Sigma Aldrich, 1998; Simpson, 2000; Borgund *et al.*, 2007).

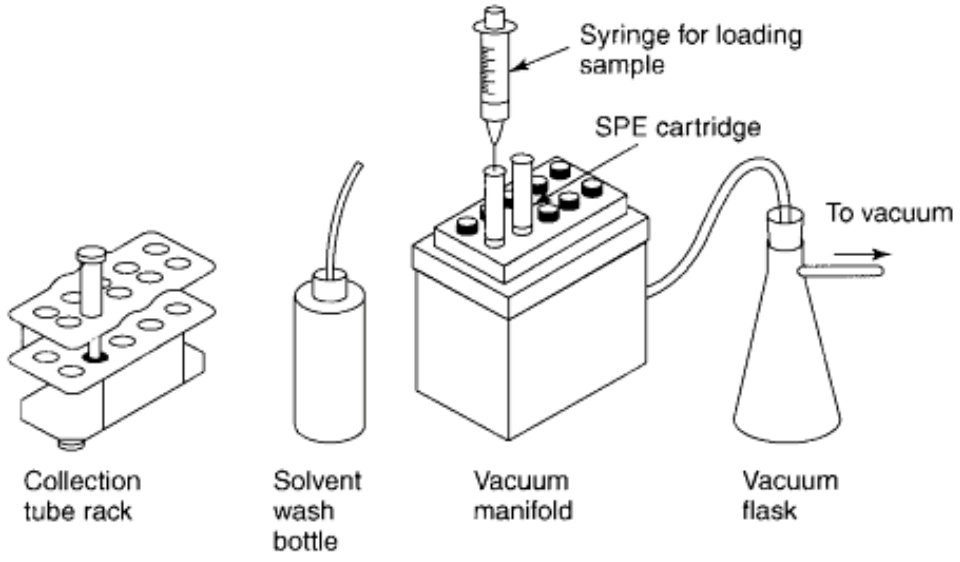

Figure 2.3.1: Setup for a SPE (Miller, 2009).

2.4 Total acid number titration

Titration is a technique used to determine an unknown concentration of a solution by adding a solution of known concentration. The equivalence point in a titration is when the titrant and analyte are chemically equivalent, in other words the same amount of moles are present. Equation 2.4.1 illustrates how the base neutralizes the acidic components present in the crude oil. Indicators are often used to determine the endpoint of the reaction, but since crude oils are colored solutions, the use of indicators becomes impossible (Harris, 2010).

$$KOH + R{-}COOH \rightleftarrows K{-}OOCR + H_2O \qquad \textbf{Equation 2.4.1}$$

Total acid number(TAN) is the assessment of how acidic a crude oil is by potentiometric titration. Potentiometric titration is a technique where the potential difference, between a reference electrode and an indicating electrode, in the solution is measured. The indicating electrode responds to changes in concentration of one of the ions involved in the reaction. The TAN is determined by the amount of potassium hydroxide (KOH) it takes to neutralize the acidic components present in one-gram oil. Crude oils are deemed high acid crudes with TANs over 0.5mg KOH/g oil (Harris, 2010; Schobert, 2013).

The TAN is calculated by Equation 2.4.2.

$$TAN\left(\frac{mg\ KOH}{g\ oil}\right) = \frac{C_{KOH} \times (V_{KOH(EP)} - V_B) \times Mm_{KOH}}{m_{oil}} \qquad \textbf{Equation 2.4.2}$$

Where C_{KOH} is the concentration of the titrant, $V_{KOH(EP)}$ is the volume of titrant used at the equivalent point, V_B is the volume of the blank, Mm_{KOH} is 56.11 g/mol and m_{oil} is the mass of the oil sample.

The acid number determination is very dependent on C_{KOH} and due to its instability, the concentration of the titrant has to be calibrated against potassium hydrogen phthalate (KHP). Dissolving known amounts of KHP in the titration solution and titrating it against the KOH solution gives a plot with a straight line. This results in the following equations:

$$n_{KOH} = n_{KHP} + n_B \qquad \textbf{Equation 2.4.3}$$

Where Equation 2.4.3 can be rewritten as follows:

$$C_{KOH} \times V_{KOH(EP)} = m_{KHP} \times M'_{KHP} + n_B \qquad \textbf{Equation 2.4.4}$$

Where m_{KHP} is the mass of KHP added to the titrant solution, M'_{KHP} is the molality of the solution, calculated by Equation 2.4.5, and $Mm_{KHP} = 204.22\ g/mol$.

$$Molality = \frac{moles\ of\ solute}{Kg\ of\ solvent} \qquad \textbf{Equation 2.4.5}$$

Equation 2.4.4 can be plotted as a straight line, where $V_{KOH(EP)}$ is plotted against m_{KHP} and can give C_{KOH} and n_B as a result.

$$V(KOH) = \left(\left[\frac{M'(KHP)}{C(KOH)}\right] \times m(KHP)\right) + \left(\left[\frac{1}{C(KOH)}\right] \times n(blank)\right) \qquad \textbf{Equation 2.4.6}$$

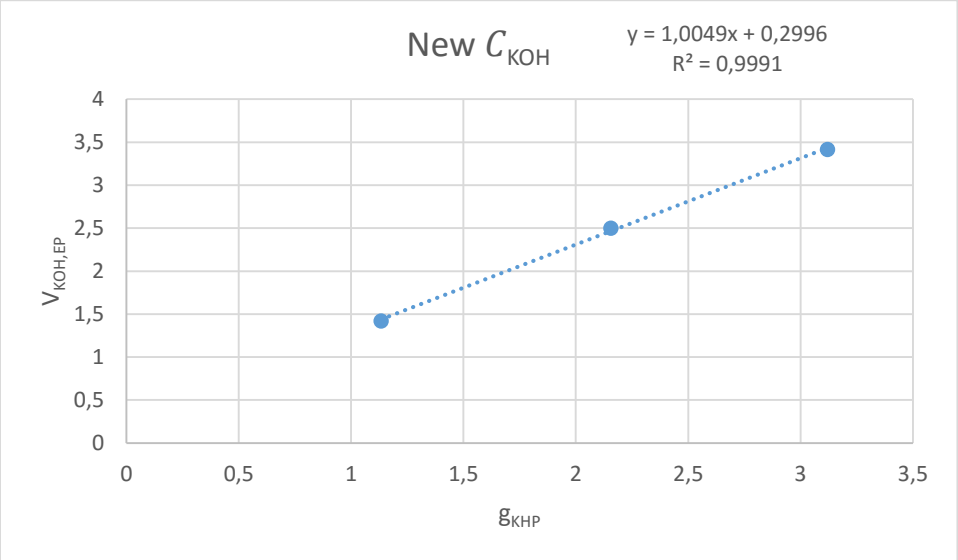

Figure 2.4.1: Plot of the new concentration of C_{KOH}.

The linear function y = ax + b will then give the new concentration of C_{KOH} as shown in Equation 2.4.7.

$$a = 1.0049 = \left[\frac{M'_{KHP}}{C_{KOH}}\right] \leftrightarrow C_{KOH} = \frac{M'_{KHP}}{1.0049} = 0.049 \qquad \textbf{Equation 2.4.7}$$

$b = 0.2996 = n_B$, this value is used continuously in further calculations.

The concentration of the titrant and the blank are now known.

2.5 Infrared Spectroscopy

Spectroscopy is a tool used to find structural information for known or unknown molecules using light in the electromagnetic spectrum. Fourier transform infrared spectroscopy (FT-IR) uses the infrared region and measures the vibrational and rotational energies of the chemical bonds in a molecule. Each peak in an infrared spectrum corresponds to a different functional group. The normal frequency region for an infrared spectrum is 4000 – 650 cm^{-1} (Pavia, 2009).

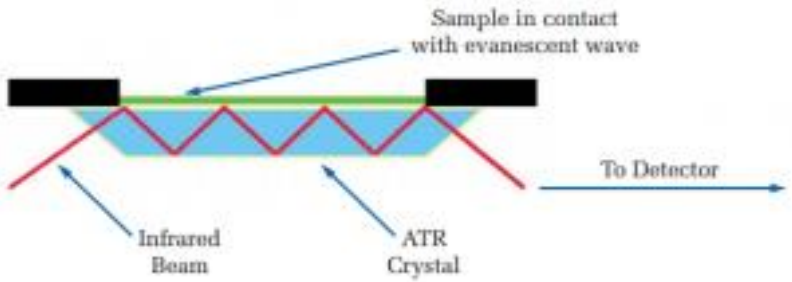

Figure 2.5.1: Illustration of ATR (PerkinElmer, 2016)

In Fourier transformation IR (FT-IR) the entire frequency range of the IR spectrum is applied. The beam is split into two beams of varying lengths. This results in both constructive and destructive interferences, which produces an interferogram. Fourier transformation is a mathematical program which converts the acquired data from, the interferogram, into a frequency-domain spectrum. This conversion makes it easy to manipulate the spectrums, allows increased signal-to-noise ratio by summarizing multiple scans and the possibility to switch units on both axes (Silverstein, 2005).

Attenuated total reflection(ATR) IR spectroscopy is used to analyze the crude and deasphalted oils and the fractionated oil samples. This simplified method of IR has revolutionized solid and liquid sample analysis due to its easy procedure and its reproducibility. The horizontal setup, shown in Figure 2.5.1, consists of a crystal with a high refractive index, so that the light is internally reflected several times. The beam is in contact with the sample at the reflecting surface, and goes to a depth of a few micrometers, which is enough to produce an adsorption spectrum (Durig, 1990).

2.6 ^{31}P NMR

Nuclear magnetic resonance (NMR) is a non-destructive nuclei specific spectroscopic method used to determine the structure of organic compounds.

Neutrons and protons make up the nucleus, which in some cases act as if they are spinning. This can be described by using the angular momentum quantum number (I) and the magnetic quantum number (m). All nuclei have (2I+1) different values of directional quantum number, which means that a ^{1}H – isotope with I= ½, has two possible spin states (+ ½ and – ½) and the two spin states are used in simple NMR. Some common isotopes, ^{1}H, ^{13}C, ^{19}F and ^{31}P, have I = ½, therefore the theory will be limited to I= ½ . NMR analyzes samples based on certain properties that only atomic nuclei with either an odd mass, an odd atomic number or one with both, possesses. These spinning molecules will have a magnetic moment (μ):

$$\mu = \gamma I \qquad \textbf{Equation 2.6.1}$$

Where γ is the gyromagnetic ratio, which is important for the detection sensitivity of a nuclide. A nucleus with high γ is said to be sensitive and is easily observable in NMR, while a small γ is insensitive. γ is a constant for each nucleus. The magnetic moment makes the nuclei act as small magnets. In the absence of a magnetic field, $B_{0,}$ the spin states are random and have identical energies (Pavia, 2009).

When an NMR experiment is run, the sample is subjected to an external B_0, which causes an uneven distribution in energy. This is due to the now charged particles own generated magnetic field. Figure 2.6.1 shows an example of how a proton, which has two possible spin states (+ ½ and – ½)., can point in two different directions, depending on which way it is spinning when introduced to an external field B_0. The spin state + ½ has a lower energy as it is parallel to B_0, while – ½ has a higher energy because it is opposite B_0.

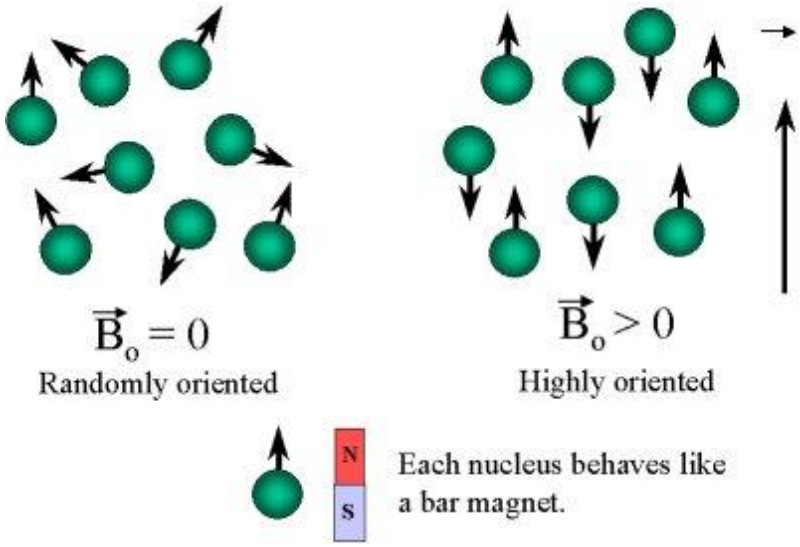

Figure 2.6.1: Illustration of how nuclei act if a magnetic field is absent or present (University of Maine, 2002).

When nuclei parallel with the external magnetic field absorbs energy, the nuclei changes spin direction. This is called magnetic resonance. The energy absorbed must be equal to the energy difference (ΔE) between the two spin states. The energy difference is dependent on the force of the applied magnetic field, where a stronger B_0 will result in an increased ΔE (Pavia, 2009).

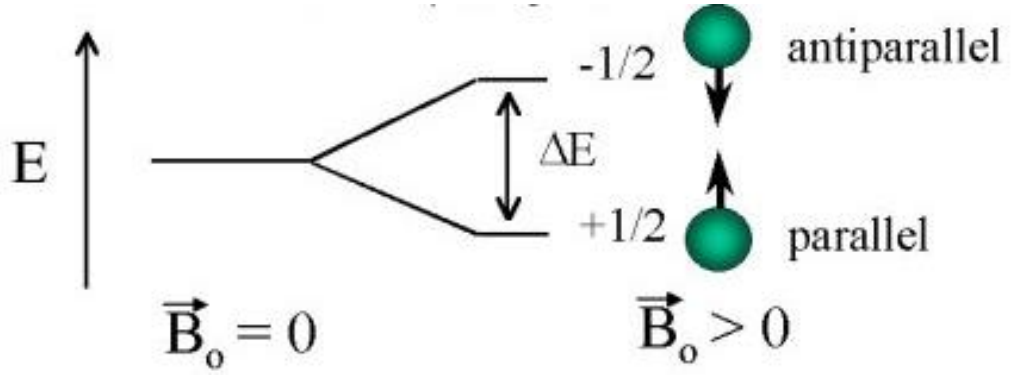

Figure 2.6.2: Illustration of energy difference in the spin state (University of Maine, 2002).

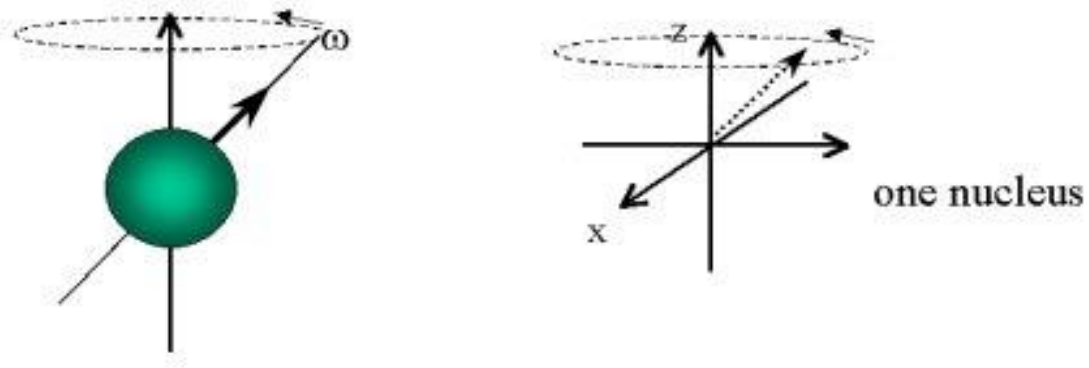

Figure 2.6.3: Illustration of a nucleus precessing around its own axis (University of Maine, 2002).

Figure 2.6.3 illustrates what happens when spinning nuclei are subjected to a magnetic field. This phenomena is called precession and at that moment the nuclei starts to "wobble" around its own axis with an angular frequency ω, also called the Larmor frequency. The frequency of precession is directly related to the strength of B_0.

As mentioned earlier, the nucleus is charged. Due to this, the precession generates an oscillating electric field of the same frequency as the Larmor frequency. If a radio wave of the identical frequency is sent into that field, the nuclei can absorb the energy and change spin direction. This is termed resonance (Pavia, 2009).

In a molecule, protons experience different electromagnetic environments because they are shielded to a certain degree by the surrounding electrons. Due to this, protons with a small difference in environment will have resonance at different frequency and it is therefore possible to detect all different protons present in the molecule.

In modern NMR instruments, a brief but strong energy pulse is sent through the sample during analysis. All the specific and detectable nuclei absorb this energy and switch spin state. When the energy pulse is turned off, the nuclei relax back to their original state and send out energy in the form of electromagnetic radiation. Due to the difference in electron shielding in the molecule, the electromagnetic radiation will have different frequency. The signals are collected and Fourier transformed by a computer program, resulting in a NMR-spectrum (Friebolin, 2011).

2.6.1 ^{31}P-NMR

When investigating the polar components of a crude oil sample, it would be ideal to do NMR on ^{17}O, ^{12}N or ^{33}S nuclei, but because of the poor detection possibilities due to their very low abundances, their quadrupolar nature and their low receptivity this is not feasible. Instead, heteroatom functional groups such as CO_2H, NH and SH, containing a single hydrogen prone to chemical change, can be reacted with certain reagents. Specific methods can then be used to analyze the functional groups of the derivatives (Wroblewski *et al.*, 1988).

^{31}P is the only isotope of phosphor. It fulfills the requirement of NMR detection by having an odd atomic number. Also, the odd-numbered isotope has a natural abundance of 100%, making it easily detectable (Argyropoulos, 1995).

In this thesis, ^{31}P-NMR is used to analyze the different hydroxyl groups present in the crude oil, asphaltene precipitate and the two most polar fractions in the maltene fractionation. To be able to see the hydroxyl groups, they need to be introduced and reacted with a molecule that has a phosphor atom. Figure 2.6.4 shows how the phosphitylation reaction with labile protons proceeds, where 2-chloro-4,4,5,5-tetramethyl-1,3,2-dioxsafosfolane(TMDP) is the chosen reagent based on the previous work done by Laugerud (2015). The reaction results in the central phosphorous atom being surrounded by three oxygen atoms, which ensures that these derivatives only show as singlets, with no coupling information, in the NMR spectrum (Argyropoulos, 1995).

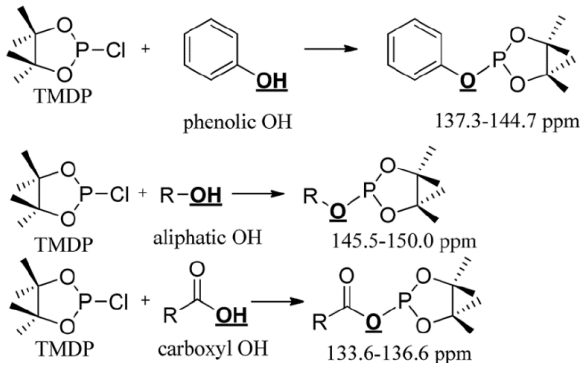

Figure 2.6.4: TMDP reaction with different hydroxyl groups (Ben *et al.*, 2016).

Pyridine and deuterated chloroform is used to make the solvent mixture. Pyridine is chosen as the base, in order to neutralize the hydrogen chloride produced in the reaction and to push the slightly exothermic phosphitylation reaction to complete conversion. The chloroform has to be deuterated because it is used as a frequency lock in NMR. Chromium (III) acetylacetonate ($Cr(acac)_3$) is added to the solvent mixture as a relaxation agent (Pu *et al.*, 2011; Melone *et al.*, 2013).

2.7 Physiochemical properties

The physiochemical properties are provided by Kolltveit (2016). A brief review of her experimental methods are given.

2.7.1 Interfacial tension

The measurements were obtained by the pendant drop method on a contact angle measurement instrument (OCA 20). An inverted needle was used, due to the density differences between the crude oil and brine. The results were collected and analyzed by variation in salinity, ionic strength and pH of the solution (Berg, 2010; Farooq *et al.*, 2013).

2.7.2 Contact Angle

The contact angle measurements were conducted on the OCA20, by the sessile drop method using a glass plate system. The results were obtained by variation in salinity, ionic strength and pH. The contact angle measurements are used to describe wettability. Wettability is the preference of a solid to be in contact with one fluid rather than another. The contact angle, θ, is completely water-wet when $\theta = 0°$ and completely oil-wet when $\theta = 180°$ (Standal *et al*., 1999; Berg, 2010).

2.7.3 Zeta potential

The zeta-potentials were measured using a zetasizer by Malvern with a u-shaped cell. The results were obtained by variation in salinity, ionic strength and pH (Berg, 2010; Farooq *et al.*, 2013).

Chapter 3

Experimental Method

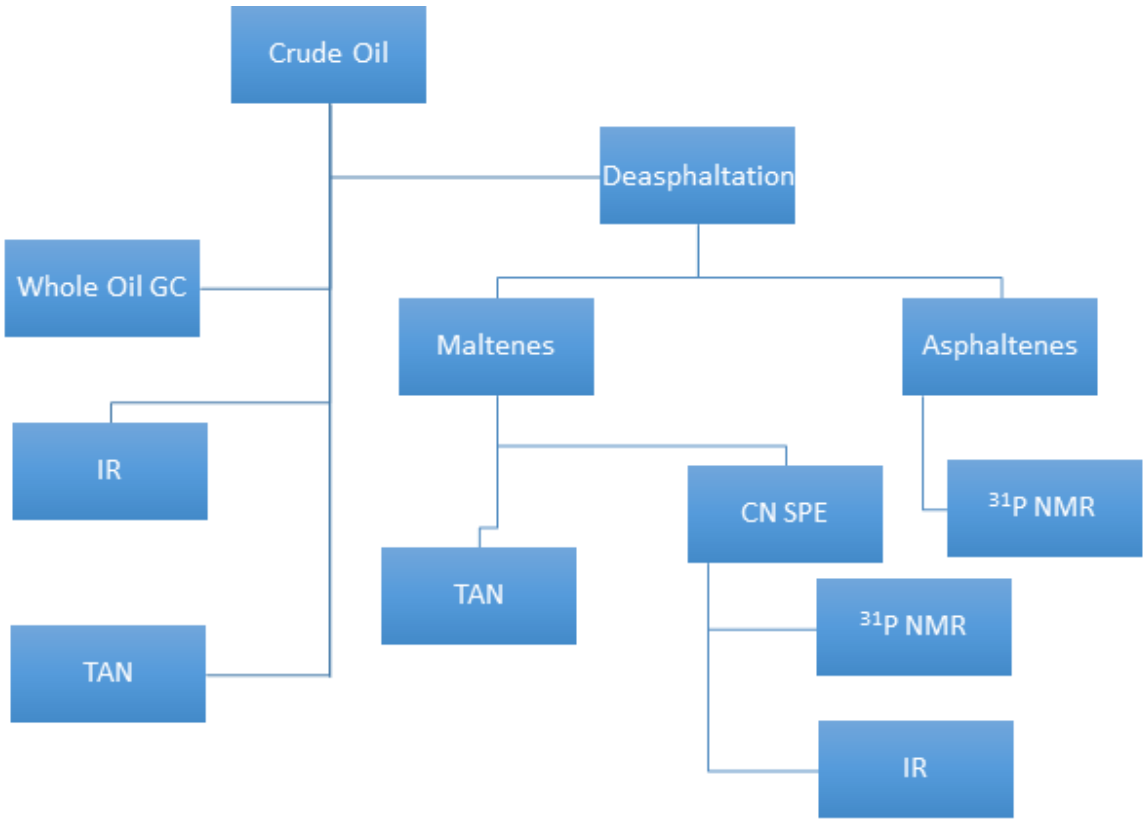

Figure 3.1: Flowchart summarizing the fractionation and analysis methods used.

3.1 Oil Samples

Six oil samples, distributed over five oil fields, were supplied by Statoil. Aliquots of the oils are transferred from jerry cans to smaller sample containers after heating to 60°C and reaching homogenization. Samples E1 and E2 stem from the same well. E1 has no chemical additives in the sample, while E2 has been added a demulsifier.

3.2 Determination of asphaltene content

The asphaltenes are determined by precipitation of insoluble compounds from the crude oil in a 40 times excess (by volume) of n-hexane. The solution is shaken vigorously before storage in a fridge for approximately 24 hours. The precipitated asphaltenes are collected through filtration through a Whatman GF/C glass fiber filter. The collected asphaltenes are then dried for 30 minutes at 50°C and stored in a glass vial sealed with nitrogen gas.

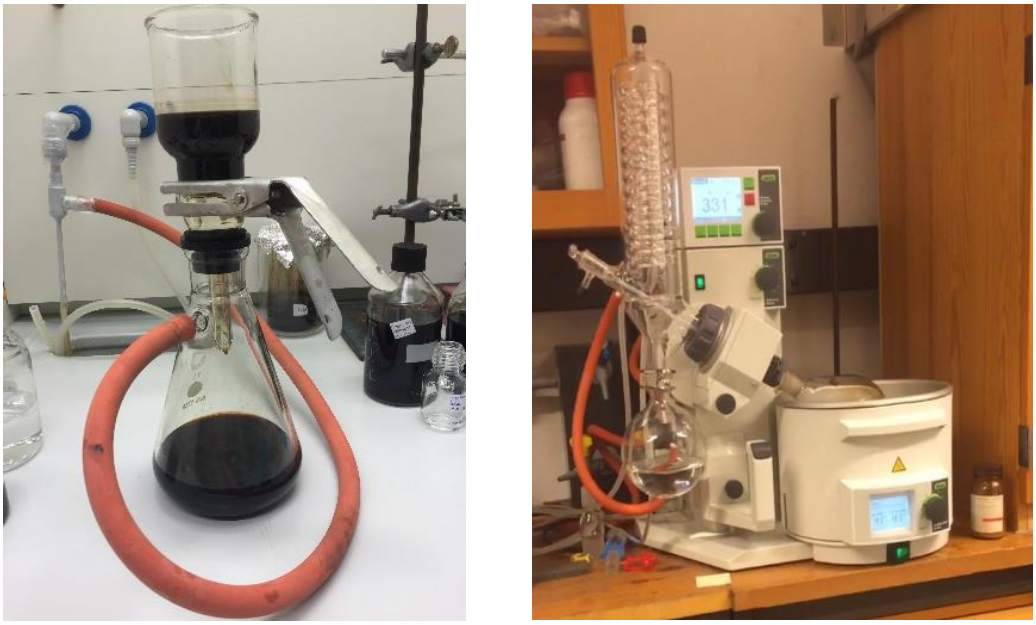

Figure 3.2.1: Experimental setup for the determination of asphaltenes and for removing excess hexane in the maltene fraction by rotavapor.

3.3 SPE cyano column - maltene fractionation

After the asphaltenes are precipitated from the solution, the excess hexane present in the maltene solution is removed by rotavapor and N_2-gas treatment. The remaining oil is then subjected to further separation and analysis.

Isolute SPE cyano columns (end-capped) from Biotage with a 1000mg sorbent mass and 6ml reservoir volume are used to fractionate the samples. The first eluent is used to wet the column and approximately 30mg of oil sample dissolved in 0.075ml of DCM:MeOH 93:7 (v/v) is introduced to the column. The solvents and volumes are given in Table 3.3.1.

Table 3.3.1: SPE procedure for fractionation of deasphalted oils (Borgund *et al*., 2007)

Fraction	Solvent	Volume of Solvent (mL)	Compound Types	Abbreviation
1	Hexane:DCM 90:10 (v/v)	20	Non-Polar	**F1**
2	Hexane:DCM 90:10 (v/v)	30	Intermediate Fraction	**F2**
3	DCM:MeOH 93:7 (v/v)	20	Polyfunctional and Phenols	**F3**
4	MEOH:DCM 70:30 (v/v) + MeOH:Formic Acid 95:5 (v/v)	~2 ~10	Highly Polar Compounds	**F4**

3.4 WOGC

A Hewlett Packard 5890 series II gas chromatograph, equipped with a FID detector is used to analyze the crude oil samples. The GC is fitted with a HP-ULTRA 2 column from Aligent Technologies, with the dimensions 25m x 0.20mm x 0.33µm. The program Chromeleon^{TM}, version 7.2 (delivered by Dionex) is used to obtain and treat the chromatograms.

Homogenous samples are ensured by placing the crude oil samples in a heating cabinet at 50°C for 30 minutes, where the sample is shaken every 10 minutes.

A 10 µL Hamilton syringe is used to collect the samples of approximately 0.5±0.1µL. The syringe is cleaned three times with DCM:MeOH (93:7v) and three times with hexane before, in-between and after use. The sample is manually introduced into the GC via the injector, which holds a temperature of 260℃ and the FID temperature is kept at 350°C. The injection is split in a 75:1 ratio. Helium is used as the mobile phase. The temperature program is shown in Table 3.4.1. Chromatograms of all the oils are shown in the A1-appendix.

Table 3.4.1: Temperature program used for WOGC

Temperature Interval (℃)	**Hold Time (min)**	**Ramp (℃/min)**	**Total Time (min)**
30	10	-	10
30 → 60	-	1.5	20
60	0	-	0
60 → 300	-	4.0	60
300	0	-	0

3.5 TAN Titration

A Metrohm autotitrator, model 809 Titrando, connected to a Metrohm Solvotrode easyClean combined LL pH glass electrode (model 6.0229.010) is used to determine the acid number. The computer software Tiamo 1.3 (delivered by Metrohm) is used to store and analyze data.

The standardized potentiometric titration procedure, ASTM D664-89, is used to determine the acid numbers. At least three parallel titrations of the crude oil samples are conducted, using 5-20g of oil in each titration.

3g of KOH is mixed with 1L of iso-propanol in a round bottom flask. The mixture is heated under reflux, until the salt is completely dissolved. It cooled for two days in room temperature. Nitrogen gas is used to eliminate the remaining dissolved CO_2. Precipitated carbonate is removed by filtration.

To avoid forming solid deposits under titration, KCL pellets are used when the titrant is connected to the autotitrator (Negash, 2004).

Table 3.5.1: Titration Solution mixture

Solvent	**Amount (wt%)**
Distilled water	0.5
Iso-Propanol	49.5
Toluene	50

The standard solution is made from hydrogen phthalate (KHP). Approximately 3g of KHP is dried at 100 °C for 2-3 hours and cooled in a desiccator. Exactly 1.01g of KHP is dissolved in 100g water. Air is removed by N_2-gas substitution.

A minimum of three parallels are measured, in order to obtain an average and standard deviation. The electrode is washed after each measurement, first with DCM, then titrant solution and finally with distilled water. The electrode is put in distilled water in between measurements. The electrode is stored in electrode solution after the measurements are conducted. Titration curves are found in the Appendix.

3.6 FTIR Analysis

All of the measurements are performed on a Nicolet iS5OR FT-IR spectrometer equipped with a Diamond Attenuated Total Reflection (ATR) sample cell. The computer program OMNIC integrated software (delivered by Thermo Fisher) is used to collect the sample spectra. The spectra are recorded from 600 to 4000cm^{-1} using 32 scans, where a background spectrum is collected first in order to cancel out bands from water vapor, CO_2 and other noise present.

Prior to collecting the spectra, all the samples are warmed in a heating cabinet at 50°C to homogenize. Toluene and ethanol is used to clean the sample surface before, in-between and after the runs.

To increase the sample present in F1-F4, N_2-gas is used to evaporate the bulk solvent. Approximately one drop is left, which is then evaporated on the sample cell before the spectrum is collected.

3.7 ^{31}P NMR Analysis

The experimental procedure is based on the method developed by Jasiukaityte et al. (2010) and Laugerud (2014). The samples are run on a Bruker Biospin AV 500 and analyzed using TopSpin 3.5pl5 (delivered by Bruker).

Table 3.7.1: 500mHz ^{31}P NMR parameters

td	sw (ppm)	o1p (ppm)	o1 (Hz)	p1 (µs)	pl1 (dB)	d1 (s)	ns	aq (s)
52901	261,3222	70.273	14227,21	11.25	3.00	25	64	0.4999238

The parameters shown in Table 3.7.1 were developed by Laugerud (2014) and used in this analysis.

The solvent mixture contains pyridine and deuterated chloroform, (1,6:1 v/v). $Cr(acac)_3$ is added to the solution so that the concentration is 5 mg/ml.

30mg of sample is dissolved in 500µL of the solvent mixture and 10µL cyclohexanol is added as an internal standard. Finally, 100µL of the reagent TMDP is added to the solution before it is shaken.

The NMR solvent mixtures are made the day before analysis and stored in room temperature.

3.8 Multivariate Analysis

Multivariate analysis is performed on the data collected, using the SIRIUS^{TM} program, version 10.0 (SIRIUS, 2004). Principal component analysis (PCA) models are built using the limited data collected in this thesis and by Kolltveit (2016), in order to investigate the possibility of predicting physiochemical properties from the chemical composition (Grung, 1996; Isaksson *et al.*, 1996).

The data collected directly from the experimental methods is called raw data and may contain noise, baseline drift, dominant variables and other factors that may conceal the significant information in the dataset (Karstang, 1996). The raw data is therefore standardized in order to give the variables equal-variance. By using PCA, the raw data matrix is also centered, in order to observe object similarities and variable covariance relative to their placement around the mean value of the dataset. The principle components (PCs) are in other words arranged in a variable and object space according to the direction of maximum variation, where the center point of the graph contains no variation.

Chapter 4

Results

4.1 WOGC

The results are interpreted by comparison to a chromatogram of a Norwegian standard oil (NSO) (Weiss, 2000). This analysis is conducted in order to determine the level of biodegradation in each crude oil according to the system developed by Peters and Moldovan. The results of this evaluation can be found in Table 4.1.1.

The chromatogram in Figure 4.1.1 shows how the short hydrocarbons and the small naphthenes appear first. The normal distribution of the larger hydrocarbons, nC_{10+}, start eluting at approximately 28 minutes. Two important "doublet" peaks present themselves at ~60 and ~62 minutes. These doublet peaks represent the reference peaks for the biomarkers pristane and phytane, where nC_{17} and pristane elute first at ~60 and nC_{18} and phytane elute after at ~62 minutes. These biomarker peaks are important because they are more resilient towards biodegradation and can therefore be used in determining the biodegradation level of crude oils.

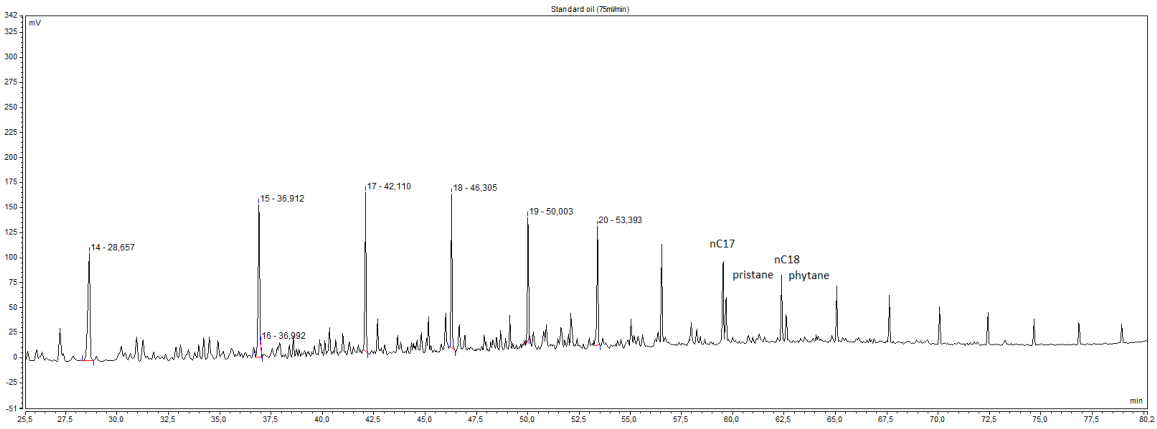

Figure 4.1.1: Normal distribution of nC_{10+} alkanes in a Norwegian standard oil chromatogram. The x-axis has units in time (min) and the y-axis has units of mV.

Table 4.1.1: Results of evaluation of biodegradation in crude oil from their chromatogram.

Crude Oil	C8-C15 alkanes	Pristane/C17 Pristane/Phytane ratio	UCM	Peters and Moldowan Biodeg. Value
A	To some degree intact	0.88 2.07	Yes	3/2 slight
B	To some degree intact	0.85 1.86	Yes	3/2 slight
C	Not intact	3.71 1.86	Yes	4/3 slight/moderate
D	Intact	0.70 1.58	No	1 very slight
E1	Intact	0.62 1.55	No	1 very slight
E2	Intact	0.60 1.56	No	1 very slight

One of the biodegradation trends in Peters and Moldovans system is the degree of missing n-alkanes. This absence can clearly be seen in the upper chromatogram in Figure 4.1.2, especially when comparing it to the chromatogram underneath. The lack of n-alkanes will vary depending on the amount of biodegradation the crude oil has been subjected too. The chromatograms show that the crude oils A, B and C all experience a varying degree of n-alkane deficiency, while the chromatograms for crude oils D, E1 and E2 show nice normal distributions of the n-alkanes.

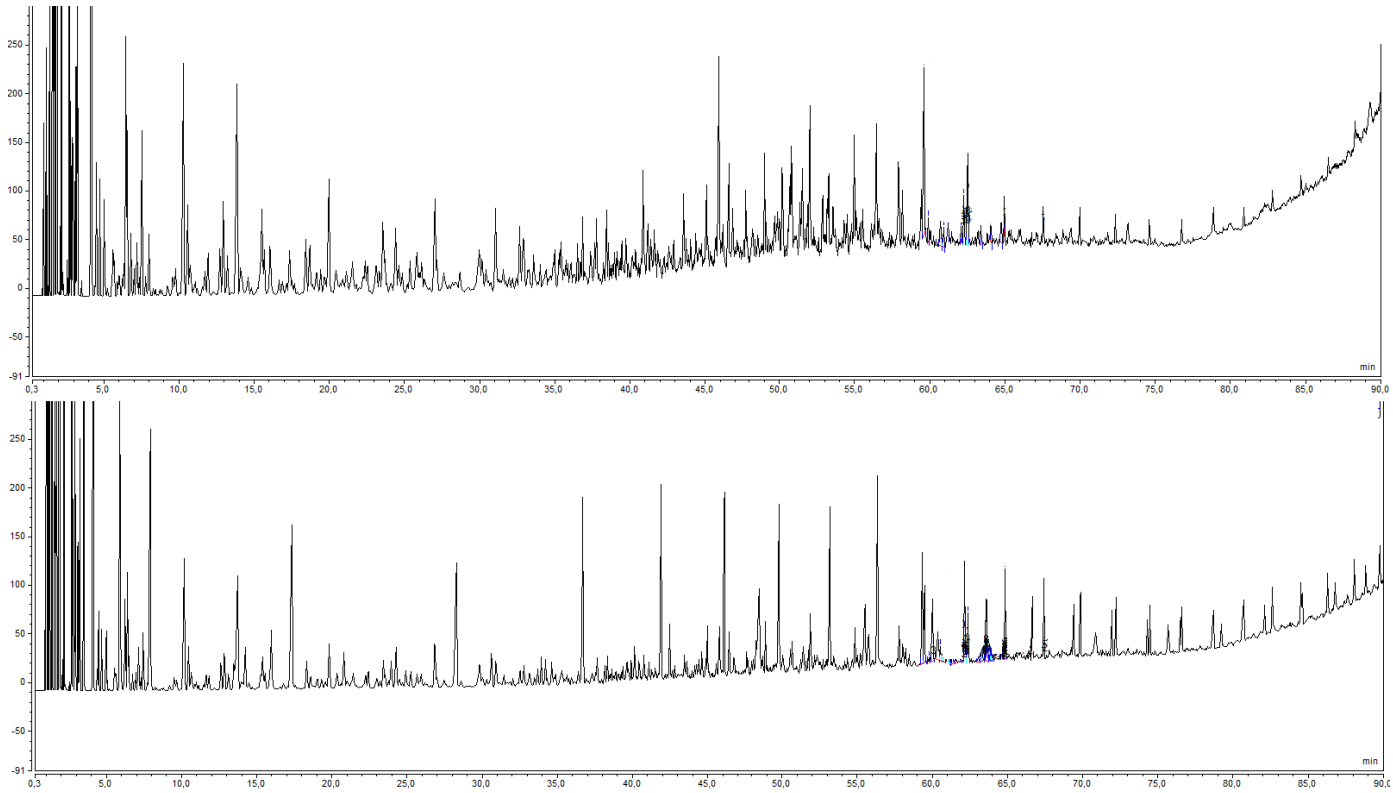

Figure 4.1.2: Upper chromatogram (crude oil C) shows a biodegraded sample and the bottom chromatogram (crude oil D) shows a non-biodegraded sample.

In Figure 4.1.2, the upper chromatogram shows a non-linear baseline. This curved baseline is another biodegradation trend and is a phenomena referred to as an UCM. The bacteria that cause biodegradation "eat" the smaller hydrocarbons, resulting in an indistinguishable hump where the n-alkanes used to be (Gough *et al*. 1990; Tomren *et al*., 2014). The UCM hump is found in the chromatograms of crude oils A, B and C, where the chromatograms of A and B can be found in the A1-appendix.

Another biodegradation indication is the ratio between the "doublet" biomarker peak and their n-alkane peak. In Figure 4.1.3 the difference between nC_{17} and pristane in a biodegraded and a non-biodegraded sample is shown. On the left hand side, the crude oil C shows how the pristane peak is more intense than the nC_{17} peak, indicating biodegradation. On the right hand side, crude oil D shows how this ratio can be less distinct, which can indicate less or no biodegradation.

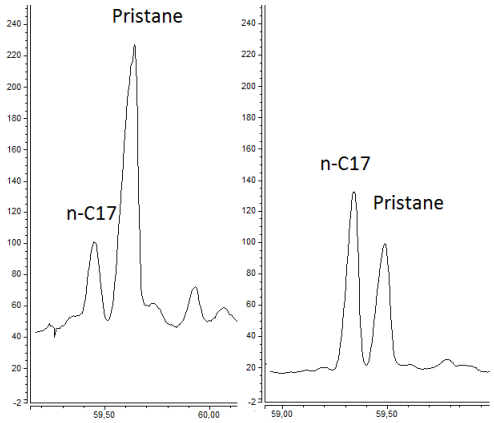

Figure 4.1.3: The nC_{17} and pristane peak, where the ratio between the two determine the level of biodegradation. To the left is a biodegraded sample (crude oil C) and to the right is a non-biodegraded sample (crude oil D).

4.2 Crude oil deasphalting

A detailed table of the results from precipitating the asphaltenes from the crude oil can be found in Table A2-1 in the appendix.

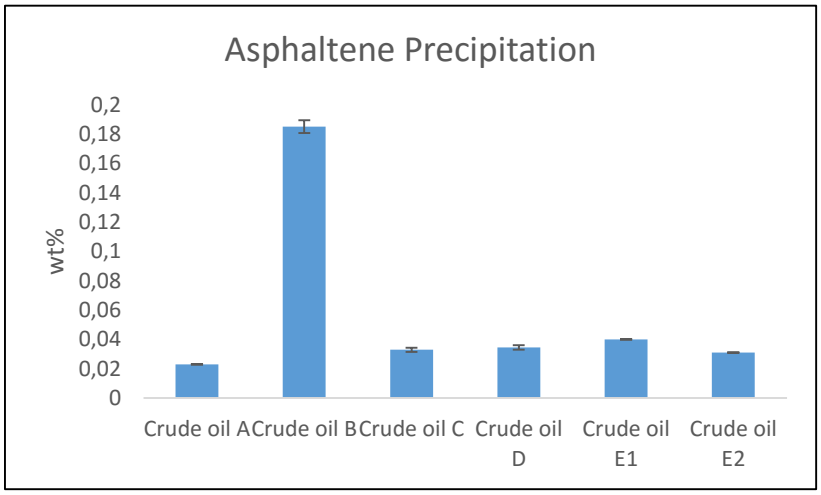

Figure 4.2.1: Amount of asphaltenes (wt%) present in each crude oil.

From Figure 4.2.1 it is obvious that crude oil B has the highest amount of asphaltenes. Crude oil E1 and E2 should be close in asphaltene amounts as they are the same crude oil, where E1 has not been chemically modified and E2 has been added a demulsifier. Crude oil A has the smallest amount of asphaltenes.

The reproducibility of the asphaltene measurement was tested for crude oil B, C and D. The selection of these crude oils was based on the amount of accessible crude oil. A relative standard

deviation of less than 5% was the ideal goal and for both crude oil B and C the reproducibility goal was achieved. Crude oil D on the other hand had a deviation of 7.4%.

4.3 SPE – Maltene fractionation

No quantitative or qualitative information is gained in this process. The fractions are further analyzed by the following processes. Figure 4.3.1 shows how the different components in the crude oil have different affinities for the column and the solvent by eluting at different steps in the procedure. At F4 there is still some sample left on the column. This is not surprising as some irreversible adsorption is expected.

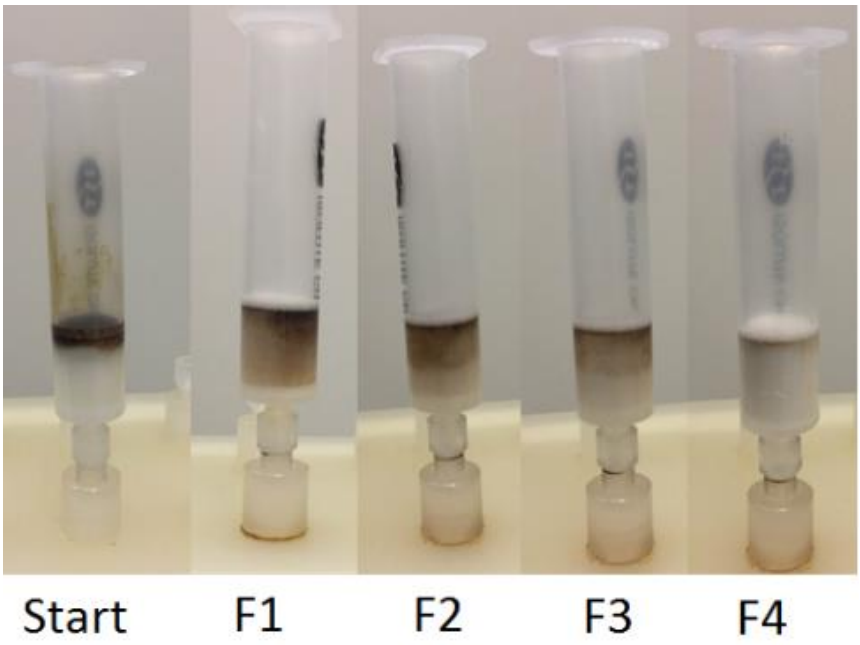

Figure 4.3.1: Illustration of the SPE columns during the fractionation process.

4.4 Infrared Spectroscopy

The crude oils, the deasphalted oils and their deasphalted maltene fractions(F1-F4) are analyzed by FT-IR spectroscopy. The maltene fractions were treated with N_2 gas in order to increase the sample concentration and decrease the amount of solvent in the spectra. In addition to this, when the sample was added to the sample plate, the remaining solvent was evaporated before the sample spectra was collected.

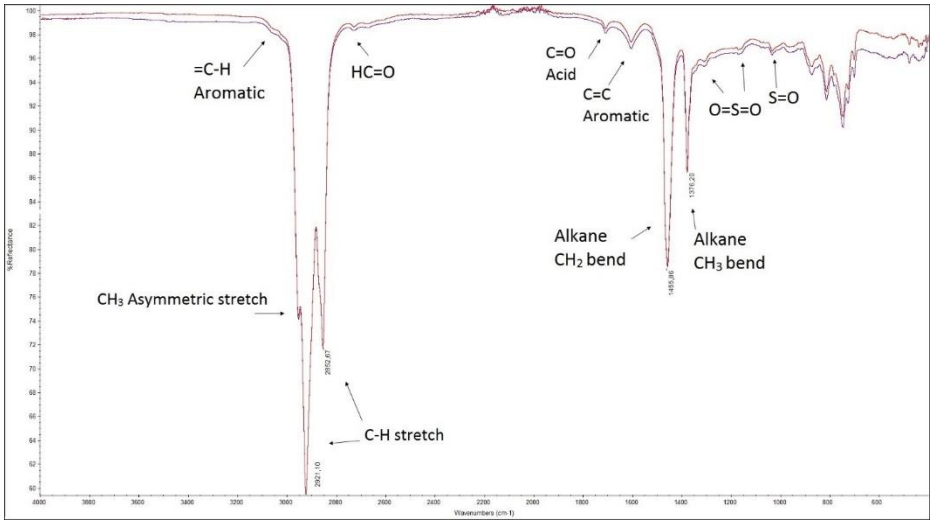

Figure 4.4.1: Spectra for crude oil B and its deasphalted sample. The marked bands are typical functional groups found in crude oil. The purple spectrum represents crude oil B and the red spectrum represents the deasphalted oil.

Spectra of the crude and deasphalted oils appear almost identical and an example is shown in Figure 4.4.1. The marked bands in this figure represent typical functional groups found in crude oils and Table 4.4.1 shows a more detailed list. The first bands appearing at 2953 cm^{-1} to 2852 cm^{-1} represent the C−H stretch in alkanes, often accompanied by a band at 1455cm^{-1}, indicating asymmetrical methyl bending, and one at 1375cm^{-1} indicating symmetrical methyl bending. A weak band at ∼2800 cm^{-1} might indicate HC=O in an aldehyde. Weak bands also appear at 1705cm^{-1} and 1604cm^{-1}, where the first represents the C=O stretching for carboxylic acids and the second suggest aromatic C=C bonds, where conjugation might have played a role in lowering the frequency. The bands found in the fingerprint region, around 1300-1000 cm^{-1} of the spectra, might be indicators of sulfoxide and sulfone.

Table 4.4.1: Major bands found in the crude and deasphalted oil spectra. The intensity of a band is denoted; strong band = +++, medium band = ++, weak band = + and no band = 0.

Wavenumber (cm^{-1})	**Possible Source**		**A**	**B**	**C**	**D**	**E1**	**E2**
>3000	=C-H Alkane Stretch	Crude Oil	+	+	+	+	+	+
		Deasphalted Oil	+	+	+	+	+	+
2953	CH_3 Asymmetrical Stretch	Crude Oil	++	++	++	++	++	++
		Deasphalted Oil	++	++	++	++	++	++
2919	C-H Alkane Stretch	Crude Oil	+++	+++	+++	+++	+++	+++
		Deasphalted Oil	+++	+++	+++	+++	+++	+++
2852	C-H Alkane Stretch	Crude Oil	++	++	++	++	++	++
		Deasphalted Oil	++	++	++	++	++	++
2800	HC=O Aldehyde	Crude Oil	+	+	+	+	+	+
		Deasphalted Oil	+	+	+	+	+	+
1705	C=O Carboxylic Acid	Crude Oil	+	+	+	0	0	0
		Deasphalted Oil	+	+	+	0	0	0
~1600	C=C asymmetrical Conjugated Alkanes or Aromatics	Crude Oil	+	+	+	+	+	+
		Deasphalted Oil	+	+	+	+	+	+
1455	CH_2 Methyl Bending	Crude Oil	++	++	++	++	++	++
		Deasphalted Oil	++	++	++	++	++	++
1375	CH_3 Methyl Bending	Crude Oil	++	++	++	++	++	++
		Deasphalted Oil	++	++	++	++	++	++
~1030	S=O Sulfoxide	Crude Oil	+	+	+	+	+	+
		Deasphalted Oil	+	+	+	+	+	+
~1300 and ~1100	O=S=O Sulfone	Crude Oil	+	+	+	+	+	+
		Deasphalted Oil	+	+	+	+	+	+
~750	Alkane Long-chain band	Crude Oil	+	+	+	+	+	+
		Deasphalted Oil	+	+	+	+	+	+

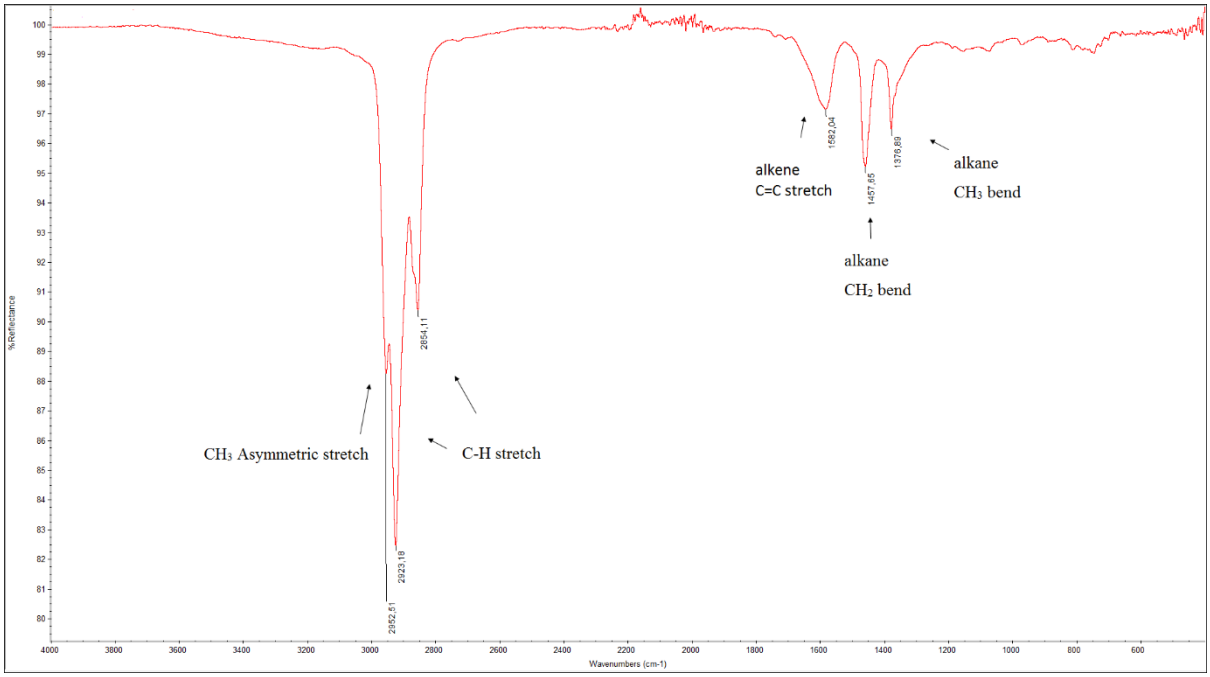

Figure 4.4.2: The spectrum of crude oil A F1.

Table 4.4.2: Common wavelengths found in F1. Symbol description can be found in Table 3.3.1.

Wavenumber (cm^{-1})	**Possible Source**	**A**	**B**	**C**	**D**	**E1**	**E2**
~2953	CH_3 Asymmetric stretch	++	++	++	++	++	++
~2919	C-H Alkane stretch	+++	+++	+++	+++	+++	+++
~2852	C-H Alkane stretch	++	++	++	++	++	++
~1582	C=C Alkene stretch	++	+	+	+	++	+
~1455	C-H Methyl asymmetrical bending	++	++	++	++	++	++
~1375	C-H Methyl symmetrical bending	++	++	++	++	++	++

F1 is the least polar fraction and does therefore not contain any polar functional groups. Figure 4.4.2 shows a spectrum of F1 for crude oil A, which clearly shows the common C-H alkane stretches at 2953-2852 cm^{-1}, 1455 cm^{-1} and 1375 cm^{-1}. Also for crude oil A and E1 there is a medium intensity band at 1582cm^{-1} which might indicate C=C for alkenes.

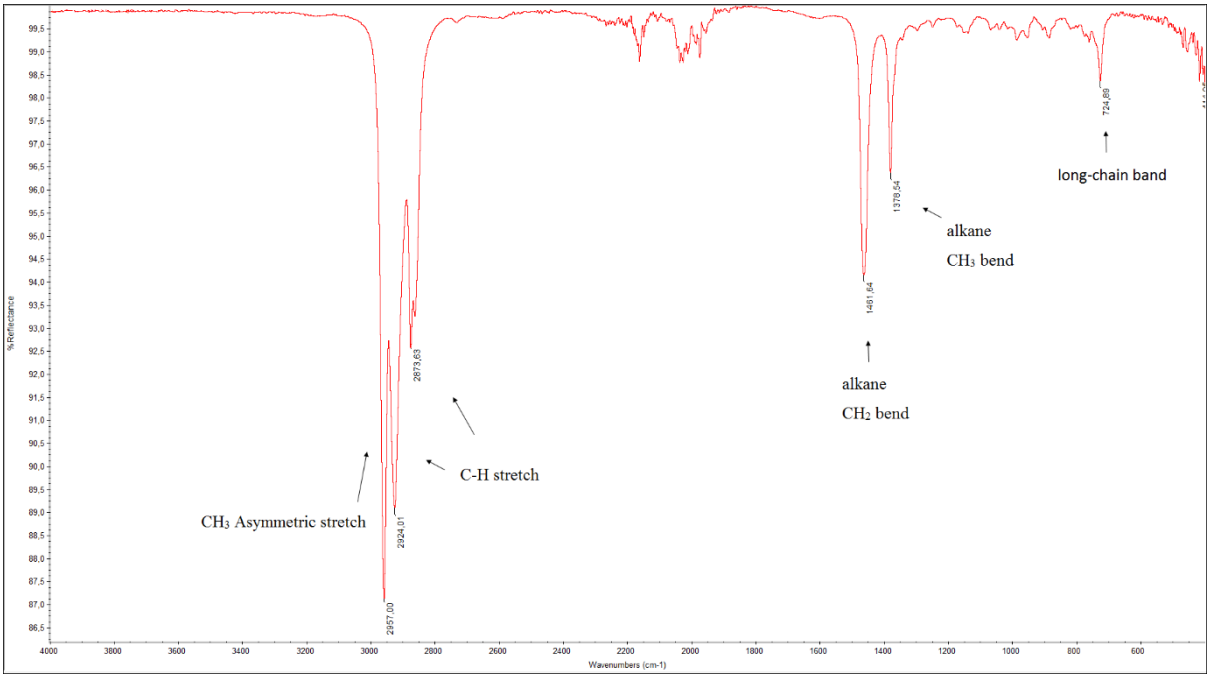

Figure 4.4.3: The spectrum of F2 for crude oil A.

Table 4.4.3: Common wavelengths found in F2. Symbol description can be found in Table 3.3.1.

Wavenumber (cm^{-1})	**Possible Source**	**A**	**B**	**C**	**D**	**E1**	**E2**
~2953	CH_3 Asymmetric stretch	+++	++	+++	+++	+++	+++
~2919	C-H Alkane stretch	++	+++	++	++	++	++
~2852	C-H Alkane stretch	++	++	++	++	++	++
2800	HC=O Aldehyde	+	+	+	+	+	+
~1455	C-H Methyl asymmetrical bending	++	++	++	++	++	++
~1375	C-H Methyl symmetrical bending	++	++	++	++	++	++
724	Indication of long-chain band	+	0	+	+	0	+

F2 is an intermediate fraction. Figure 4.4.3 and Table 4.4.2 shows the common C-H alkane stretches just mentioned. The difference in these spectra is that the intensity of the asymmetric CH_3 band is more intense than the C-H stretch, indicating more branched structures. It also has a weak band at 2800cm^{-1} indicating HC=O for an aldehyde. An addition to this spectra, is the band at 724 cm^{-1}, which may be an indication of a long-chain alkane band (Pavia, 2009).

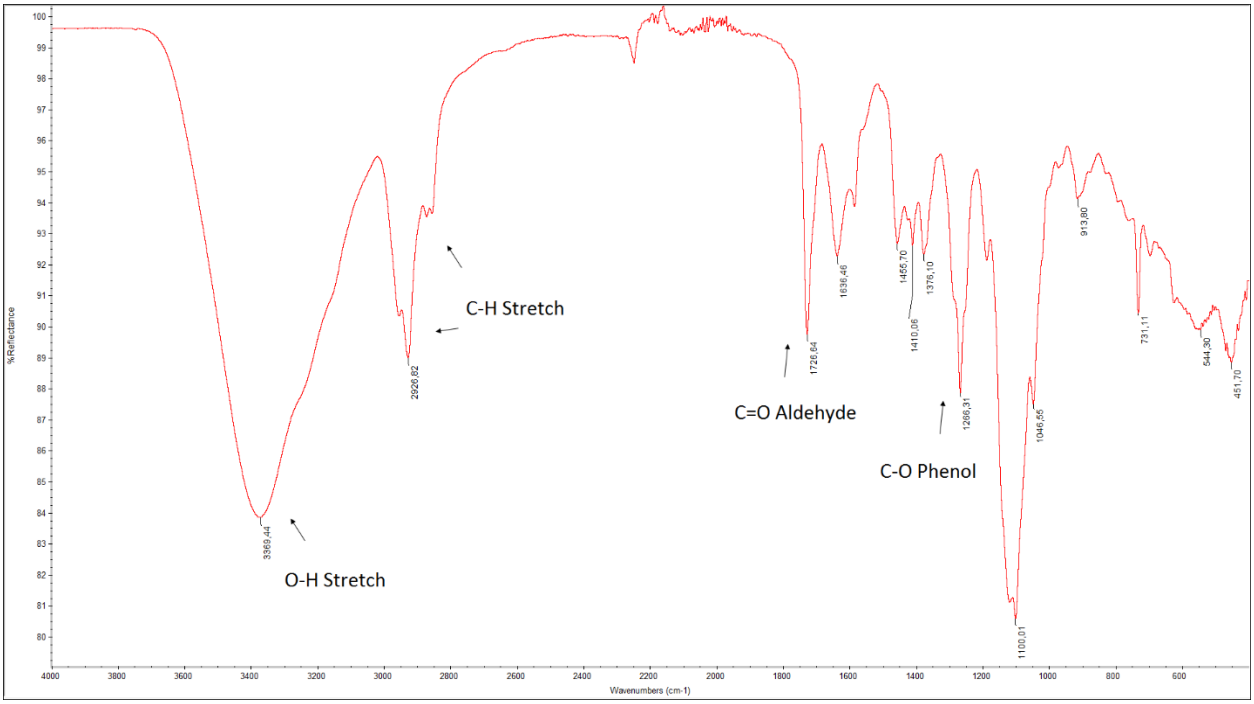

Figure 4.4.4: The spectrum for crude oil A F3.

Table 4.4.4: Common wavelengths found in the F3. Symbol description can be found in Table 3.3.1.

Wavenumber (cm^{-1})	**Possible Source**	**A**	**B**	**C**	**D**	**E1**	**E2**
3400-3300	O-H Alcohol/Carboxylic acid stretch	+++	++	+++	++	+++	+++
~2960	CH_3 Asymmetric stretch	++	+++	++	++	++	++
~2850	C-H Alkane stretch	+	++	+	+	+	+
1726	C=O Aldehyde/ester	++	0	0	0	++	++
1705	C=O Carboxylic Acid	0	+	+	+	0	0
1636	C=C Alkene stretch	+	+	++	+	++	+
1450	C-H Methyl asymmetrical bending	+	++	+	+	+	+
1375	C-H Methyl symmetrical bending	+	+++	+	+	+	+
1264	C-O Phenol	++	0	0	0	++	++
1300-1000	C-O ether/ester	+++	0	+++	+++	+++	++

Borgund et al found that F3 contained polyfunctional and phenolic compounds. This is consistent with the spectra obtained in F3. Figure 4.4.4 shows that F3 has the familiar broad O-H stretch at $\sim 3400\ cm^{-1}$ indicating either alcohol or carboxylic acids. There is also a band with medium intensity occurring at 1264 cm^{-1}, which might indicate C-O in phenols. The alkane bands are not very intense which indicates aromatic structures. Due to low concentration of sample in F3, some information may be lost in noise from the baseline.

Table 4.4.5: Common wavelengths found in the F4. Symbol description can be found in Table 3.3.1.

Wavenumber (cm^{-1})	**Possible Source**	**A**	**B**	**C**	**D**	**E 1**	**E2**
~3370	O-H Alcohol/Carboxylic acid stretch	+	+	+	++	+ +	+
~2960	CH_3 Asymmetric stretch	+	+	+	+	0	+
~2850	C-H Alkane stretch	+	+	+	+	0	0
1705	C=O Carboxylic Acid	+	+	+	++	+	+
1625	C=C Alkene stretch	+	0	+	++	+	+
1587	C=C Aromatic stretch	0	++	0	0	0	0
1450	C-H Methyl asymmetrical bending	0	+	0	0	0	0
1390	C-H Methyl symmetrical bending	+	0	+	+	+	+
1208	C-O Carboxylic Acids	+	0	+	+	+	+

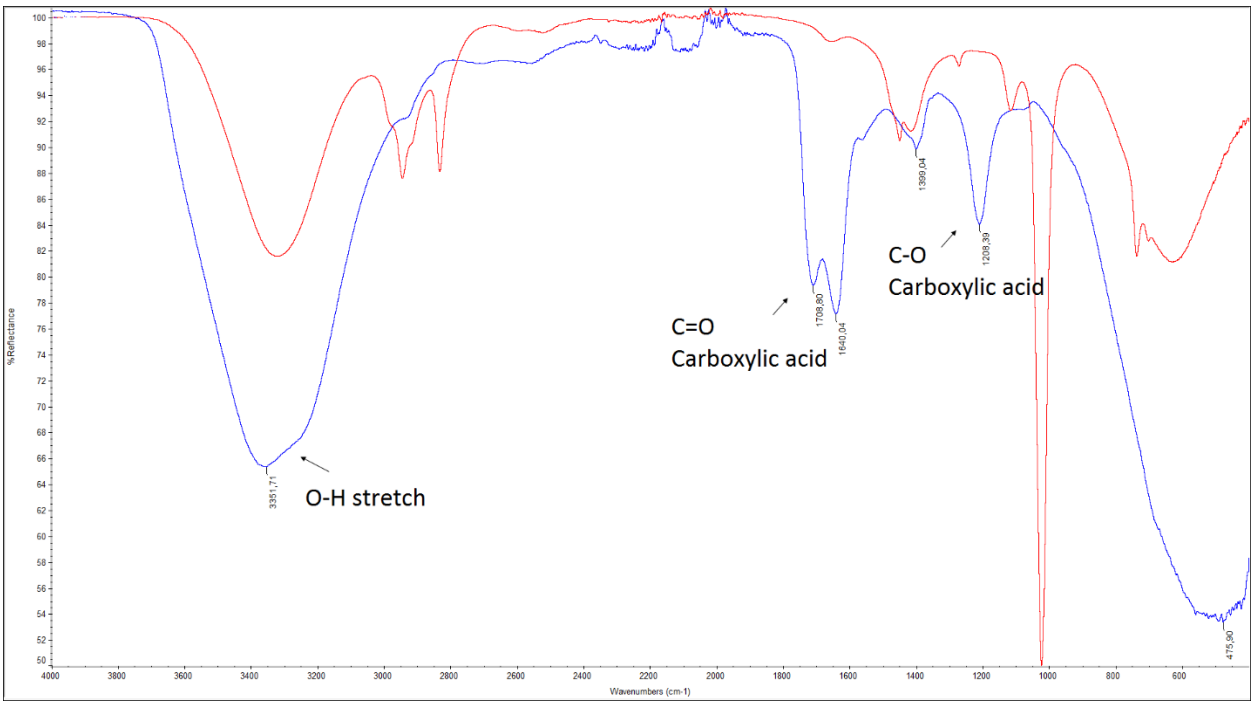

Figure 4.4.5: Spectra of solvent used in F4 (Red) and the evaporated F4 sample (blue).

Figure 4.4.5 shows that F4 has more polar bands belonging to carboxylic acid with a broad band at $\sim 3400 cm^{-1}$ representing the O−H stretch and the complimentary peaks at $\sim 1705 cm^{-1}$ and $\sim 1205 cm^{-1}$, indication C=O and C−O. Due to very low concentrations of sample in the last fraction, the spectra where difficult to obtain, thus increasing the presence of noise. The sample spectra are checked against the solvent spectra in order to confirm any suspicion of contamination from the solvent.

4.5 Total Acid Number

Table 4.5.1 and Table 4.5.2 show the measured TAN values for the crude oil samples and their deasphalted maltene samples. Crude oil A, B and C have TANs that are classified as highly acidic, where crude oil A is the most acidic of the three. Crude oil D, E1 and E2, and their maltene samples, do not have sufficient amounts of acidic components to be detectable in this TAN procedure.

By comparison of the crude oil and their deasphalted oil samples, one can conclude that the asphaltenes do not contribute to the TAN.

The titration curves are located in the A3 and A4 appendix.

Table 4.5.1: Results of crude oil TAN measurements.

Crude Oil	**Total Acid Number (mg KOH / g oil)**	**SD (mg KOH / g oil)**	**%RSD**
Crude oil A	3.01	0.04	1.21
Crude oil B	2.04	0.09	4.23
Crude oil C	0.98	0.04	4.28

Table 4.5.2: Results of deasphalted crude oil measurements.

Deasphalted Oil	**Total Acid Number (mg KOH / g oil)**	**SD (mg KOH / g oil)**	**%RSD**
Crude oil A	3.09	0.05	1.52
Crude oil B	1.78	0.08	4.72
Crude oil C	0.94	0.03	3.58

4.6 ^{31}P NMR

The two most polar maltene fractions, F3 and F4, and their respective asphaltene fractions , are analyzed with ^{31}P NMR.

Table 4.6.1: Chemical shifts of different functional groups (Pu et al, 2011; Laugerud, 2015).

Functional Group	Chemical Shift (ppm)
TMDP	175.0
Thiol/Amine	168.8 – 167.1
Aliphatic OH	148.3 – 146.3
Cyclohexanol	145.8 – 144.7
Phenols with 2 OMe	144.5 – 141.0
Phenols with 1 OMe	140.8 – 139.6
Phenols with 0 OMe	139.6 – 137.0
Carboxylic acids	135.3 – 134.0

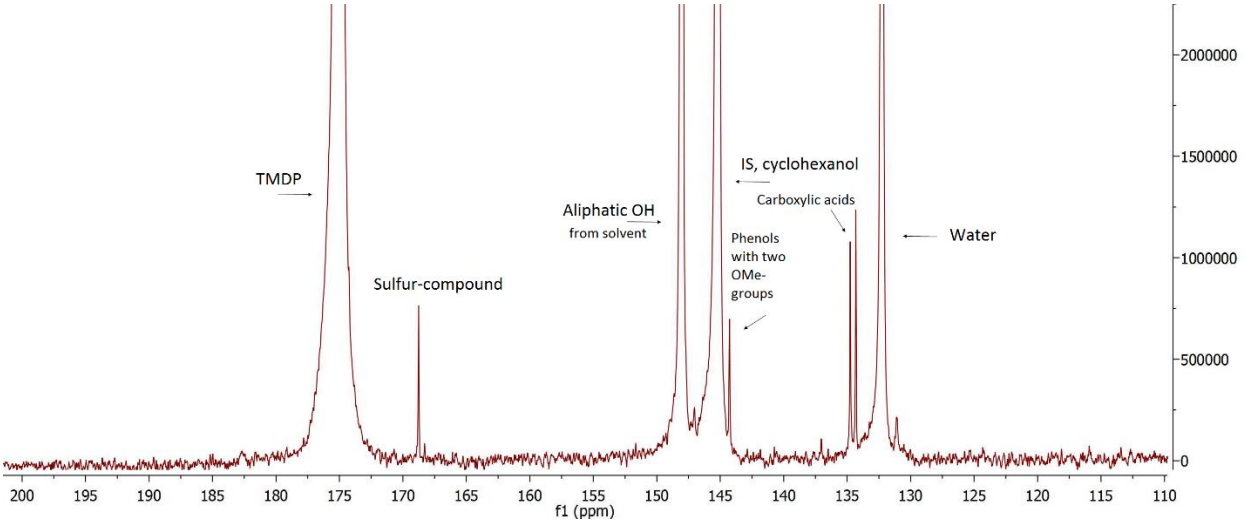

Figure 4.6.1: NMR spectrum of F3 (crude oil A), marked with possible OH-functional groups.

The spectra for crude oils are very similar, where a summarization of the peaks can be found in Table 4.6.1. The variation in the spectra lies mainly in the integration ratios, which are comparable as the internal standard is used as the reference peak.

The peak found most downfield, at 175ppm, is unreacted TMDP. The peak occuring at ~168ppm, might indicate some sort of sufur or nitrogen containing compound. Wroblewski et al. did some research into standards containing sulfur and found them to be located further downfield than the oxygen containing compounds, supporting this indication. The aliphatic OH peak occurs at ~148ppm. The internal standard is found at 145ppm and is used as the reference peak in the integration of all the spectra. The next peaks represent phenolic compounds with either two, one or no OCH_3 groups. The carboxylic acid functional groups are located further upfield, approximetely at 134 and 135 ppm. The peak at ~132ppm represents water present in the solution.

Borgund et al. found through her HPLC studies that F3 contained polyfunctional and phenolic compounds. This conclusion is supported by the findings in the F3 spectra as the functional groups for alcohols, phenols and carboxylic acids are present.

In Figure 4.6.1 all the peaks that are of interest are very small in comparison to the IS peak at 145ppm, except for the aliphatic OH peak which is very intense. This peak is most likely a product of the solvent used in the maltene fractionation and it is therefore difficult to asses how much or if any aliphatic OH can be found in F3.

By integration of the peaks relative to the IS, the most abunandt functional groups are found in each sample. Crude oils A and E1 have approximatley the same amounts of the phenolic functional group with two OCH_3 and the carboxylic acid at 134ppm. Crude oils B, D and E2 are most abundant in the carboxylic functional group located at 134ppm, while crude oil C has the highest ratio of the phenolic compound with two OCH_3.

An interesting observation made when comparing the spectra of E1 and E2. Figure 4.6.2 shows how E2 has three additional peaks.

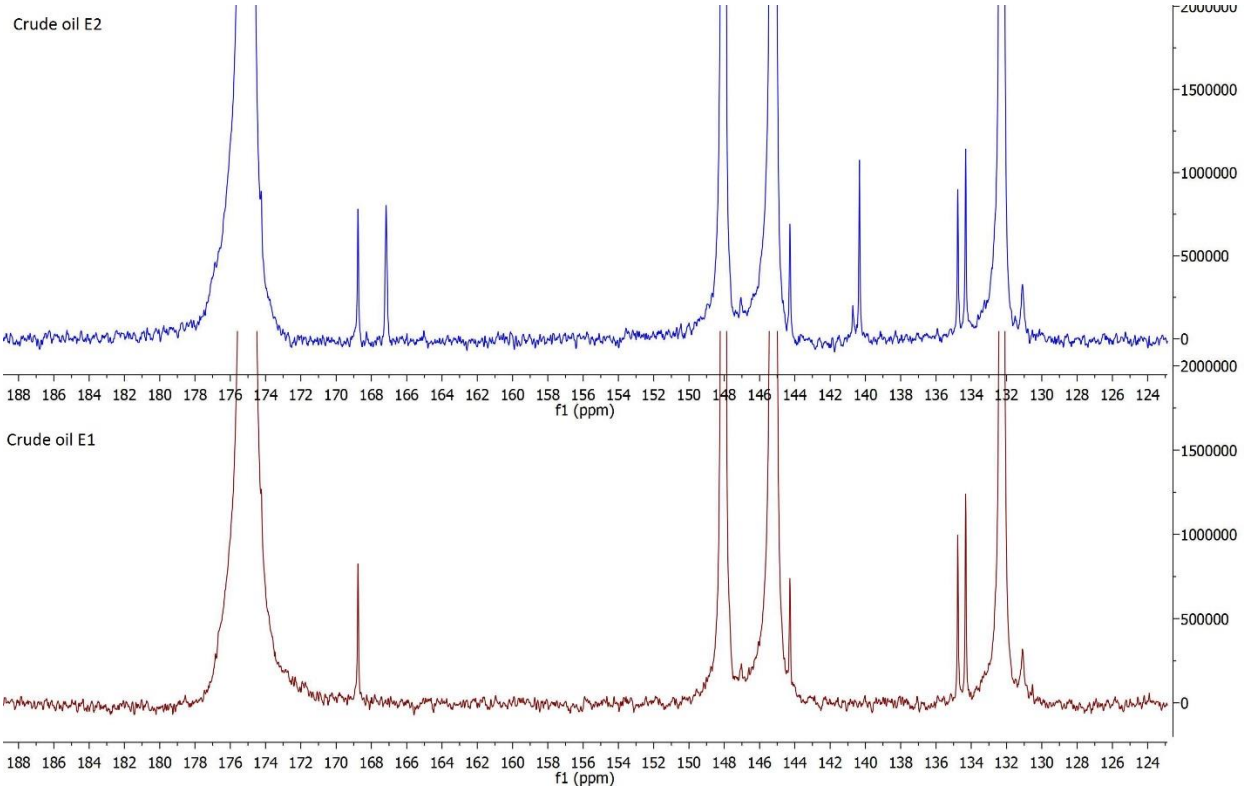

Figure 4.6.2: Crude oil E1 vs E2. The difference is that one has an demulsifier and the other does not.

The first peak is found downfield at ~167ppm. As mentioned earlier, this might indicate some sort of thiol or amine functional group. Further analysis is needed to make any definite conclusions. Also, two additional peaks are found at ~140ppm. These are indications of compounds containing phenols with either one or two OCH_3 groups. It is uncertain why these two crude oils from the same well have so different spectra. One indication might be contamination in crude oil E2. Another indication might be that there is a demulsifier in E2 that has polar components in its structure made apparent in the NMR analysis. However, these are only educated guesses and have to be further examined in order to make any certain conclusions.

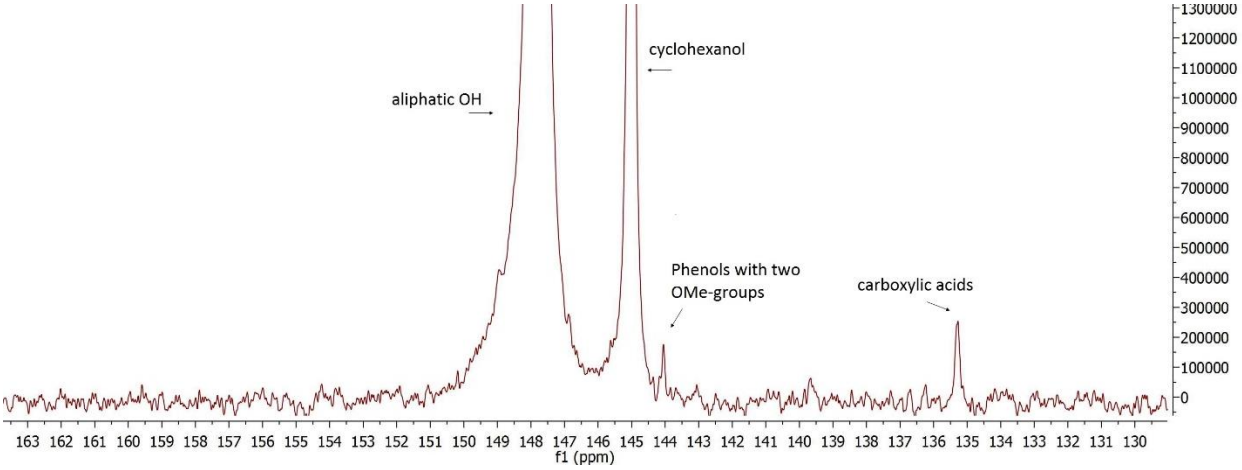

Figure 4.6.3: F4 spectra (crude oil A).

Borgund et al. found that F4 contained highly polar compounds. The spectrum in Figure 4.6.3 show peaks for phenols with two OCH_3 and peaks for carboxylic acids, which validates what Borgund found in her studies.

F4 is the last fraction and there is some uncertainty surrounding the amount of sample present. By comparing the spectra found for F4, some peaks might be lost in the noise of the baseline due to too little sample reaction with TMDP. Crude oil A might have a small peak at 144 ppm and crude oil B might have a small peak at 134ppm, but further analysis is needed to confirm these indications.

Through integration of the peaks relative to the IS, all the crude oils are most abundant in the carboxylic functional group appearing at ~135ppm. This is not the same carboxylic acid functional group that is most abundant in F3. F4 is a more polar fraction and a slightly different chemical environment causes this peak to be located further downfield.

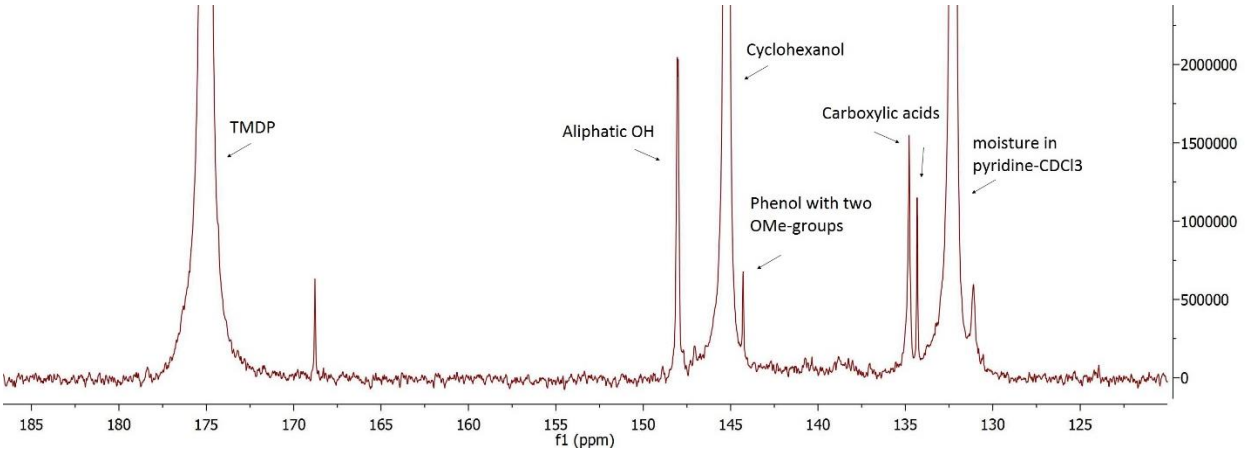

Figure 4.6.4: ^{31}P NMR spectra of crude oil B asphaltenes.

In Figure 4.6.4, a marked spectrum of the asphaltenes from crude oil B shows the polar functional groups present in the fraction. The first observation made is that the aliphatic OH peak is in the same intensity range as the other functional groups and can now be integrated with no uncertainty surrounding its origin. Another observation made is that crude oil A is the only sample that does not have this peak.

The integration of the peaks relative to the IS, shows that crude oils B, C, E1 and E2 have the highest ratio of aliphatic OH present. In crude oils A and D on the other hand, the carboxylic acid functional group at ~134ppm is most abundant.

Figure 4.6.5: The picture shows cloudy precipitation formed upon mixing F4 with NMR solvent.

When F4 is mixed with the NMR solvent, white precipitation formed instantly. Figure 4.6.5 shows the difference between a sample from F3 and F4, where the F4 sample to the right has precipitation at the bottom of the tube. When the mixture is shaken, small white crystals coat the inside walls of the NMR tube. The solution is to reduce the presence of solvent in the F4 solution by N_2-gas evaporation.

4.7 Physiochemical measurements

Table 4.7.1: A condensed list over physiochemical properties measured by Kolltveit.

		IFT				Zeta potential				CA		
Brine solution	**pH**	**A**	**B**	**C**	**pH**	**A**	**B**	**C**	**pH**	**A**	**B**	**C**
0.03M NaCl	**3**	26.1	27.2	18.5	**3**	26	41	22	**3**	-	-	-
	6	22.9	30.1	17.5	**6**	-30	-16	-43	**6**	-	-	-
	9	21.5	27.4	17.0	**9**	-76	-87	-54	**9**	-	-	-
	11	-	0.1	-	**11**	-102	-89	-101	**11**	-	-	-
0.12M NaCl	**3**	22.9	23.8	19.3	**3**	6	29	11	**3**	30	40	55
	6	20.5	25.8	17.6	**6**	-12	-16	-14	**6**	27	31	32
	9	9.1	21.0	15.0	**9**	-37	-24	-64	**9**	49	70	60
	11	-	0.2	0.1	**11**	-63	-39	-64	**11**	-	-	-
2.40M NaCl	**3**	12.3	9.60	11.5	**3**	-	-	-	**3**	56	43	62
	6	9.6	10.1	9.3	**6**	-	-	-	**6**	30	55	59
	9	0.5	0.2	0.9	**9**	-	-	-	**9**	97	61	57
	11	-	0.2	0.2	**11**	-	-	-	**11**	-	-	-
0.04 mole fraction $CaCl_2$	**3**	25.3	37.0	20.6	**3**	25	41	25	**3**	34	44	54
	6	23.2	27.9	18.7	**6**	-37	-24	-28	**6**	28	19	51
	9	16.2	15.6	12.6	**9**	-50	-59	-39	**9**	42	37	55
	11	14.4	6.3	11.0	**11**	-96	-91	-83	**11**	-	-	-

Table 4.7.1 is a condensed list of the measured physiochemical properties by Kolltveit, where the entire dataset can be found in her thesis.

Kolltveit observed that the contact angles at pH 9, acted water-wet during the measurements, but this cannot be seen in the results collected and are therefore deemed uncertain.

Chapter 5

Discussion

Chemical composition

Modern elemental analysis of petroleum has made it possible to identified more than 150,000 distinct elemental compositions in a bitumen sample by using advanced mass spectroscopy techniques (McKenna *et al.*, 2010). The spectroscopic and chromatographic methods used in this thesis can only give limited specific molecular information regarding the chemical compounds present, but they can give indications of functional groups that are important to surface activity. Table 5.1.1 and Table 5.1.2 summarizes the measured oil composition.

Table 5.1.1: Summary of the crude oil properties.

Crude Oil	**Asphaltene content** (wt%)	**Biodegradation** (Peters and Moldowan)	**TAN** (mg KOH/g oil)	**Density** (g/cm^3)	**Viscosity** (cS)	**Asphaltenes** Most abundant functional group (^{31}P NMR)
A	0.25	3/2	3.01	0.905	35	Carboxylic
B	2.04	3/2	2.04	0.934	270	Aliphatic OH
C	0.38	4	0.98	0.891	21	Aliphatic OH
D	0.43	0	BDL	0.836	N/A	Carboxylic
E1	0.48	0	BDL	0.82	N/A	Aliphatic OH
E2	0.43	0	BDL	0.82	N/A	Aliphatic OH

Biodegradation

Bacterial degradation is a reoccurring problem in many reservoirs and the impact it has on the oil quality can be very significant (Wenger *et al.*, 2002; Barth *et al.*, 2004). It is therefore important to understand how the chemical composition is altered and what effects this alteration has on the physical properties of the oil. From the results shown in Table 5.1.1, the Peters and Moldovans scale value indicates that crude oil C is the most biodegraded sample. The measured properties show that the normal distribution of the n-alkanes are not intact, it has the highest pristane/C17

ratio of 3.7 and an UCM hump. These factors combined give it a slight to moderate biodegradation ranking. The reasons crude oils A and B are given only a slight biodegradation ranking is because they do not show the deviation from the normal distribution of the n-alkanes and also because they do not have a comparably high pristane/C17 ratio. The remaining crude oil samples are unaltered and given a zero value in the ranking, making them non-biodegraded.

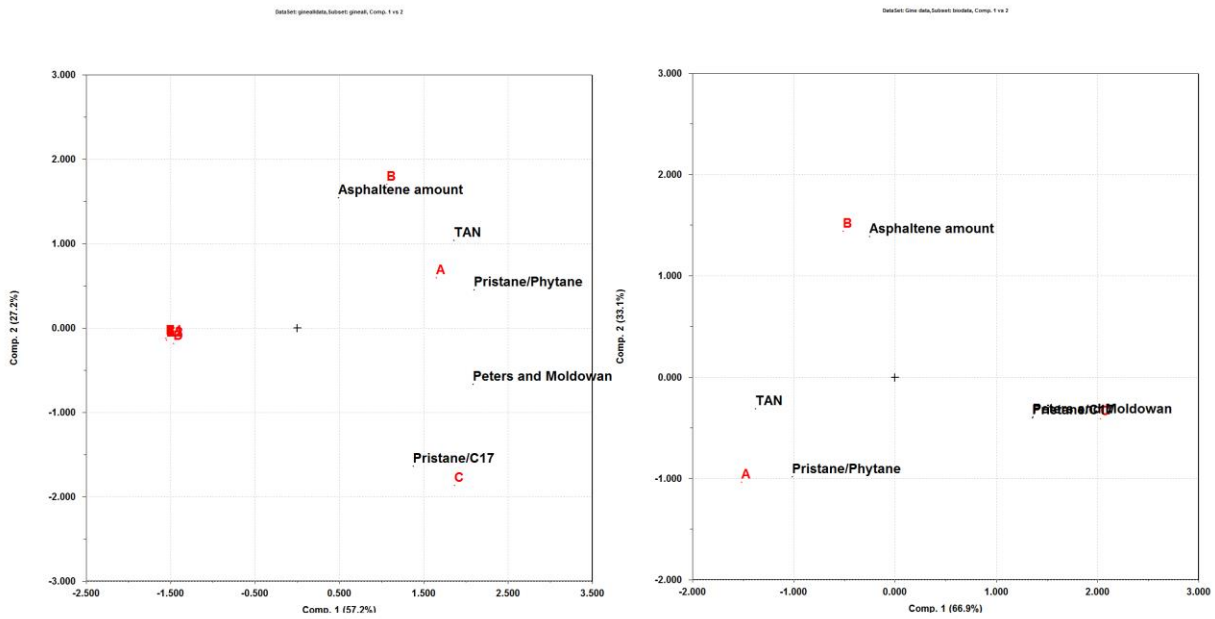

Figure 5.1.1: Bi-plot of measured properties. Left: all the crude oil samples. Right: only the biodegraded samples (A-C) (Sirius, 2004).

The bi-plot in Figure 5.1.1 displays some of the information found in Table 5.1.1 in an easy and straightforward way. On the left hand side, Figure 5.1.1 shows the bi-plot with all six crude oils and the correlation selected properties. The plot on the left clearly shows that crude oils D, E1 and E2 are very similar to each other, since they plot together in the PCA plot. The bi-plot also shows that the samples are negatively correlated to the biodegradation parameters, such as the Peters and Moldovan system and the pristane/phytane ratio. They are not correlated with pristane/C17. All these correlations demonstrate that the samples are non-biodegraded.

When the three non-biodegraded crude oils are removed from the subset, the bi-plot shows the correlation between the more biodegraded samples. On the right hand side of Figure 5.1.1 crude oil C is found to be highly correlated with the biodegradation parameters, supporting that it is the most biodegraded sample.

Previous work done by Barth *et al.* (2004) showed that extracted acids from biodegraded crude oils typically consisted of more carboxylic and aliphatic acids, while the non-biodegraded were found to be more phenolic. As just mentioned the crude oils are divided into two groups by their biodegradation ranking. The first group, consisting of crude oils A, B and C, have similar crude and deasphalted oil FT-IR spectra. These crude oils have a weak band at 1705cm^{-1}, indicating the carbonyl functional group for carboxylic acids. The second group, with the remaining crude oils, do not have this indication. Using the information gathered in the F3 FT-IR spectra, the crude oils can reveal further indications of biodegradation. Crude oils B, C and D have the have the familiar carbonyl stretch at 1705cm^{-1}, for carboxylic acid, while crude oils A, E1 and E2 have their carbonyl stretch at 1726cm^{-1}, indicating aldehyde or esters. In addition, crude oils A, E1 and E2 have a very intense O-H stretch, indicating alcohol functional groups and a band at 1264cm^{-1}, indicating C-O for phenols or esters. These findings further support the information gather by WOGC, where crude oils D, E1 and E2 are found to be non-biodegraded. Based on FT-IR observations alone, crude oil A would be classified as non-biodegraded. This however contradicts the results found in WOGC. This might thus indicate that in addition to being slightly biodegraded, crude oil A might also be immature.

Maturity vs. biodegradation

Crude oils are complex mixtures of chemical species derived from once living organisms and catagenetic products of kerogen maturation. (Oldenburg *et al.*, 2014) In other words, an immature crude oil tends to have higher concentrations of heteroatoms compared to a biodegraded sample, because it has not yet experienced the chemical modifications that it would have undergone during catagenesis. Young and/or shallow crude oils have larger molecules and higher concentrations of heteroatoms. Considering these facts, it might point to crude oil A being more immature than the crude oils B and C, as it is only slightly biodegraded, yet it has a very high TAN. On the other hand, Peters *et al.* (1993) found that the ratio between pristane/phytane generally increased with increasing thermal maturity. This is directly contradictory to the indications pointing to crude oil A being immature, as it has the highest ratio of pristane/phytane ratio of the six crude oils. As mentioned, crude oils are complex molecules, and if crude oil A stems from source rock and/or biomass with high amounts of heteroatoms, it can explain why a mature oil has a high TAN.

As just mentioned, crude oil C is classified to be the most biodegraded sample. However, extensive biodegradation typically increases oil viscosity, increases the density and increases the asphaltene content. With this in mind, looking at Table 5.1.1, crude oil B stands out as the most biodegraded by definition of fluid properties. Nevertheless, these properties may also occur as a result of immaturity. The reason crude oil B is deemed immature and not heavily biodegraded, is because of its chromatogram, which has few indications of being severely biodegraded.

Polar components

The six crude oils can be loosely divided into two groups by looking at their crude and deasphalted oil FT-IR spectra, which are nearly identical. Table 5.1.2 shows that the crude oils A, B and C, have a weak band indicating a carbonyl for carboxylic acids, at 1705cm^{-1}. Crude oils D, E1 and E2, on the other hand, have no indications of this carboxylic functional group in these spectra. However, when looking into their F3 fraction spectra, E1 and E2 have indications of alcoholic and phenolic (or ester) functional groups. Crude oil D on the other hand, has a weak band indicating carboxylic acid in the F3 spectra, which indicates that it has a less carboxylic character than the crude oils in the first group.

The carboxylic functional group found in the crude oil spectra for crude oils A, B and C, does not stem from the asphaltenes, as it also appears in the deasphalted FT-IR spectra. Through a study of acid fractions, Hoeiland *et al.* (2001) emphasized the importance of the acid structures and types present in the fractions compared to the acid concentrations. Even though crude oil acid fractions cannot be directly compared to crude oils, this can indicate that there is a correlation between the molecular structure of the acids and the TAN due to the observation that the TAN values are only detectable in the crude oils which have the carboxylic carbonyl indication in the crude and deasphalted FT-IR spectra. In addition, the results for the TANs shown in Table 4.5.2 support the indication that the TAN is not dependent on the asphaltenes, indicating that the polar acidic components are also found in the maltene fractions.

Table 5.1.2: Summary of functional groups found using the different spectroscopic methods.

Crude Oil	**Type of acidity** crude & deasphalted oil (FTIR)	**Type of polar compound** in maltene F3 (FTIR)	**Type of Acidity** In maltene F3 (NMR)
A	Carboxylic	Phenolic/Ester	Carboxylic/Aliphatic OH
B	Carboxylic	Carboxylic	Carboxylic
C	Carboxylic	Carboxylic	Carboxylic/Aliphatic OH
D	No Indication	Carboxylic	Carboxylic
E1	No Indication	Phenolic/Ester	Carboxylic/Aliphatic OH
E2	No Indication	Phenolic/Ester	Carboxylic

By integration of the peaks found in the F3 fraction ^{31}P NMR spectra, the most abundant functional groups can be detected in each crude oil fraction. In Table 5.1.2 the results show that crude oils A, C and E1 have almost equal amounts of the aliphatic OH compound and the carboxylic compound at 134 ppm. Crude oils B, D and E2 on the other hand, are most abundant in the carboxylic compound found at 134ppm. These findings are in partial agreement with the findings in the F3 FT-IR spectra. The reason for the slight deviation in functional group characterization of the F3 spectra is that the carboxylic and alcoholic O-H and C-O stretch overlaps in FT-IR and is therefore hard to distinguish between the two. In NMR however, a slight change in the chemical environment gives a peak at a different shift and makes it easier to distinguish between the two.

In the F4 NMR spectra, as in the F4 FTIR spectra, the carboxylic compound, found at 135.3 ppm, is the most abundant in all of the samples. It should be noted that the carboxylic compounds found in F3 and F4 are not the same. The carboxylic compound in F4 is shifted slightly more downfield, indicating a different chemical environment then the compound found in F3.

The composition of asphaltenes has been subjected to extensive analysis with varying results (Acevedo, *et al.,* 2005; Barth *et al.,* 2005) because they are defined by solubility and therefore do not have one specific composition. In this sample set, the first analysis revealed that crude oil B has the highest amount of asphaltenes by a factor of four. Through ^{31}P NMR, the integrals of the peaks present in the spectra reveals the most abundant functional groups. Crude oils B, C, E1 and

E2 have asphaltenes with high amounts of aliphatic OH functional groups. The peaks with the highest integral in the spectra of crude oils A and D are carboxylic acid functional groups.

Correlation to physiochemical properties

The analytical data was combined with physiochemical measurements in the monovalent brine solutions and subjected to multivariate analysis. The variables were standardized and decomposed into principal components (PC), which explained 60.6% of the total variation. Graphical representation of the PC's is shown in Figure 5.1.2. The score plot, on the right hand side, shows that the experiments are grouped by which crude oil they originate from, where the red color represents crude oil A, the blue color represents crude oil B and the purple color represents crude oil C. The loading plot, on the left hand side in Figure 5.1.2, shows that out of all the methods used to measure the crude oil properties, the contact angle measurements contain the very little variance (Isaksson *et al.*, 1996). The entire experimental setup and the coding used, is located in the A7-appendix.

Before the chemical composition of the crude oils can be compared and correlated to the different physiochemical properties, it is important to understand that the data-set is not large enough to make any conclusions. However, trends can be observed and give indications of what might be important in future work.

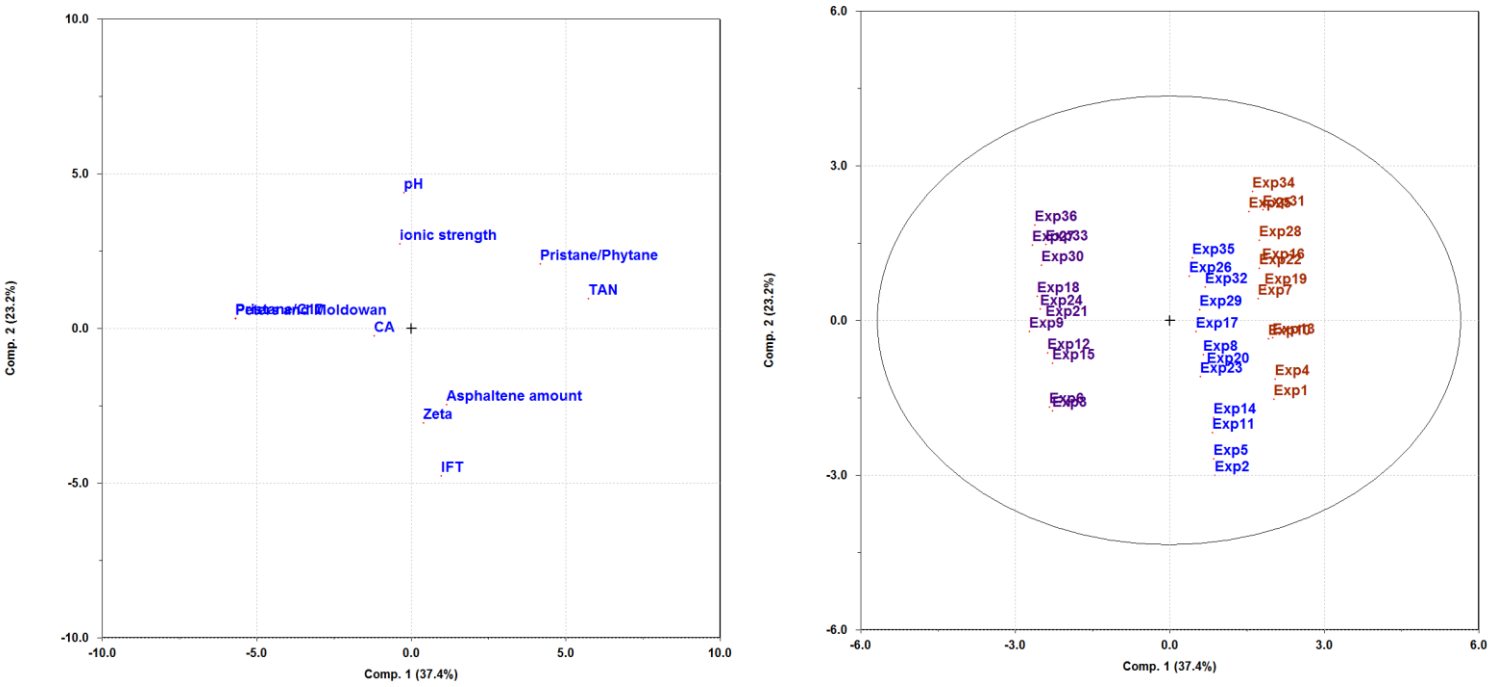

Figure 5.1.2: A loading and score plot of the experiments objects and variables. The red color represents crude oil A, the blue color represents crude oil B and the purple color represents crude oil C in the score plot. The coding of the variables can be found in the A-7appendix (Sirius, 2004).

Asphaltene correlation to physiochemical properties

The loading plot in Figure 5.1.2 shows a strong correlation between the asphaltene amount and the two physiochemical properties measured by Kolltveit, IFT ($r^2 = 0.98$) and zeta potential ($r^2 = 0.97$ respectively). In the bi-plot in Figure 5.1.2, theses correlations are especially evident for the experiments conducted with crude oil B.

The zeta potential, as just mentioned, is highly correlated to the asphaltene amount ($r^2= 0.93$). As the zeta potential is negatively correlated to the pH and the ionic strength, the zeta potentials are most positive at low pH values in brine solutions with low ionic strength, as seen in Table 4.7.1. Wu *et al.* (2014) found that the zeta potential was not only related to the interfacial properties of the droplets, but also highly dependent on the environmental conditions such as ionic strength and pH. By increasing the concentration or the valence of the counterions the double layer was compressed and thus increased the electrical potential.

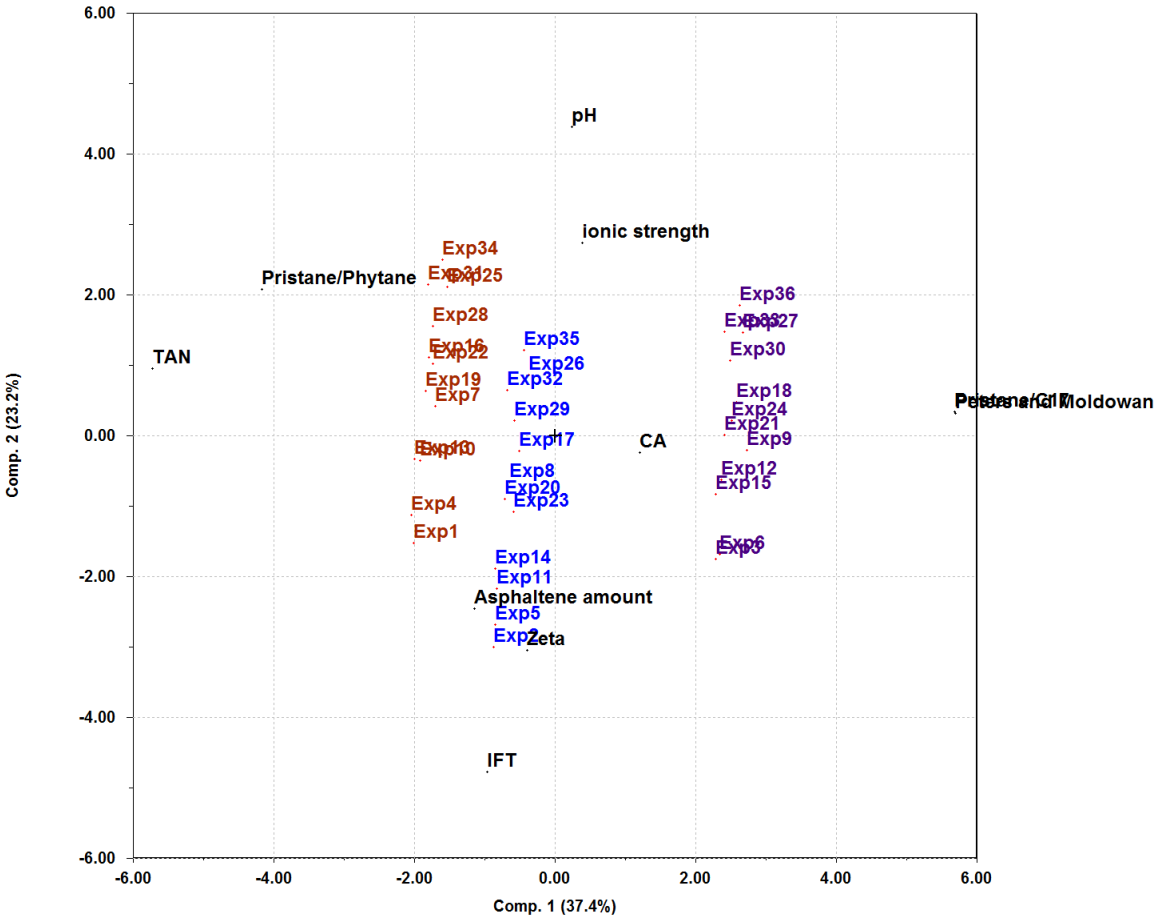

Figure 5.1.3: Bi-plot of all the data collected for NaCl brine solutions (Sirius, 2004).

Barth et al. (2005) found a correlation between the asphaltene content and the basic components present in a crude oil. Even though the author writes that the data is found to be somewhat controversial due to inconsistent data, especially in regards to determining the asphaltene content, these basic components might explain the reason for crude oil B's high positive zeta potential at low pH.

In addition to the zeta potential, the bi-plot in Figure 5.1.3 shows that the IFT is also highly correlated to the asphaltene content ($r^2 = 0.96$). The IFT tension is negatively correlated to pH and ionic strength, indicating an inverse relationship to the two parameters.

Buckley *et al*. (2007) found that heavy crude oils with high amounts of asphaltenes had higher IFT values, where the effect was most evident at pH 6. This trend is supported in Figure 5.1.4, where the red point for pH 6 is found to have the highest IFT, supporting the findings of Buckley et al. (2007). Crude oil B has much higher amounts of asphaltenes than the other crude oils and this is reflected in the significantly higher IFTs.

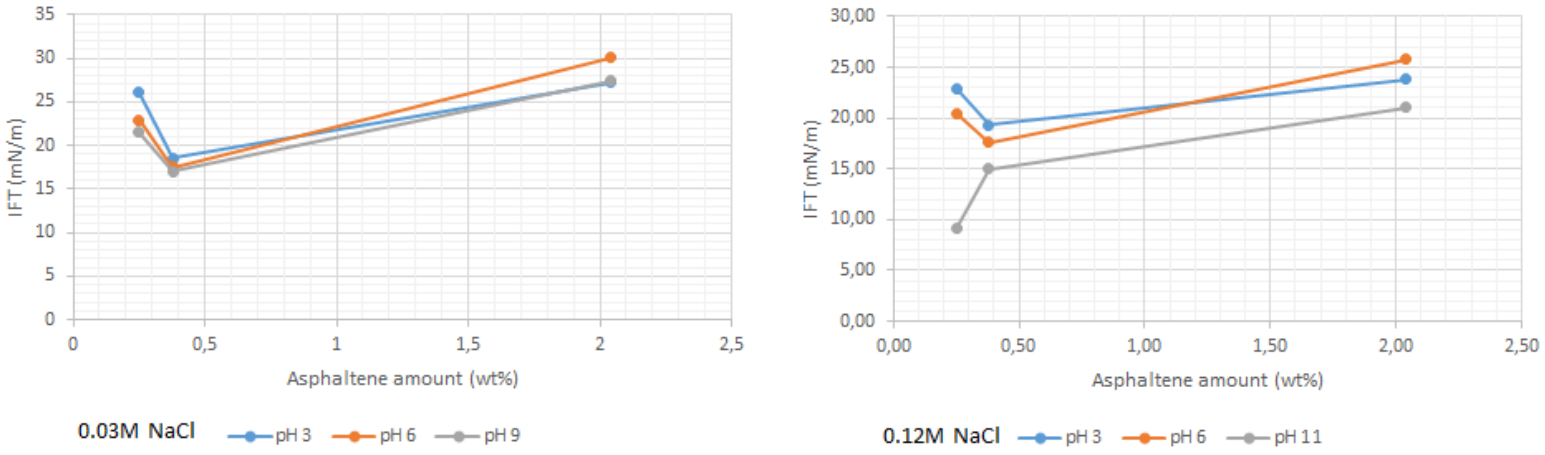

Figure 5.1.4: IFT values plotted against the asphaltene amount for crude oils A, B and C.

An interesting observation is made in Figure 5.1.4, where crude oil C is found to have the lowest IFT values. Lower IFTs indicate more surface active elements present in crude oil C, compared to the other crude oils.

Asphaltenes are amphoteric compounds and the pH is therefore very important in predicting their IFT. At high or low pH their hydrophilic behavior is increased, thus making them more surface active. Poteau *et al.* (2005) found through the study of asphaltene extraction, that increasing the concentration of asphaltenes present in a model crude oil decreased the IFT. Crude oils A and C have low weight percentages of asphaltenes, in the same range as the ones used by Poteau *et al.* They are found to follow the trend of decreasing IFT with increasing asphaltene amount. These indications, in this limited data set, support that at some point an increase in asphaltenes will no longer decrease the IFT, but rather increase the IFT as is the case for crude oil B.

Acidic components correlation to physiochemical properties

Hoeiland *et al.* (2001) found through the study of acid extracts that acid types and especially the acid structures, present in a crude oil was more important than the amount in regards to interfacial tension and contact angle measurements. In addition, the study observed that fractions enriched in alkyl acids, phenols and cyclic acids had a higher impact on the wetting properties compared to fractions with more complicated aromatic ring structures with high degrees of carboxylic compounds, which did not affect the contact angle. Even though the procedures used in Hoeiland *et al.* (2001) and Kolltveit's measurements are different and cannot be compared, the results concluded by Hoeiland *et al.* might indicate possible trends occurring in a crude oil.

The IFT measurements found in Table 4.7.1, show that the dissociation of acids becomes more significant at lower pH-values with increasing concentration of NaCl brine. This can also be seen in the bi-plot in Figure 5.1.3, where ionic strength and pH are highly correlated to each other, yet negatively correlated to IFT and uncorrelated to the TAN. The lack of correlation to the TAN may possibly be due to the difference in types of acidic compounds present in both the asphaltene fraction and the maltene fraction and not the amount as Hoeiland *et al.* also concluded.

The contact angle is found to be strongly negatively correlated to the TAN in the bi-plot in Figure 5.1.3, indicating that the amount of acids found in the crude oils affect these measurements. Acid/base interactions affect the surface charge at both the oil/water and solid/water interface. These ionized sites at the interface will influence the adsorption behavior by which polar components may alter the wettability (Hoeiland, 2001). At higher pH-values the oil/ water is increasingly negatively charged, and thus the repulsive forces between the oil/water and the water/solid interface increases, consequently lowering the contact angles. However, the contact angle data measured by Kolltveit, does not have this trend. In addition, Kolltveit concluded that the procedure used to measure the contact angles was insufficient and therefore the data was also found to be insufficient.

The change in IFT as a function of pH in basic conditions, is found to be independent of the TAN and thus the concentration of the acids in the solution. The reduction in IFT, is therefore a reflection of the interfacial activity of the specific acidic structures present in the solution, as Hoieland *et al.* (2001) concluded.

Acevedo *et al.* (1999) found indications suggesting that relatively low molecular weight and highly aliphatic mixtures of carboxylic acids played an important role in reducing the IFT values under neutral and basic conditions. The acids responsible for alteration of the IFT and the contact angle may be present in both the asphaltene fraction and the maltene fractions. From earlier in the discussion crude oil C was found to have a carboxylic acidic nature in both the crude and deasphalted oil FT-IR spectra. Crude oil A was found to have a mixture of both carboxylic and phenolic functional groups. However, no information regarding the size or structure of the acids is found, but indications of the acidic components in the maltene fraction indicates smaller molecules than at least the structures found in the asphaltene fractions. The conclusion made by Acevedo *et al.* (1999) might thus be used to explain that crude oil C has a lower IFT at neutral and basic conditions due to the difference in acidic composition and the acids ability to adsorb at the interface and pack more tightly together.

Effect of divalent cations on surface active components

The analytical data was combined with physiochemical measurements in monovalent and divalent brine solutions with an ionic strength of 0.03M and subjected to multivariate analysis

The variables were standardized and decomposed into PCs, which explained 65.7% of the total variation. Graphical representation of the PC's is shown in Figure 5.1.5. The score plot, on the right hand side, shows that the experiments are again grouped by which crude oil they originate from, where the same color coordination is used as in Figure 5.1.2. The loading plot, on the left hand side in Figure 5.1.5, shows that out of all the methods used to measure the crude oil properties, the cation object, which in this case means either a solution with only Na^+ cations or a mix with Na^+ and Ca^{2+} ions, contain very little variance.

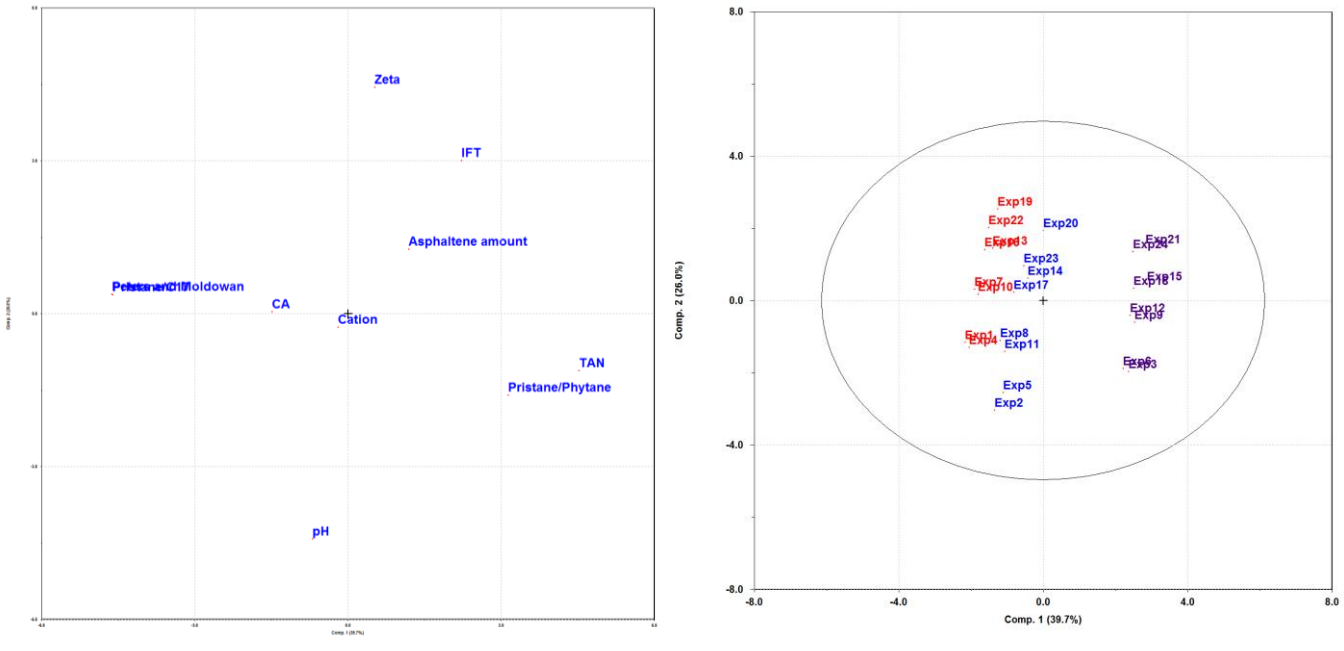

Figure 5.1.5: Loading and score plot of object and variables for the NaCl brine solution and the NaCl with $CaCl_2$ brine solution, with ionic strength of 0.03M. Coding of the variables is given in the A7-appendix (Sirius, 2004).

In the bi-plot in Figure 5.1.6, crude oil B in a pH 3 solution (Exp2) is highly correlated to the IFT and the zeta potential. The IFT is in addition highly correlated to the asphaltene amount, which indicates that the asphaltenes are important in understanding the mechanisms at the interface in crude oil B.

Tichelkamp *et al.* (2015) found that compared to 1:1 ion pairs of naphthenes and sodium ions, 1:2 ion pairs of naphthenes and calcium should show less interfacial activity. In addition, calcium was found to have bridging properties which could therefore increase the rigidity of the interfacial film and further suppress the migration of surface active components to the water phase. All the crude oils have in the divalent cation brine solution indications of this effect. Table 4.7.1 shows that all the IFT values for the basic pH solutions, are measureable and high, especially compared to the IFT values in the monovalent cation brine solutions.

The zeta potential at high pH, as seen in Table 4.7.1, seems to be consistent with the explanation of acidic dissociation at the interface. Where crude oil A, with the highest TAN has the most negative zeta potential, while crude oils B and C, with less TANs have lower negative zeta

potentials. The zeta potential does not seem to be dependent on the asphaltene amounts, which is also supported by the bi-plot in Figure 5.1.6.

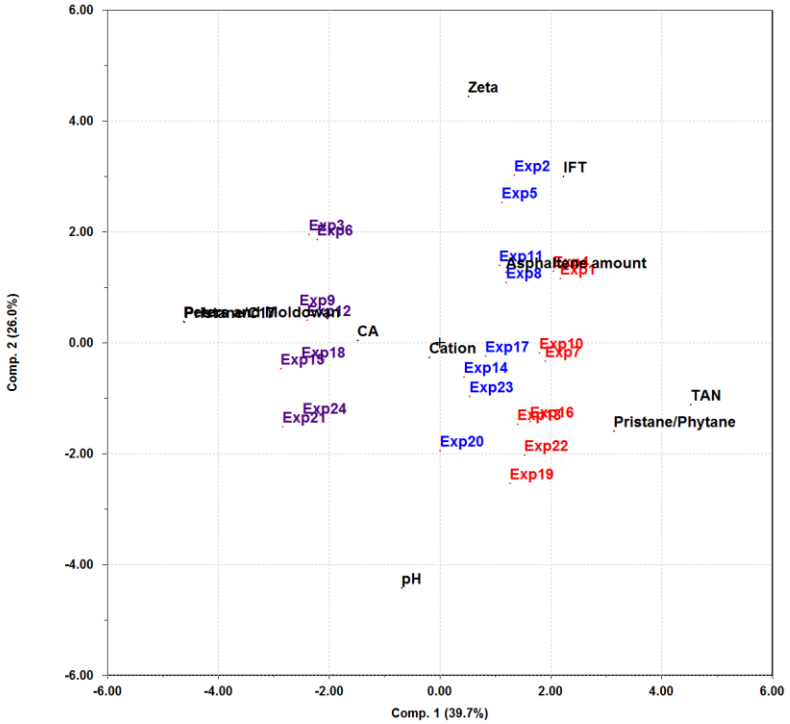

Figure 5.1.6: Bi-plot of the 0.04 mole fraction $CaCl_2$ brine solution (Sirius, 2004).

Source of error

After fractionating the deasphalted oil it is possible to quantify the polar components by electrobalance, but some of the equipment needed was not recovered and therefore it was not possible to find the mass of the fractions.

The idea behind utilizing ^{31}P NMR, is to be able to find more specific information about the polar components present in the crude oils, as well as being able to quantify them. The method used in ^{31}P NMR is developed for bio oils. The biggest difference between bio oils and crude oils is the oxygen content. Bio fuels oxygen content can range from 10-45wt%, while crude oils have usually less than two percent. It is therefore not surprising that the literature has a main focus on the oxygen related functional groups and compounds specific for bio-oils. Either way, the NMR analysis gives valuable information, but further effort to develop the procedure is needed.

Conclusion

Six crude oils have been investigated in regards to chemical composition with special interest in the polar components. WOGC was used to determine biodegradation, where crude oils A, B and C where found to be biodegraded. The results also indicated that crude oil B was of a more immature nature, which was reflected in its high density and viscosity values. Crude oils D, E1 and E2 were found to be non-biodegraded.

Fractionation of the maltene oil the FT-IR and ^{31}P NMR spectra revealed that the crude oils contained different polar functional groups as shown in Table 5.1.2. The FT-IR spectra for the crude and deasphalted oil reveal which samples were found to be highly acidic by the carboxylic carbonyl band at 1705cm^{-1}.

The asphaltene content was found to be highly correlated to both the zeta potential and IFT measurements. The amount of basic components in the asphaltenes, estimated from the asphaltene content, were found to be especially important at low pH-values in the zeta potential measurements. High amounts of basic components resulted in more stable emulsions. In addition, the crude oils with asphaltene amounts lower than 1wt% were found to decrease the IFT with increasing asphaltene amounts. However, indications point to an unknown upper limit, where the increase of asphaltene amounts no longer decreases the IFT but rather increases it.

The TAN was found to be uncorrelated to the zeta potential and IFT indicating the amount of acids was not the determining factor for these properties. Indications point to the chemical composition of the acid as more important.

The divalent cations present in the brine solution caused less surface activity at high pH due to 1:2 ion paring with acidic components and the divalent cation.

Suggestions for further work

The work presented in this thesis shows that the asphaltenes, acidic content and composition are highly correlated to the measured physiochemical properties. However, more detailed information on the chemical composition of both the asphaltene fraction and acidic compounds is needed to draw clear conclusions about their effect on physiochemical properties. Specific suggestions for further work is listed below.

More extensive data set

Due to the small data set, conclusive results are difficult to obtain. The set should be expanded to include many samples of varying degree of maturity and biodegradation. This may provide more accurate indications and conclusions regarding the importance of specific polar components in relation to the physical properties.

Develop the ^{31}P NMR method for crude oils

Standards of polar components found in the crude oil should be analyzed, thus increasing the structural information gained by ^{31}P NMR. In addition, the standards should not be limited to only oxygen containing compounds but also standards with nitrogen and sulfur.

LC-MS

By utilizing LC-MS, specific compositional information can be found. This is especially important for the acidic components present in the maltene oil fraction. In addition, more structural information in a larger data set can help give more specific conclusions.

Acid Extraction

By acid extraction, more detailed information regarding the structures and amount can be obtained. The additional information could help explain the physiochemical properties more precisely.

TBN

The total base number of the crude oils could be valuable information in regards to low pH brine solutions.

Multivariate Analysis of spectral data

The raw data collected by FT-IR and WOGC could be further analyzed by multivariate analysis, giving better peak predicting abilities and peak importance. In addition, the samples could be more easily compared.

Literature

Acevedo, S.; Borges, B.; Quintero, F.; Gutierrez, L.B. (2005) Asphaltenes and other natural surfactants from Cerro Negro crude oil. Stepwise adsorption at the water/toluene interface: Film formation and hydrophobic effects. *Energy & Fuels*. 19(5), 1948-1953.

Acevedo, S; Escobar, G.; Ranaudo, M.A.; Khazen, J.; Borges, B.; Pereira, J.C; Mendez, B. (1999) Isolation and characterization of low and high molecular weight acidic compounds from Cerro Negro extra heavy crude oil. Role of these acids in the interfacial properties of the crude oil emulsions. *Energy & Fuels.* 13(2), 333-335.

Argyropoulos, D. (1995) ^{31}P NMR in wood chemistry: A review of recent progress. *Research on Chemical Intermediates*, 21(3), 373-397.

Auflem, I.; Havre, T.; Sjøblom, J. (2002) Near-IR study on the dispersive effects of amphiphiles and naphthenic acids on asphaltenes in model heptane-toluene mixtures. *Colloid and Polymer Science*, 280(8), 695-700.

Barth, T; Høiland, S.; Fotland, P.; Askvik, K. M.; Myklebust, R.; Erstad, K. (2005) Relationship between the content of asphaltenes and bases in some crude oils. *Energy & Fuels.* 19(4), 1624-1630.

Barth, T; Høiland, S.; Fotland, P.; Askvik, K. M.; Pedersen, B. S.; Borgund, A. E. (2004) Acidic compounds in biodegraded petroleum. *Organic Geochemistry*. 35(11), 1513-1525.

Ben, H.; Ferrell, I.; Jack, R. (2016) In-depth investigation on quantitative characterization of pyrolysis oil by ^{31}P NMR. *RSC Advances*. 6(21), 17567-17573.

Berg, J. C. (2010) *An Introduction to Interfaces and Colloids. The Bridge to Nanoscience.* Hackensack, NJ: World Scientific.

Borgund, A. E.; Erstad, K.; Barth, T. (2007) Normal phase high performance liquid chromatography for fractionation of organic acid mixtures extracted from crude oils. *Journal of Chromatography.* 1149(2), 189-196.

Clemente, J. S.; Fedorak, P. M. (2005) A review of the occurrence, analysis, toxicity and biodegradation of naphthenic acids. *Chemosphere.* 60(5), 585-600.

Durig, J. R. (1990) *Applications of FTIR spectroscopy.* Amsterdam: Elsevier.

Farooq, U.; Simon, S.; Tweheyo, M.; Sjöblom, J.; Øye, G (2013) Interfacial Tension Measurements Between Oil Fractions of a Crude Oil and Aqueous Solutions with Different Ionic Composition and pH. *Journal of Dispersion Science and Technology*. 34(5), 701-708.

Farooq, U.; Simon, S.; Tweheyo, M.; Sjöblom, J.; Øye, G. (2013) Electrophoretic Measurements of Crude Oil Fractions Dispersed in Aqueous Solutions of Different Ionic Compositions—Evaluation of the Interfacial Charging Mechanisms. *Journal of Dispersion Science and Technology*. 34(10), 1376-1381.

Friebolin, H. (2011) *Basic one- and two dimensional NMR spectroscopy.* 5th ed. Weinheim: Wiley.

Gough, M. A.; Rowland, S. J. (1990) Characterization of unresolved complex mixtures of hydrocarbons in petroleum. *Nature*. 344(6267), 648-650.

Grung, B. (1996) Det matematiske grunnlaget for latent variable-metoder. *Anvendelse av kjemometri innen forskning og industri.* Bergen: Tidsskriftforlaget Kjemi AS. 121-128.

Harris, D.C. (2010) *Quantitative chemical analysis*. 8th ed. New York: Freeman.

Hoeiland, S.; Barth, T.; Blokhus, A.M.; Skauge, A. (2001) The effect of crude oil acid fractions on wettability as studied by interfacial tension and contact angles. *Journal of Petroleum Science and Engineering.* 30(2), 91-103.

Isaksson, T; Næs, T. (1996) Prinsipal komponent analyse. *Anvendelse av kjemometri innen forskning og industri.* Bergen: Tidsskriftforlaget Kjemi AS. 145-151.

Jasiukaityte, K.; Kunaver, M.; Crestini, C. (2010) Lignin behavior during wood liquefaction – Characterization by quantitative ^{31}P, ^{13}C NMR and size-exclusion chromatography. *Catalysis Today*. 156(1), 23-30.

Karstang, T.V. (1996) Forbehandling av data. *Anvendelse av kjemometri innen forskning og industri.* Bergen: Tidsskriftforlaget Kjemi AS. 129-144.

Kolltveit, Y. (2016) Relationship between crude oil composition and physical-chemical properties. MsC thesis. University of Bergen.

Larter, S. R.; Huang, H.; Adams, J.; Bennett, B.; Jokanola, O.; Oldenburg, T.; Fowler, M. (2006) The controls on the composition of biodegraded oils in the deep subsurface; Part II - Geological controls on subsurface biodegradation fluxes and constraints on reservoir-fluid property prediction. *AAPG Bulletin*. 90(6), 921-938.

Laugerud, G. (2015) NMR-analyse av LtL-oljar med fokus på kvantitative ^{31}P-NMR for analyse av hydroksylgrupper. MsC thesis. University of Bergen.

McKenna, A.M.; Purcell, J.M; Rodgers, R.P.; Marshall, A.G (2010) 1. Exhaustive compositional analysis of Athabasca bitumen HVGO distillates by Fourier Transform Ion Cyclotron Resonance Mass Spectroscopy: A definitive test of the Boduszynski Model. *Energy & Fuels.* 24(5), 2929-2938.

Melone, F.; Saladino, R.; Lange, H.; Crestini, C. (2013) Tannin structural elucidation and quantitative ^{31}P NMR analysis. 1. Model compounds. *Journal of agricultural and food chemistry*. 61(39), 9307-9315.

Meredith, W.; Kelland, S. J.; Jones, D. M. (2000) Influences of biodegradation on crude oil acidity and carboxylic acid composition. *Organic Geochemistry*. 31(11), 1059-1073.

Metrohm. *Tiamo.* Viewed 22.02.2016. Retrieved from: http://tiamo.metrohm.com/support/tiamo1_3.html?identifier=81010033&language=en&name=81010033

Miller, J. M. (2009) *Chromatography: Concepts and Contrasts*. 2nd ed. Hoboken, NJ: Wiley.

Mitchell, D. L.; Speight, J. G. (1973) The solubility of asphaltenes in hydrocarbon solvents. *Fuel*. 52(2), 149-152.

Negash, T. (2004) Distribution of petroleum acids in crude oils and distillate fractions. MsC Thesis. University of Bergen.

Norwegian Petroleum Directorate (2009) Water-flooding. Viewed 10.05.2016. Retrieved from: http://www.npd.no/en/Topics/Improved-Recovery/Temaartikler/Why-do-we-not-recover-100-per-cent-of-the-oil/

Oldenburg, T.B.P; Brown, M.; Bennet, B.; Larter, S.R. (2014) The impact of thermal maturity level on the compositions of crude oils, assessed using ultra-high resolution mass spectrometry. *Organic Geochemistry*. 75(1), 151-168.

Paukku, A. N.; Posadov, I. A.; Rozental, D. A.; Sirotinkin, N. V.; Kornilova, L. A. (1981) Study of the chemical composition of polar components of asphaltene-resin compounds of petroleum. *Petroleum Chemistry.* 21(3), 150-155.

Pavia, D. L. (2009) *Introduction to Spectroscopy.* 4th ed. Belmont, California: Brooks/Cole.

PerkinElmer (2016) ATR-FTIR. Viewed 14.03.2016. Retrieved from: http://chemists.princeton.edu/bernasek/atr-ftir

Peters, K. E.; Moldowan, J. M. (1991) Effects of source, thermal maturity and biodegradation on the distribution and isomerization of homophones in petroleum. *Organic Geochemistry*.17(1), 47-61.

Peters, K. E.; Moldowan, J. M. (1993) *The Biomarker Guide: Interpreting Molecular Fossils in Petroleum and Ancient Sediments.* Englewood Cliffs, N.J: Prentice Hall.

Poteau, S, Argillier, J.; Langevin, D.; Pincet, F.; Perez, E. (2005) Influence of pH on stability and dynamic properties of asphaltenes and other amphiphilic molecules at the oil-water interface. *Energy Fuels.* 19(4), 1337-1341.

Pu, Y., Cao, S., Ragauskas, A. (2011) Application of quantitative ^{31}P NMR in biomass lignin and biofuel precursors characterization. *Energy & Environ. Sci.* 4(9), 3154-3166.

Schobert, H. (2013) *Chemistry of Fossil Fuels.* Cambridge: Cambridge University Press.

Seifert, W. K., Howells, W. G. (1969) Interracially active acids in a California crude oil. Isolation of carboxylic acids and phenols. *Analytical Chemistry*. 41(4), 554-562.

Sheng, J. (2010) *Modern Chemical Enhanced Oil Recovery; Theory and Practice.* Burlington: Elsevier Science.

Sigma Aldrich. (1998) Guide to Solid Phase Extraction. *Supleco.*

Silverstein, R. M. (2005) *Spectrometric Identification of Organic Compounds.* 7th ed. New York: Wiley.

Simposon, N. (2000). *Solid-Phase Extraction. Principles, techniques and applications.* New York: Marcel Dekker.

SIRIUS™, Pattern Recognition System AS (PRS AS), (2004) Version 10.0 Retrieved from: http://www.prs.no/Sirius/Sirius.html

Speight, J. G. (2006) *Chemistry and Technology of Petroleum*. 4th ed. Hoboken: Taylor and Francis.

Standal, S., Haavik, J., Blokhus, A. M., Skauge, A. (1999) Effect of polar organic components on wettability as studied by adsorption and contact angles. *Journal of Petroleum Science and Engineering.* 24(2), 131-144.

Thermo Scientific. Chromeleon 7.2 Chromatography Data System. Viewed 01.04.2016. Retrieved from: http://www.dionex.com/en-us/products/chromatography-software/chromeleon72/lp-73027.html

Tichelkamp, T; Teigen, E.; Nourani, M.; Øye, G. (2015) Systematic study of the effect of electrolyte composition on interfacial tensions between surfactant solutions and crude oils. *Chemical Engineering Science.* 132(1), 244-249.

Tomren, A. L., Barth, T. (2014) Comparison of partial least square calibration models of viscosity, acid number and asphaltene content in petroleum, based on GC and IR data. *Fuel*. 120(3), 8-21.

UC San Diego (2012) Oil Window. Viewed 10.05.2016. Retrieved from: http://quakeinfo.ucsd.edu/~gabi/sio15/topics/supps/oilwindow.jpg

University of Maine, (2002), *Magnetic Moments for Spin 1/2*. Viewed 14.04.2016. Retrieved from: http://chemistry.umeche.maine.edu/CHY431/NMR/NMR-3.html

Varadaraj, R.; Brons, C. (2006) Molecular origins of heavy crude oil interfacial activity part 2: Fundamental interfacial properties of model naphthenic acids and naphthenic acids separated from heavy crude oils. *Energy & Fuels*. 21(1), 199-204.

Wang, Z., Stout, S., Fingas, M. (2006) Forensic fingerprint of biomarkers for oil spill characterization and source identification. *Environmental Forensics.* 7(2), 105-146.

Weiss, H. M.; Mills, N.; Scotchmer, J.; Hall, P. B.; Lind, K.; Brekke, T. (2000) NIGOGA – The Norwegian Industry Guide to Organic Geochemical Analysis.

Wenger, L.; Davis, C.; Isaksen, G. (2002) Multiple controls on petroleum biodegradation and impact on oil quality. *SPE Reservoir Evaluation & Engineering.* 5(5), 375-383.

Wroblewski, A. E.; Lensink, C.; Markuszewaki, R.; Verkade, J. G (1988) Phosphorus-31 NMR spectroscopic analysis of coal pyrolysis condensates and extracts for heteroatom functionalities possessing labile hydrogen. *Energy & Fuels.* 2(6), 765-774.

Wu, Y.; Li, Q.; Deng, F.; Liang, X.; Liu, H. (2014) Solvent effect on zeta potential at an aqueous/oil interface in surfactant-free emulsion. *Langmuir.* 30(8), 1926-1931.

Appendix
A1 - WOGC

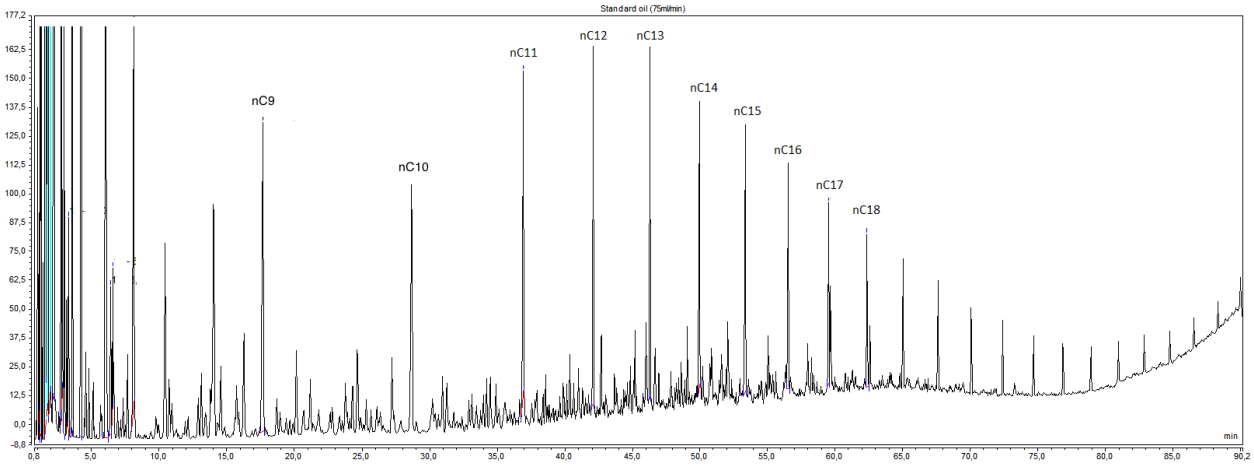

Figure A1-1: Norwegian Standard Oil

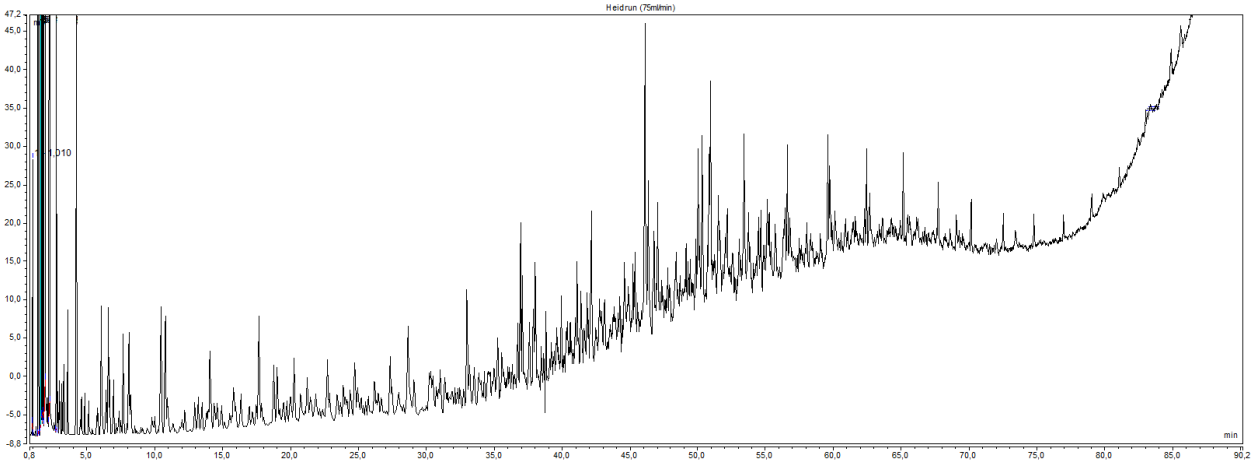

Figure A1-2: Crude oil A

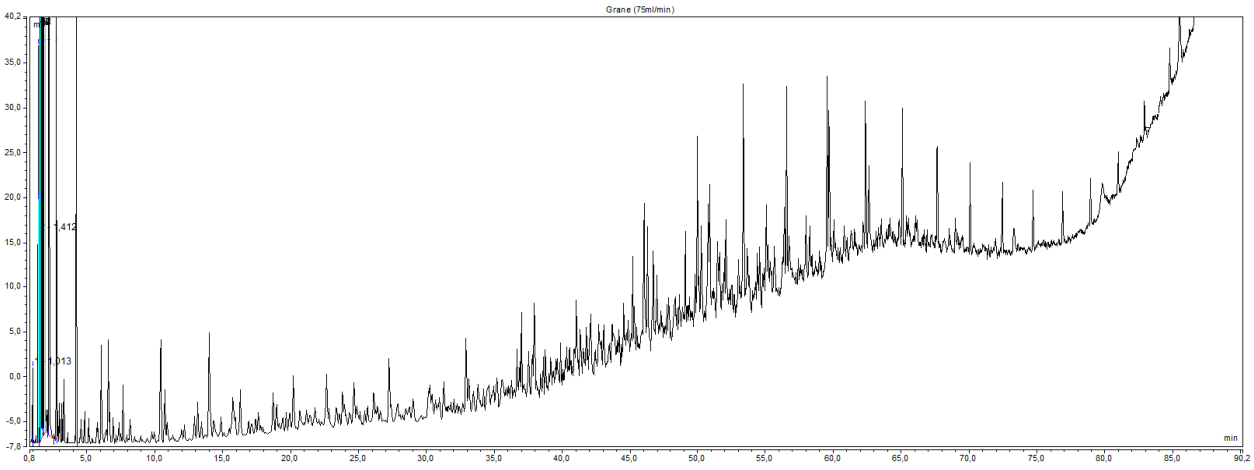

Figure A1-3: Crude oil B

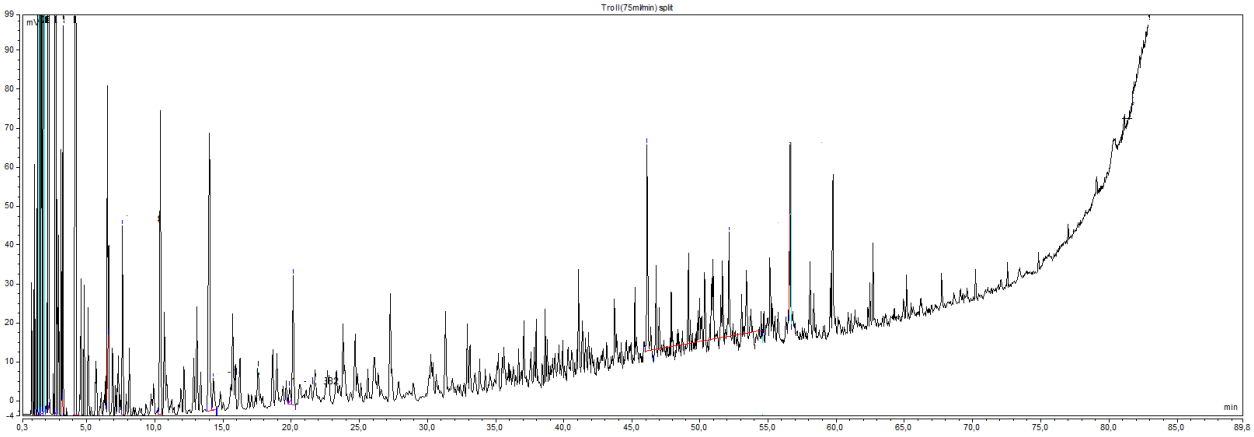

Figure A1-4: Crude oil C

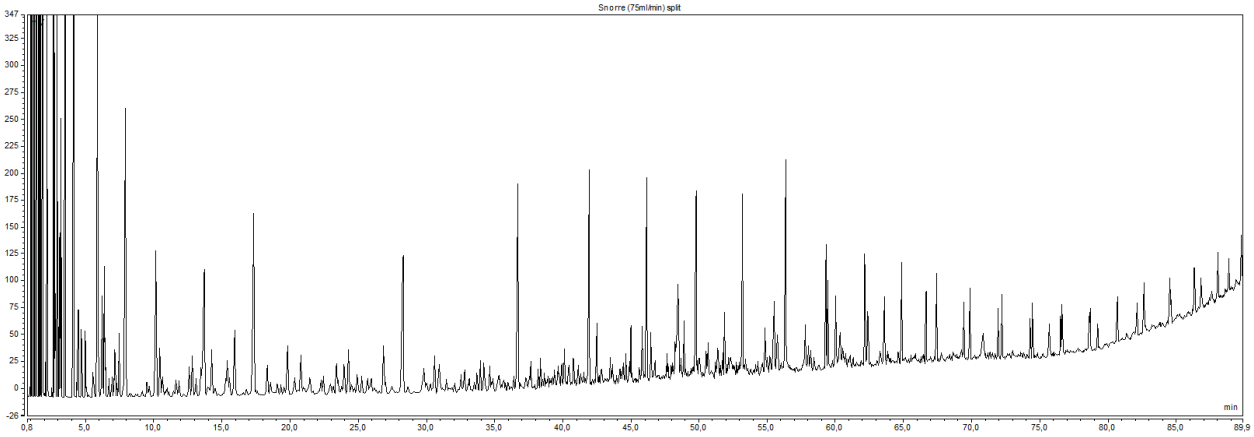

Figure A1-5: Crude oil D

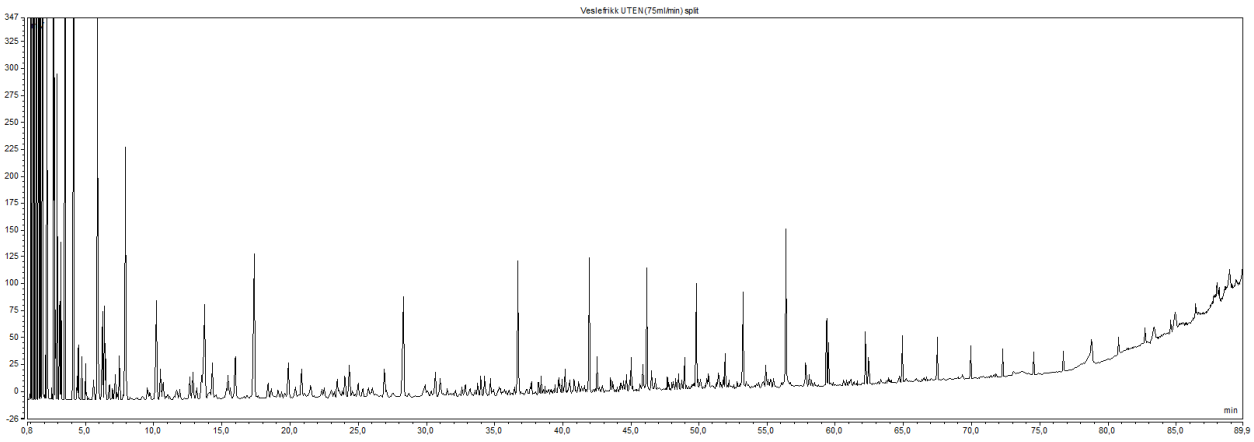

Figure A1-6: Crude oil E1

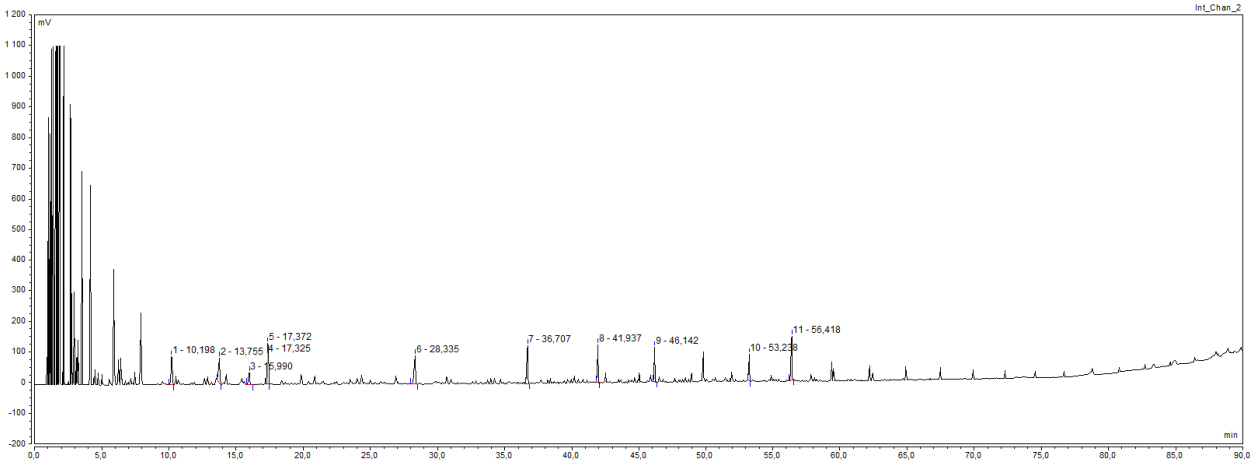

Figure A1-6: Crude oil E2

A2- Determination of asphaltenes

Table A2-1: Results from deasphalting the different crude oils

Crude oil	10mL crude oil (g)	Asphaltene (g)	Average asphaltene weight	Wt%	SD (Asphaltenes)	%RSD (Asphaltenes)
Crude oil A	9.02	0.023	-	0.25	-	-
Crude oil B	9.06 9.08 9.06	0.182 0.190 0.183	0.185	2.04	0.004	1.92
Crude oil C	8.90 8.75	0.035 0.033	0.034	0.38	0.001	2.94
Crude oil D	7.85 7.86 7.86	0.030 0.036 0.033	0.033	0.43	0.002	7.42
Crude oil E1	8.20	0.040	-	0.48	-	-
Crude oil E2	8.05	0.035	-	0.43	-	-

A3 – TAN Calculations

Figure A3-1: Crude oil A

Exp	m_{oil}	$V_{KOH,EP}$	V_B	TAN
1	4.15	5.12	0.56	3.02
2	3.20	4.06	0.56	3.00
3	4.98	6.10	0.56	3.06
4	2.09	2.80	0.56	2.95
5	5.48	6.60	0.56	3.03
		Average TAN = 3.01 ± 0.04		

Figure A3-2: Crude oil B

Exp	m_{oil}	$V_{KOH,EP}$	V_B	TAN
1	10.8	8.97	0.58	2.14
2	5.55	4.78	0.58	2.08
3	2.06	2.00	0.58	1.90
4	7.72	6.51	0.58	2.11
5	3.52	3.09	0.58	1.96
		Average TAN = 2.0 ± 0.1		

Figure A3-3: Crude oil C

Exp	m_{oil}	$V_{KOH,EP}$	V_B	TAN
1	10.57	4.18	0.58	0.94
2	14.58	5.65	0.58	0.96
3	12.56	5.30	0.58	1.03
		Average TAN = 0.98 ± 0.05		

Figure A3-4: Deasphalted crude oil A

Exp	m_{oil}	$V_{KOH,EP}$	V_B	TAN
1	2.17	2.99	0.50	3.15
2	1.70	2.42	0.50	3.11
3	2.02	2.80	0.50	3.13
		Average TAN = 3.13 $\pm$0.02		

Figure A3-5: Deasphalted crude oil B

Exp	m_{oil}	$V_{KOH,EP}$	V_B	TAN
1	2.65	2.22	0.50	1.78
2	4.01	3.24	0.50	1.88
3	4.03	3.25	0.50	1.88
4	2.15	1.83	0.50	1.70
5	1.84	1.63	0.50	1.69
		Average TAN = 1.79 $\pm$0.09		

Figure A3-6: Deasphalted crude oil C

Exp	m_{oil}	$V_{KOH,EP}$	V_B	TAN
1	2.99	1.40	0.42	0.90
2	4.47	2.02	0.42	0.98
3	3.74	1.72	0.42	0.96
		Average TAN = 0.95$\pm$0.04		

A4 – TAN titration curves

Figure A4-1: Crude oil A

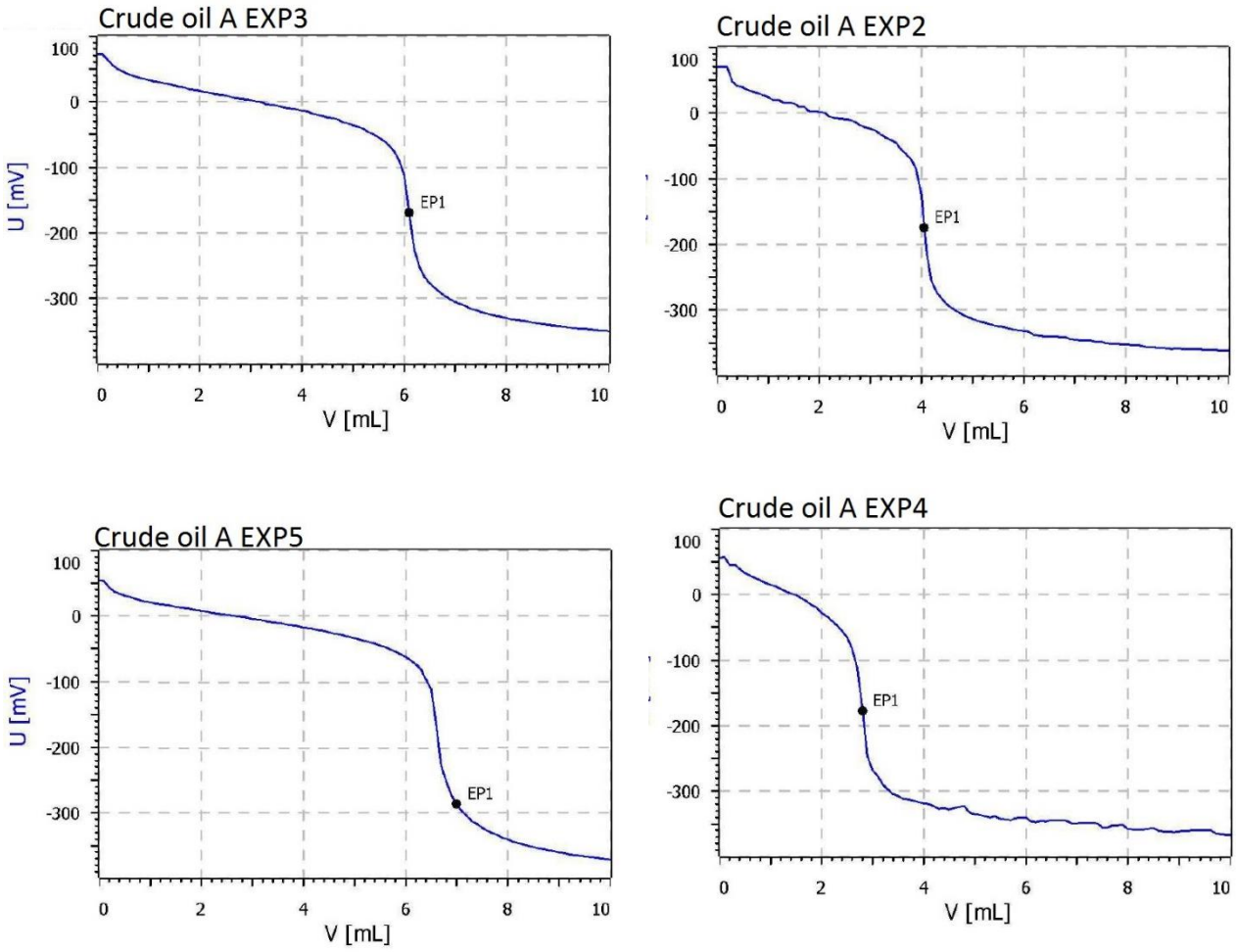

Figure A4-2: Crude oil **B**

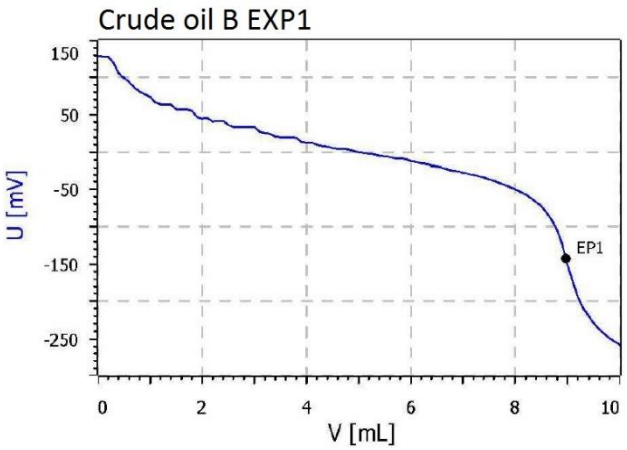

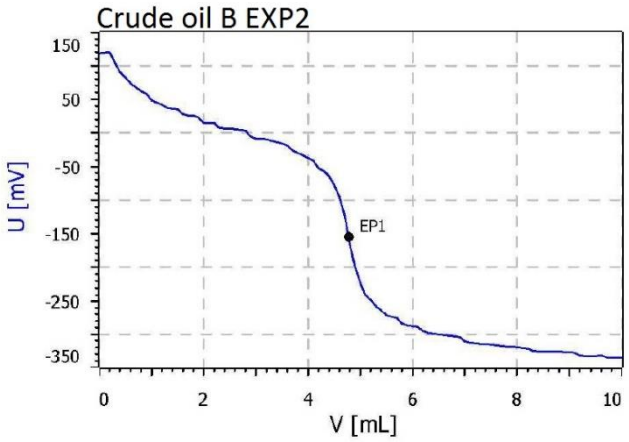

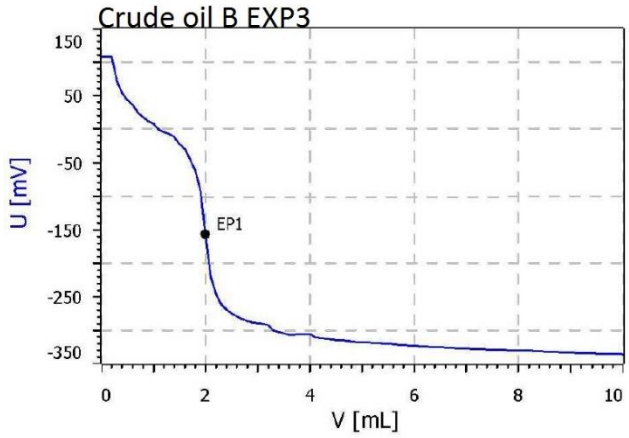

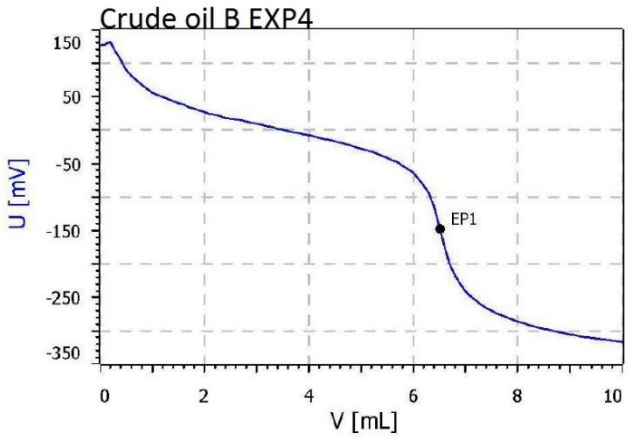

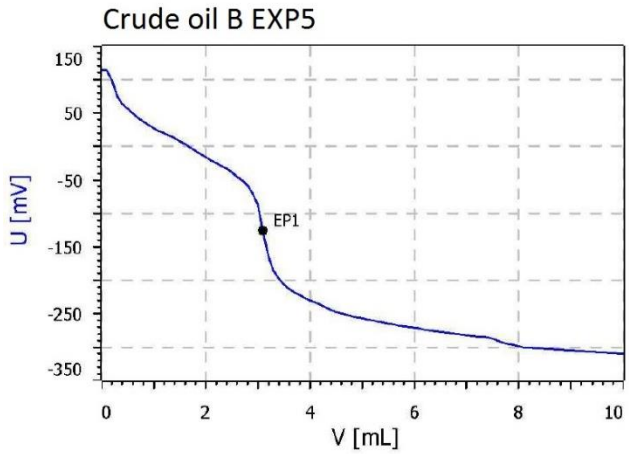

Figure A4-3: Crude oil C

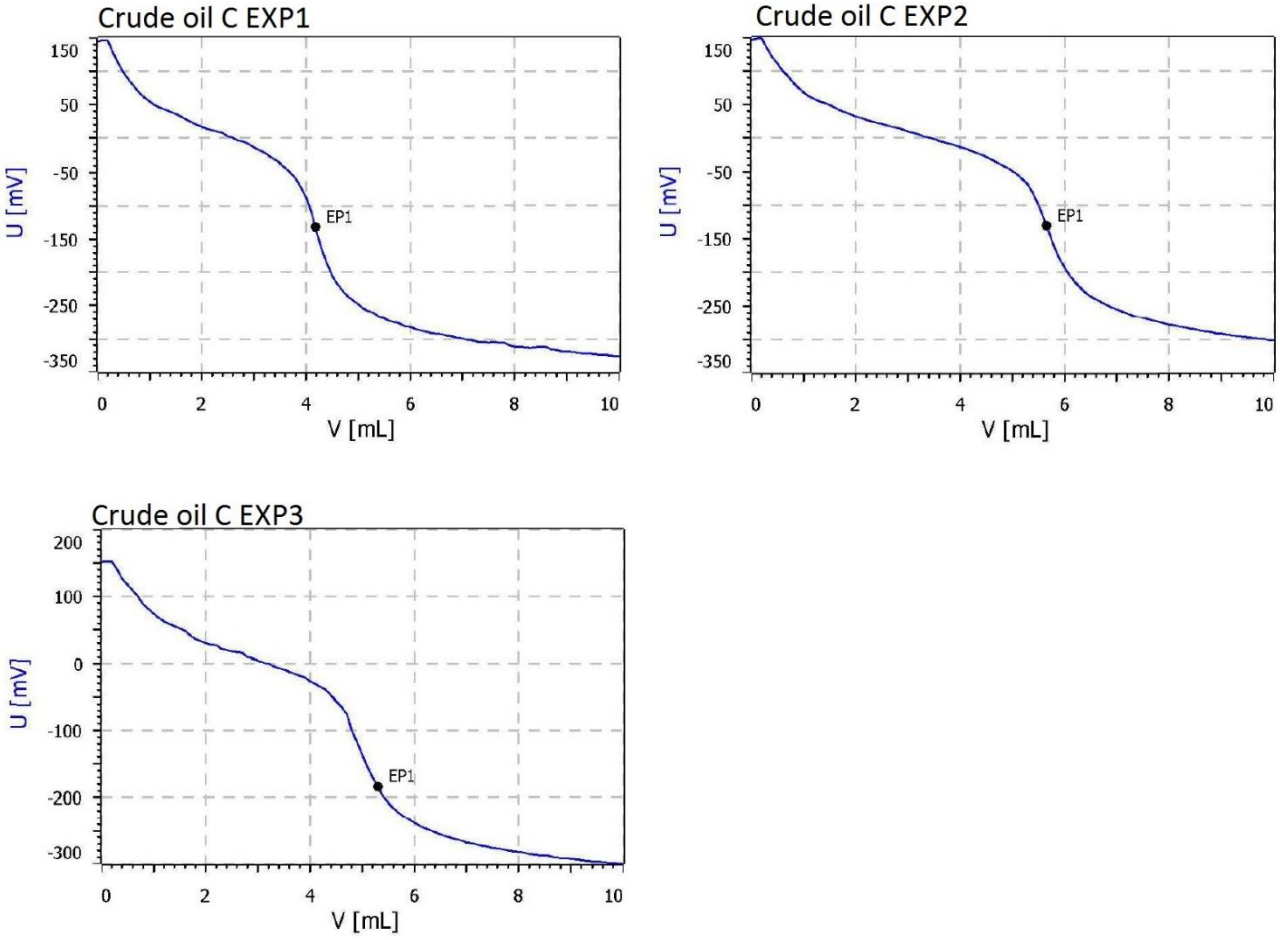

Figure A4-4: Deasphalted crude oil A

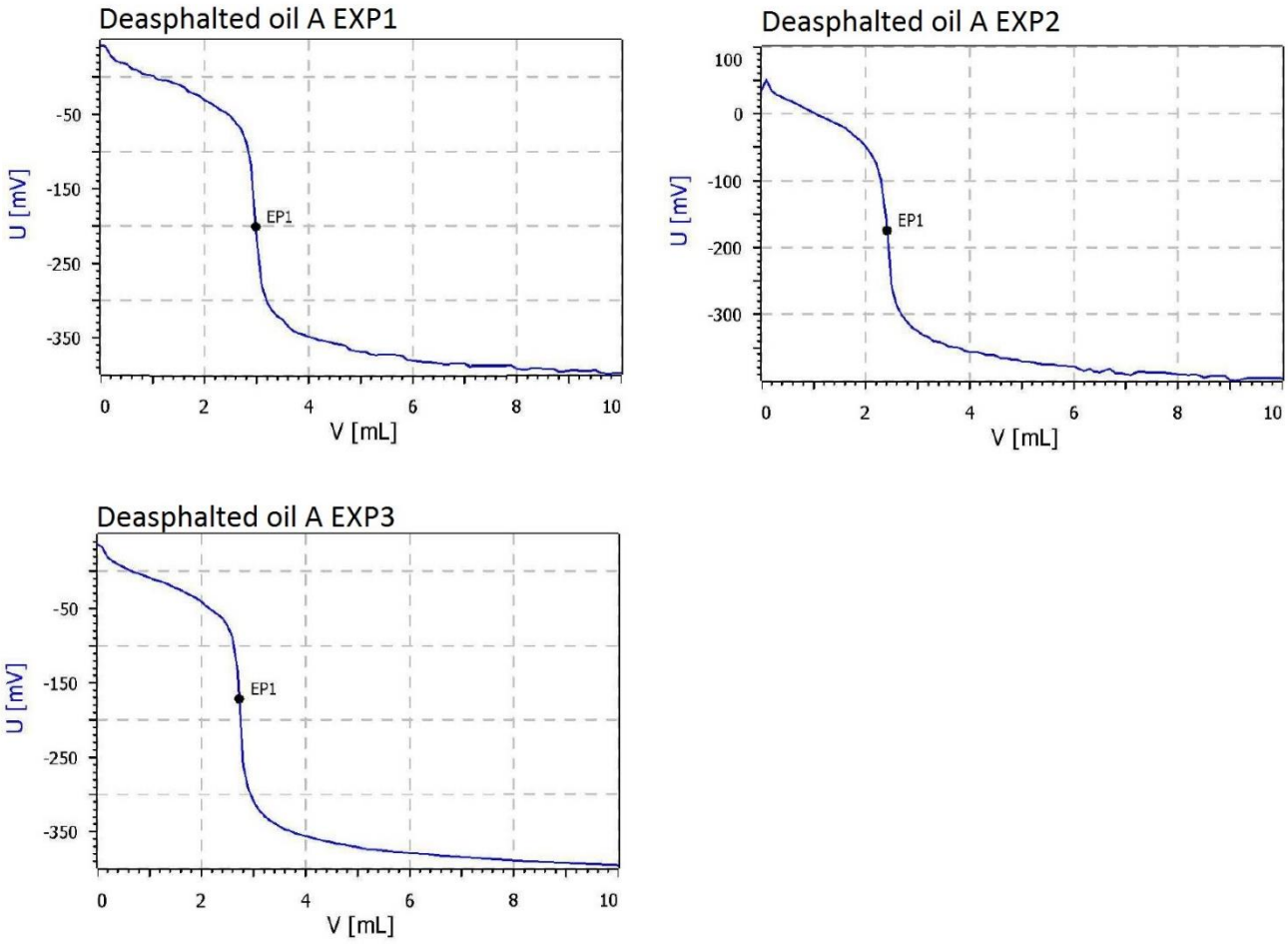

Figure A4-5: Deasphalted crude oil B

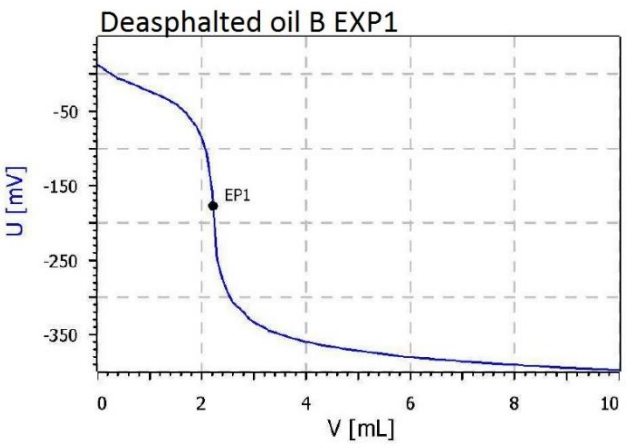

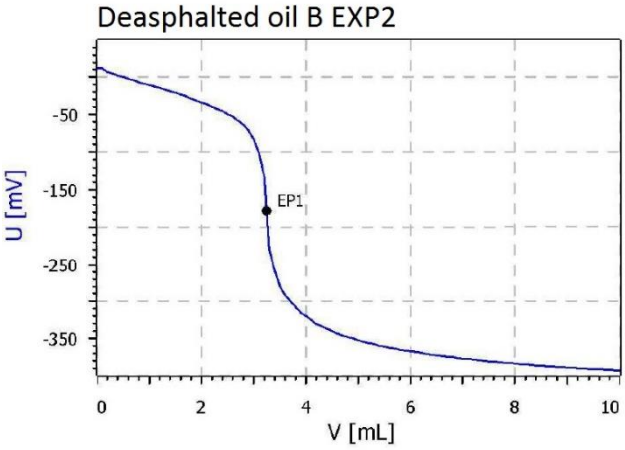

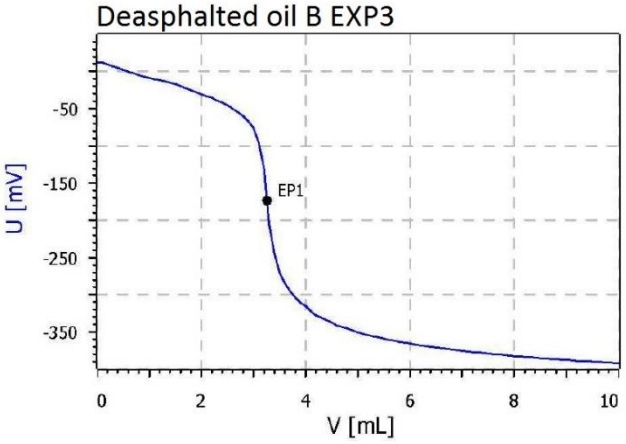

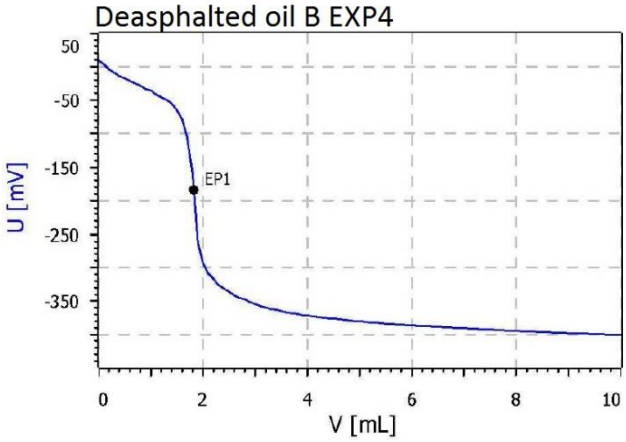

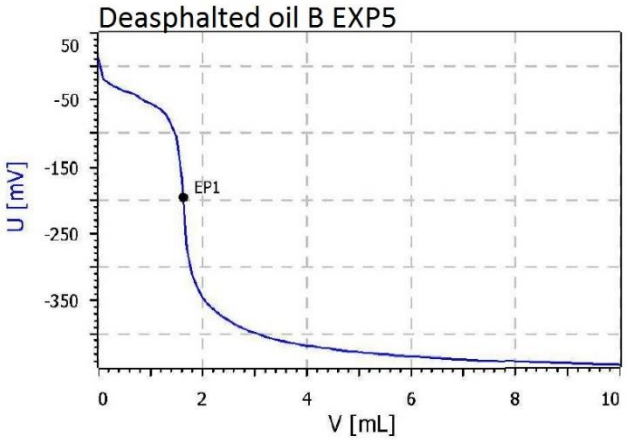

Figure A4-6: Deasphalted crude oil **C**

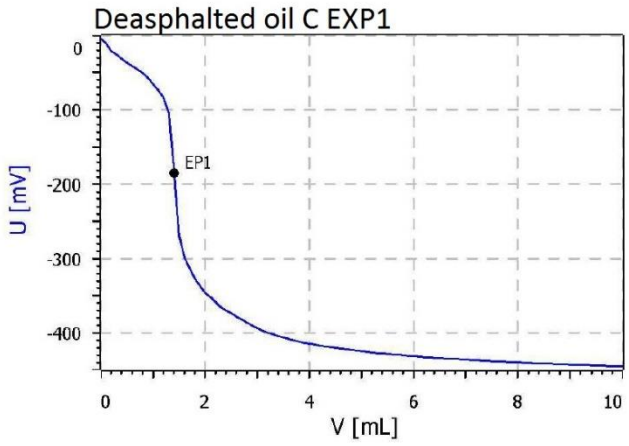

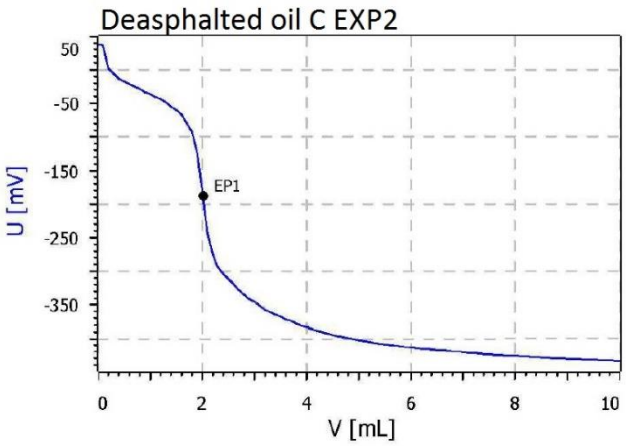

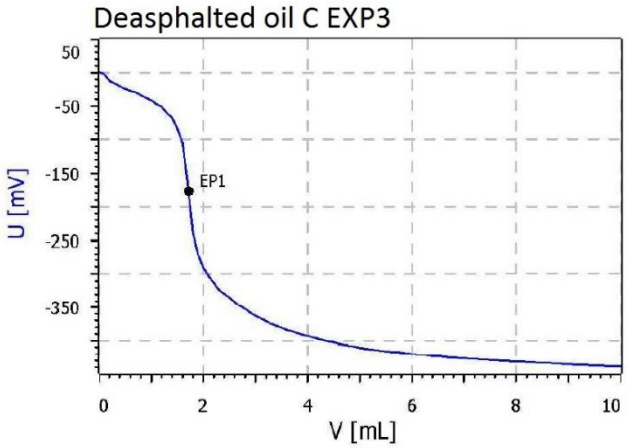

A5 FT-IR Spectra

Crude oil

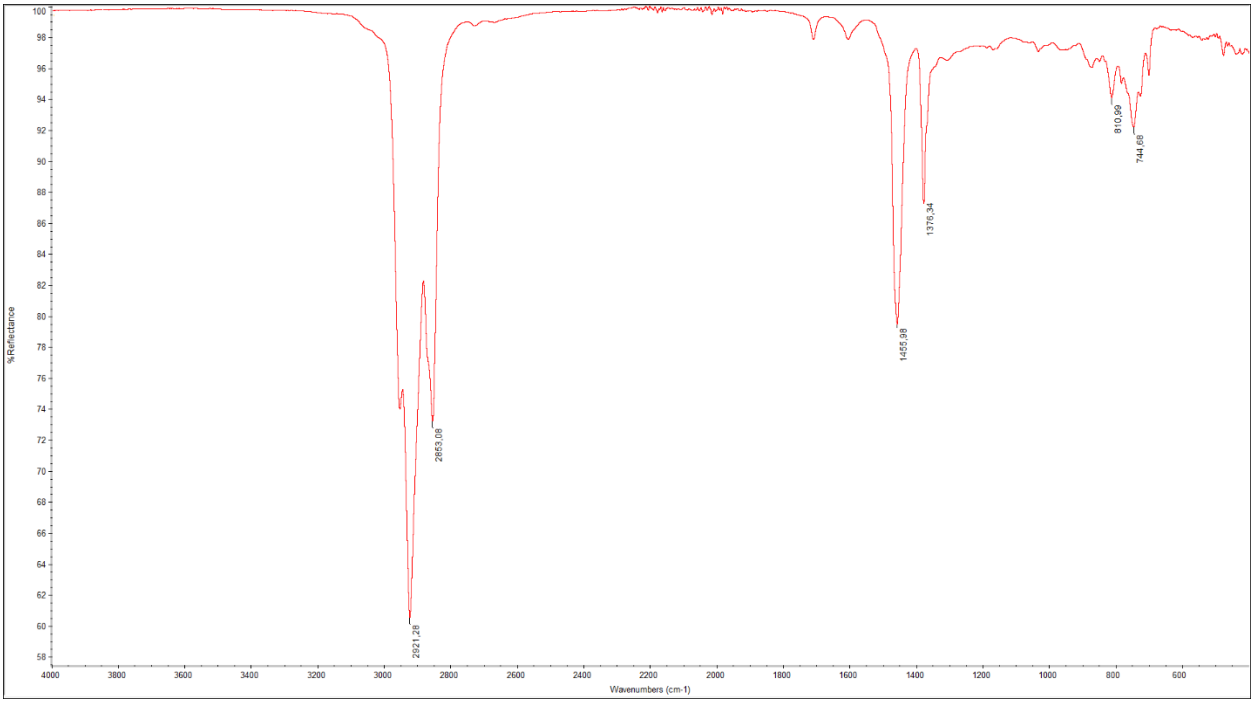

Figure A5-1: Crude oil A.

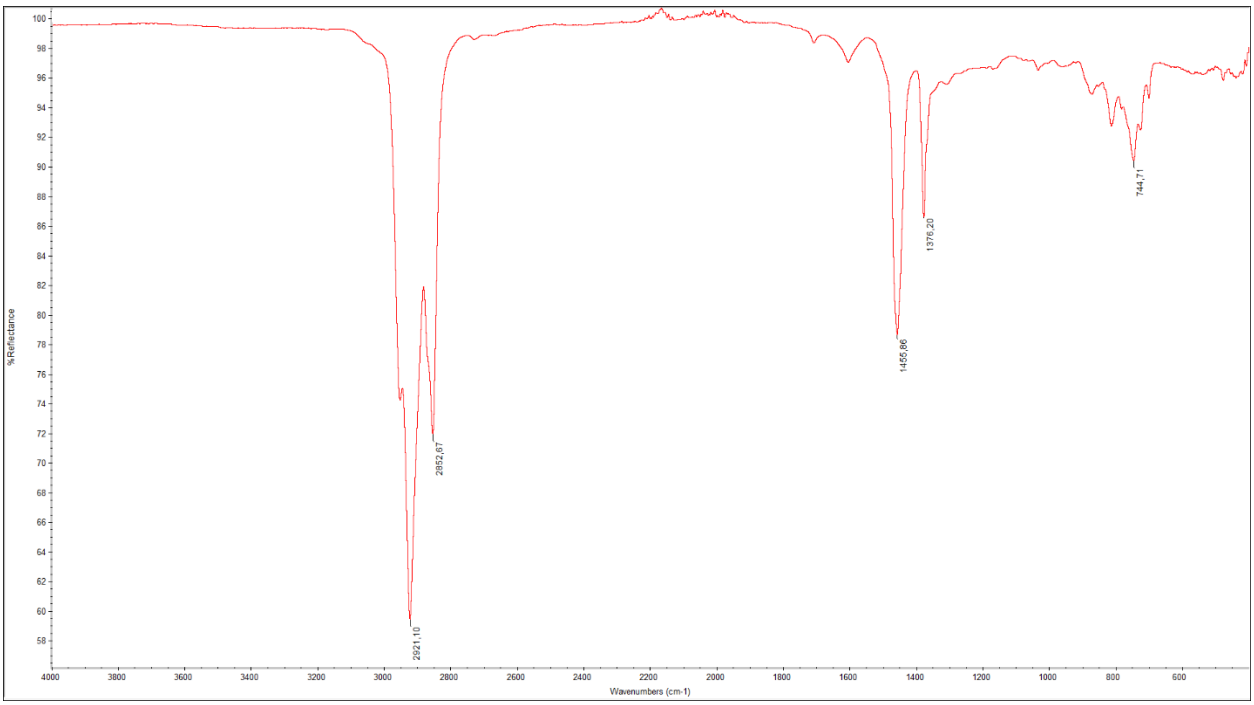

Figure A5-2: Crude oil B.

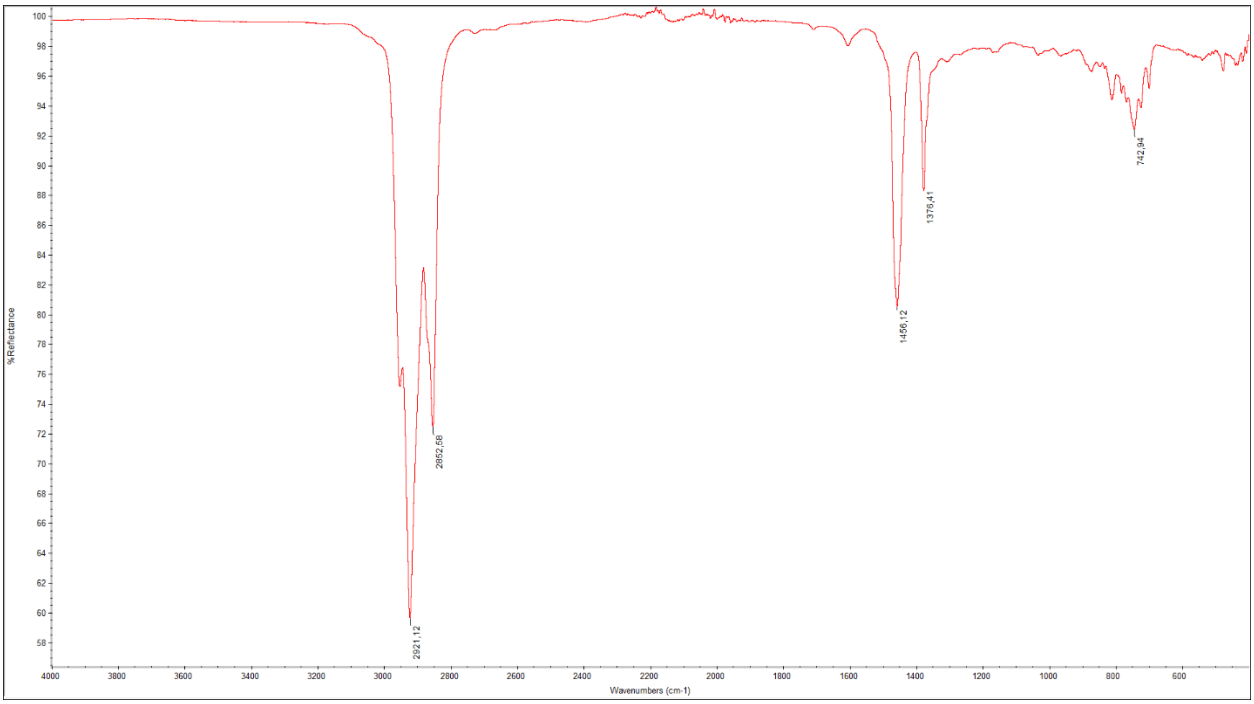

Figure A5-3: Crude oil C.

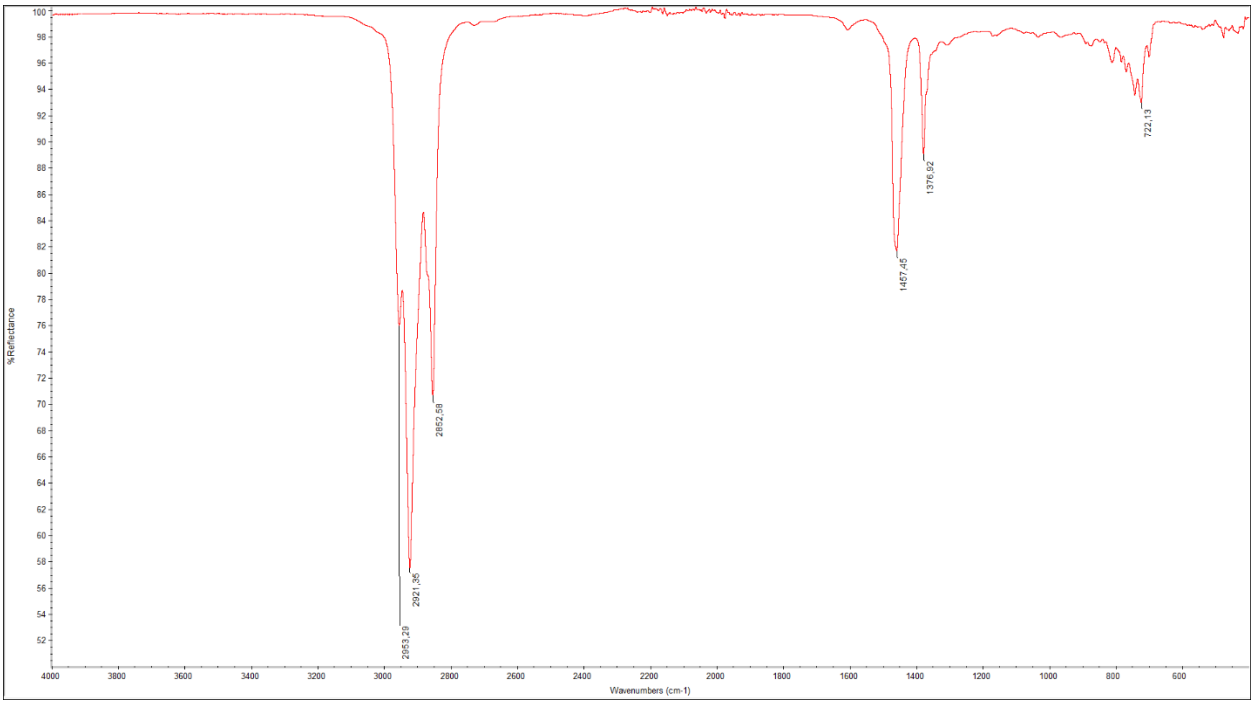

Figure A5-4: Crude oil D.

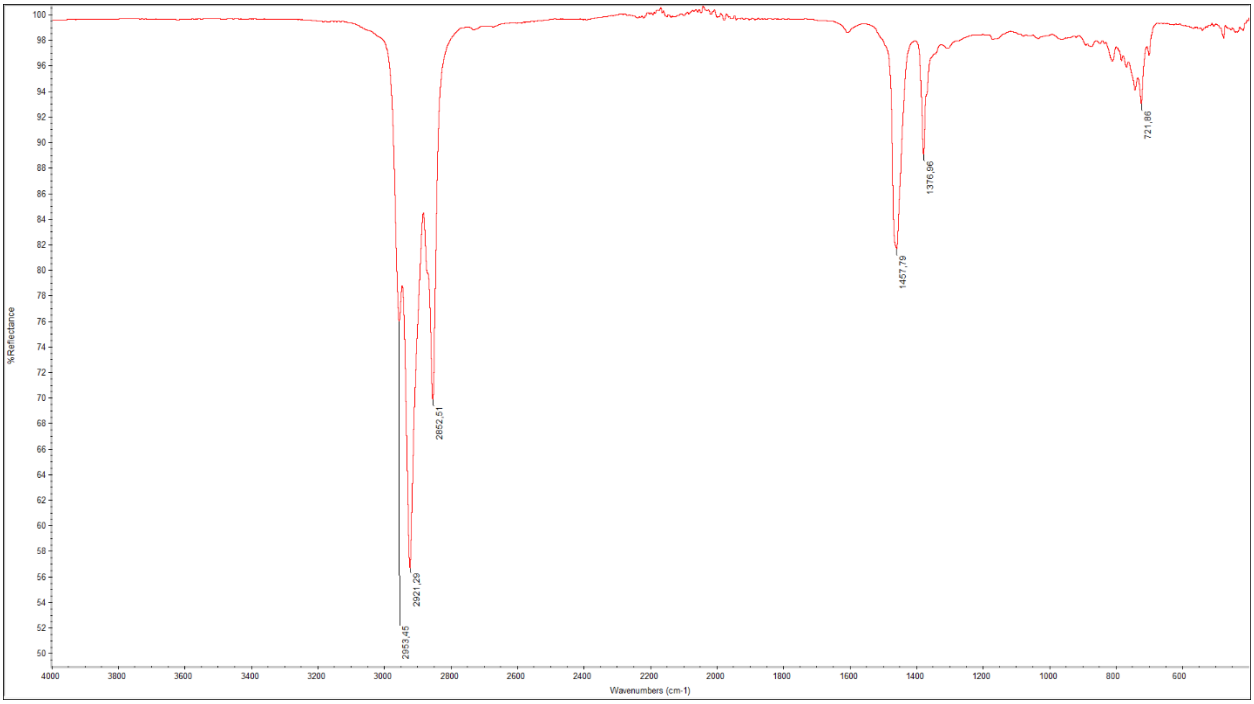

Figure A5-5: Crude oil E1.

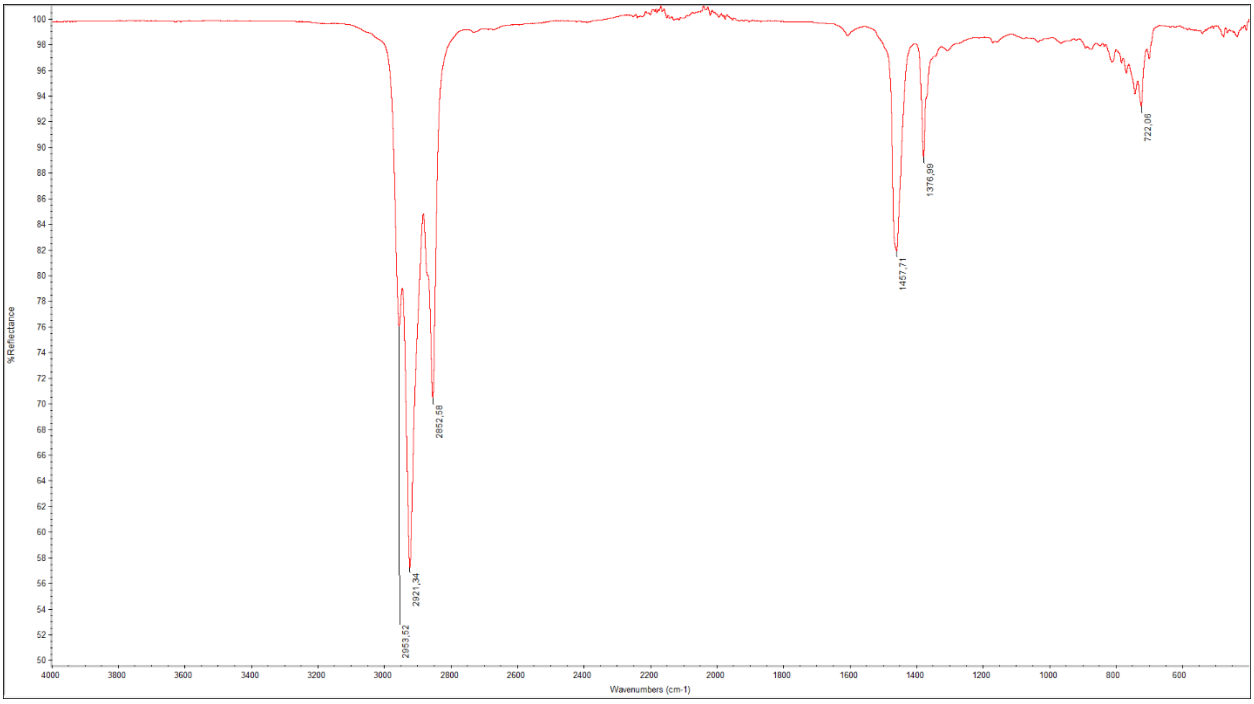

Figure A5-6: Crude oil E2.

Deasphalted oil

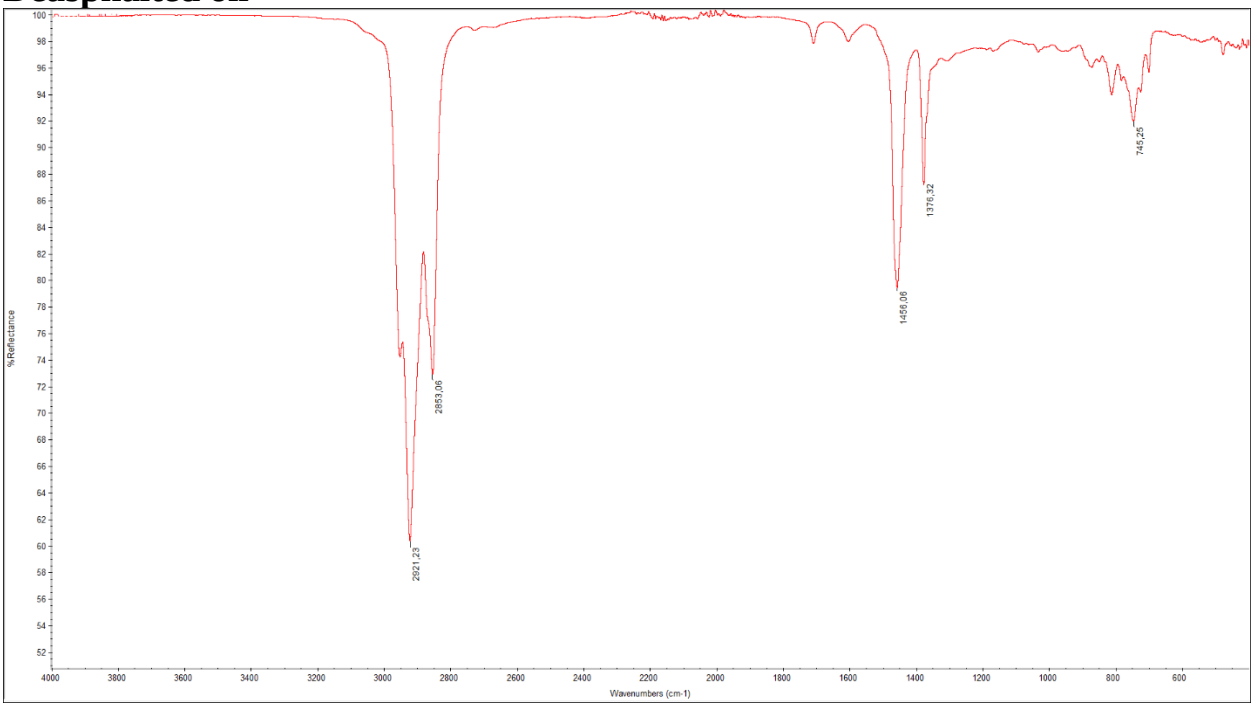

Figure A5-7: Deasphalted oil A.

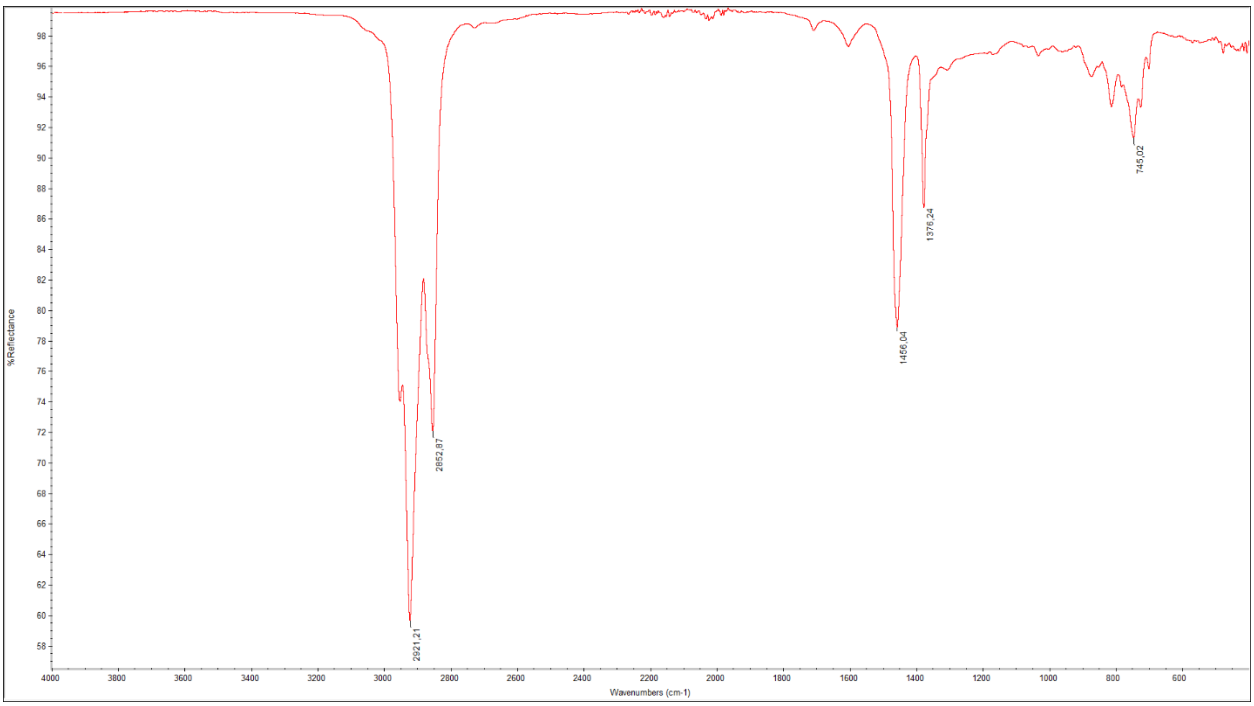

Figure A5-8: Deasphalted oil B.

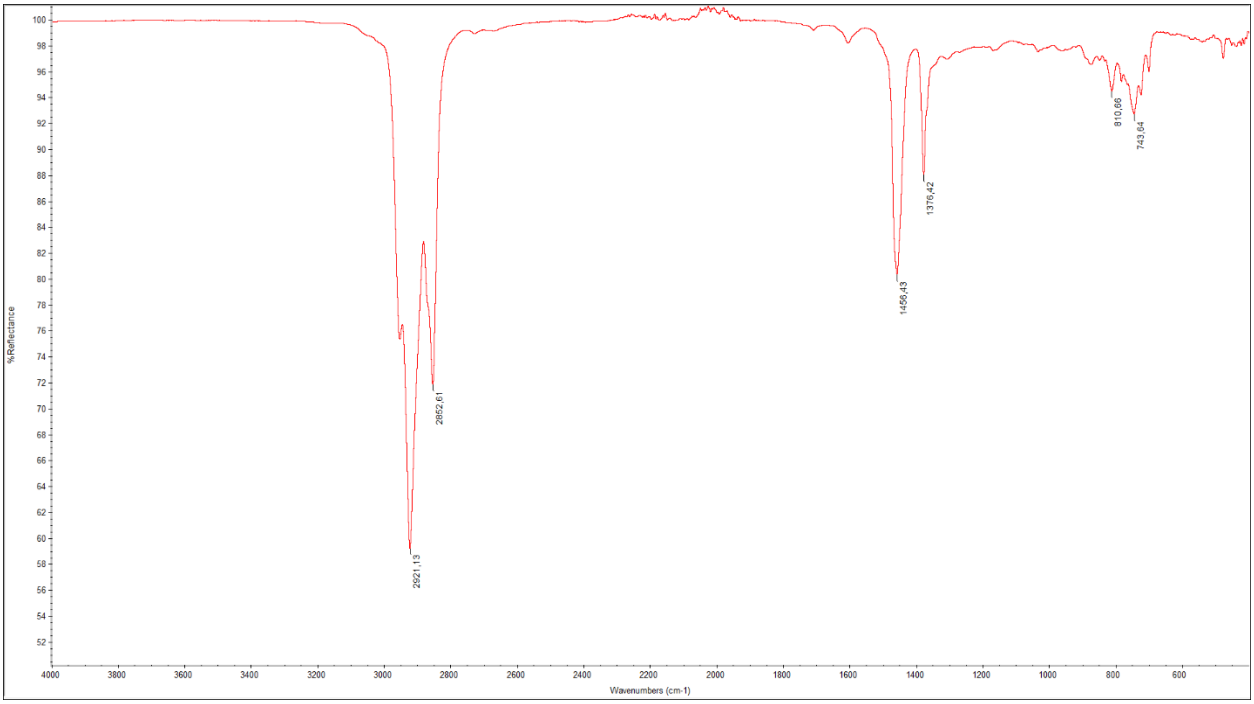

Figure A5-9: Deasphalted oil C.

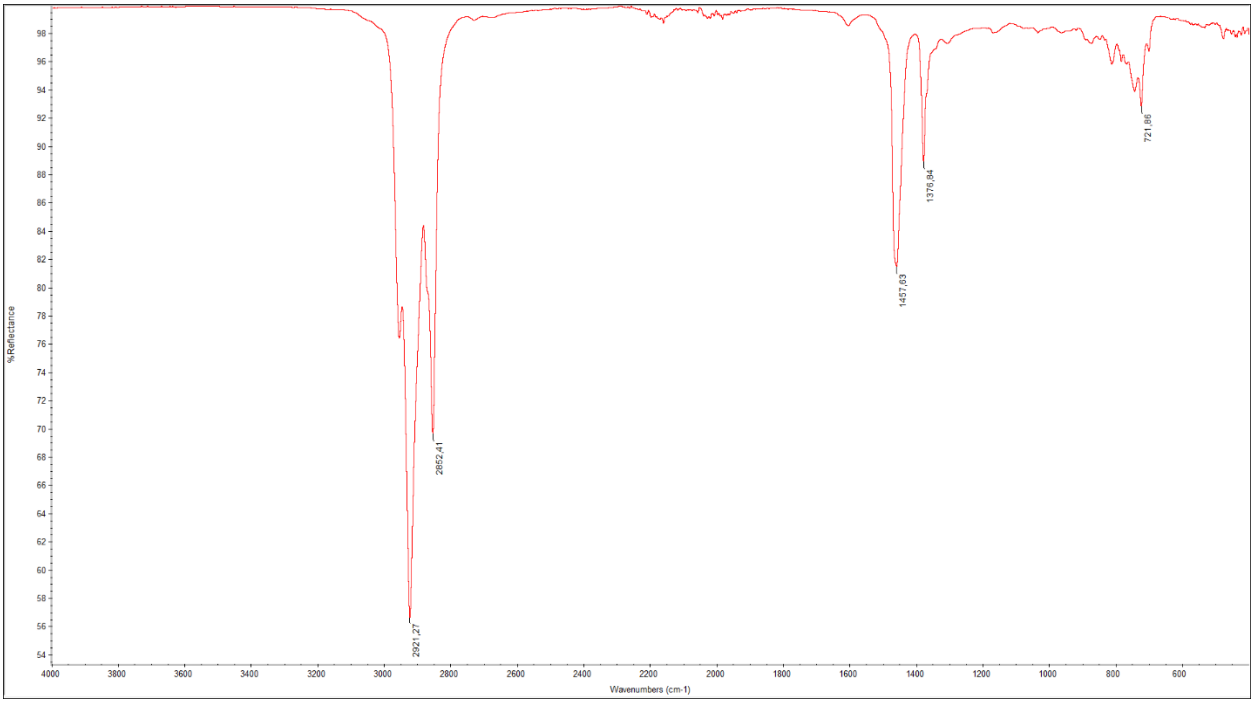

Figure A5-10: Deasphalted oil D.

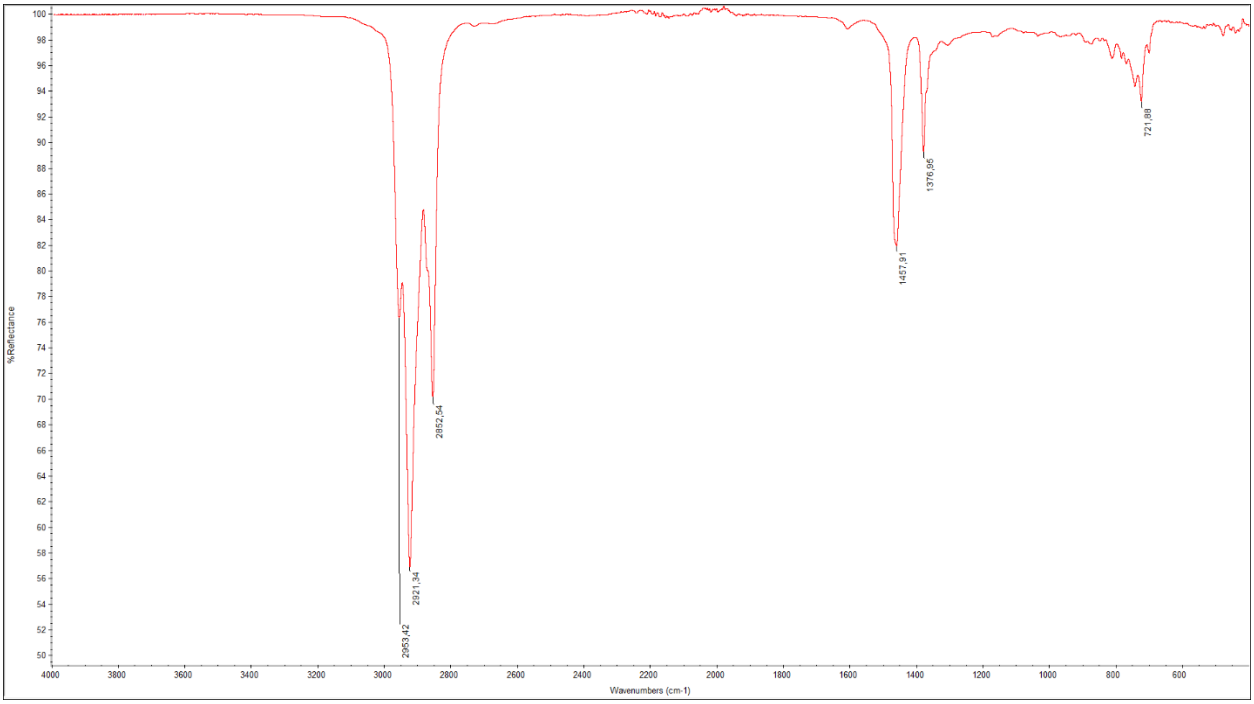

Figure A5-11: Deasphalted oil E1.

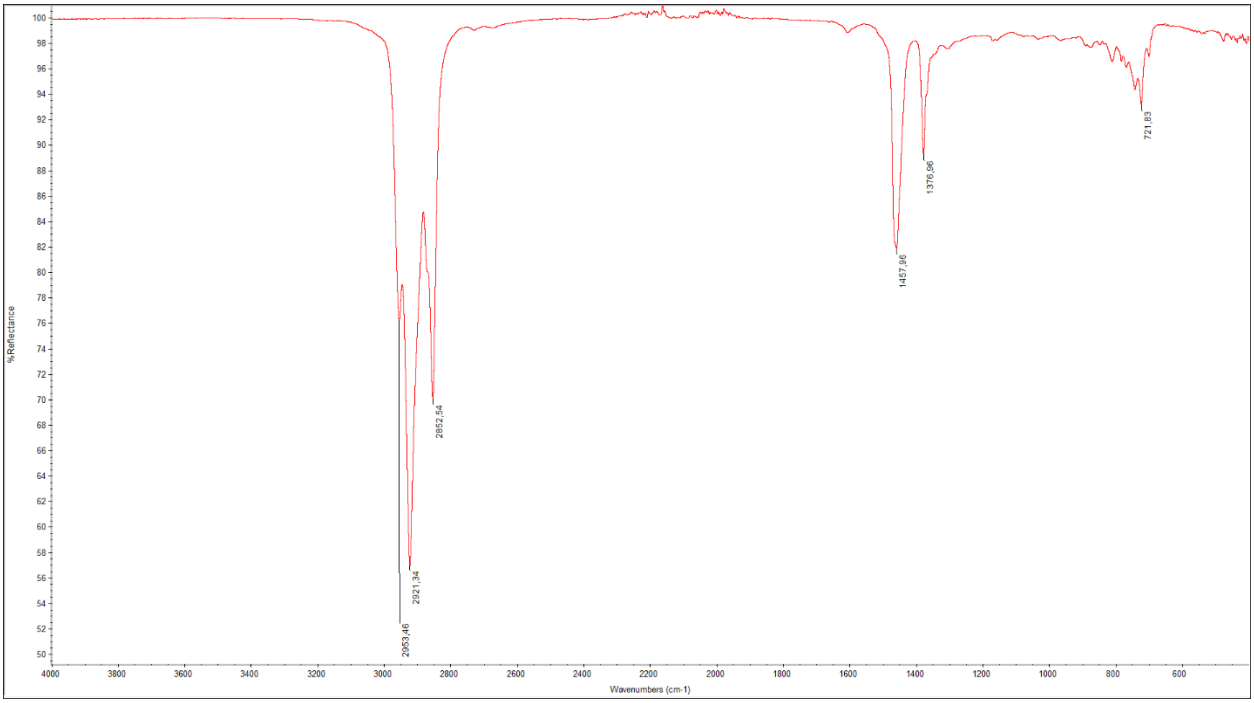

Figure A5-12: Deasphalted oil E2.

Maltene Fractions

F1

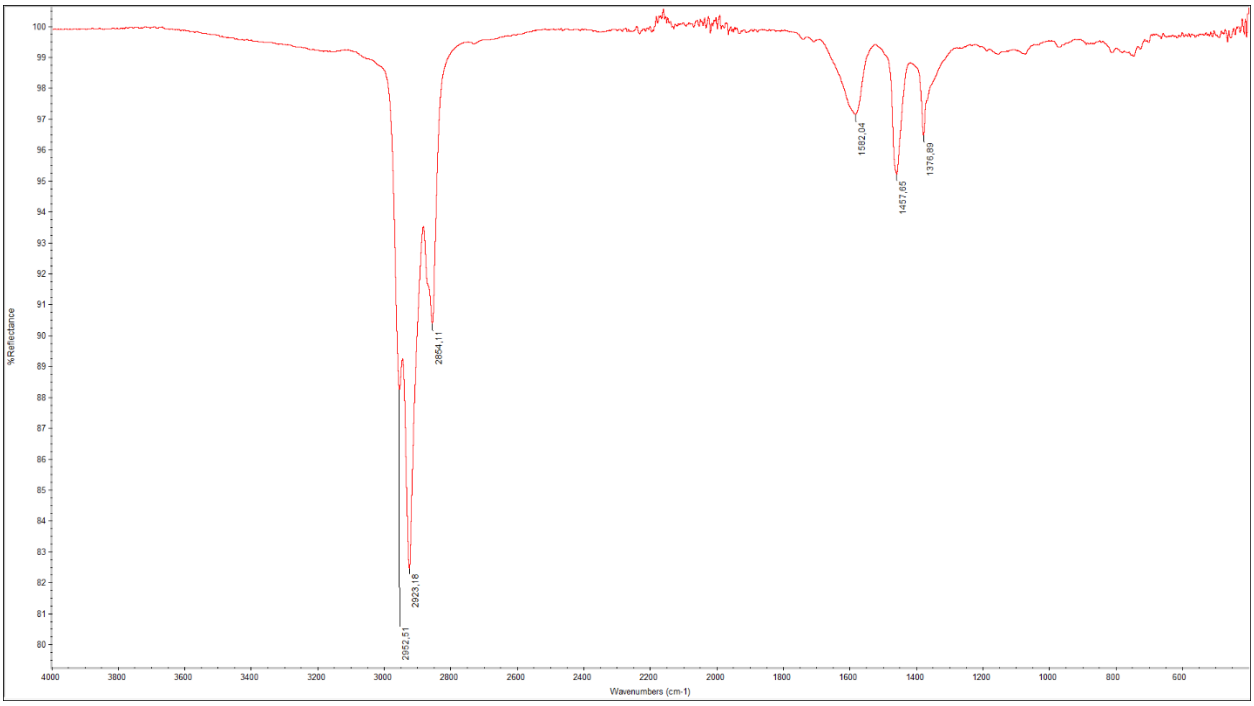

Figure A5-13: Crude oil A.

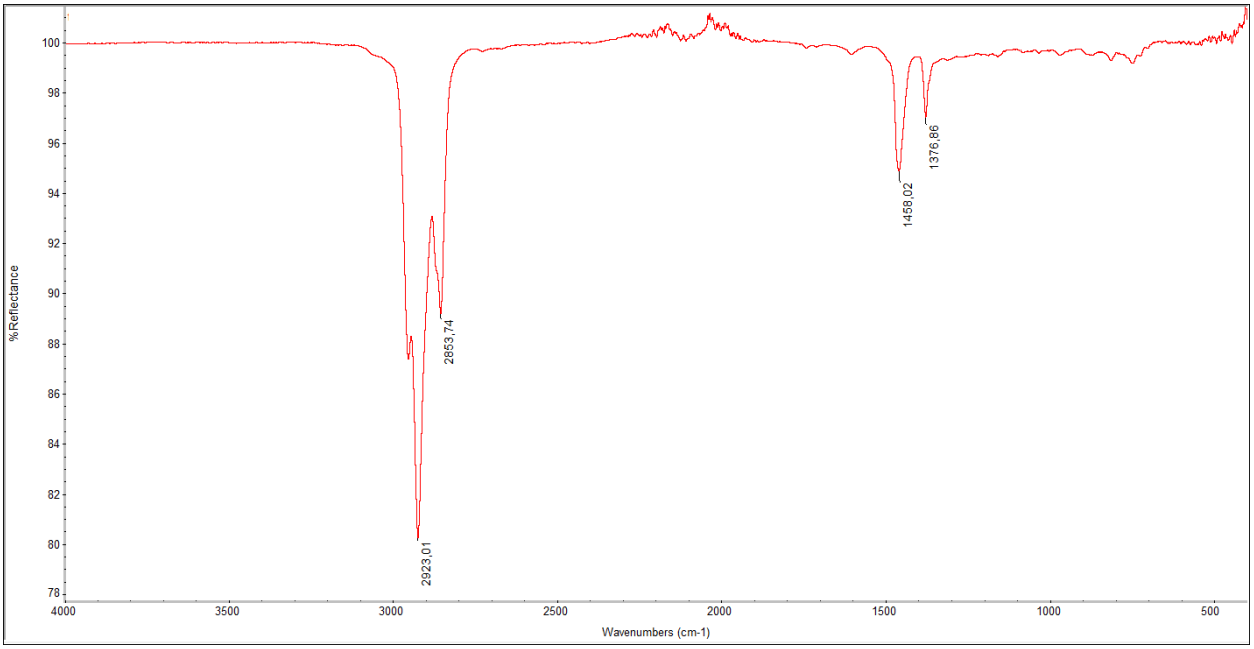

Figure A5-14: Crude oil B.

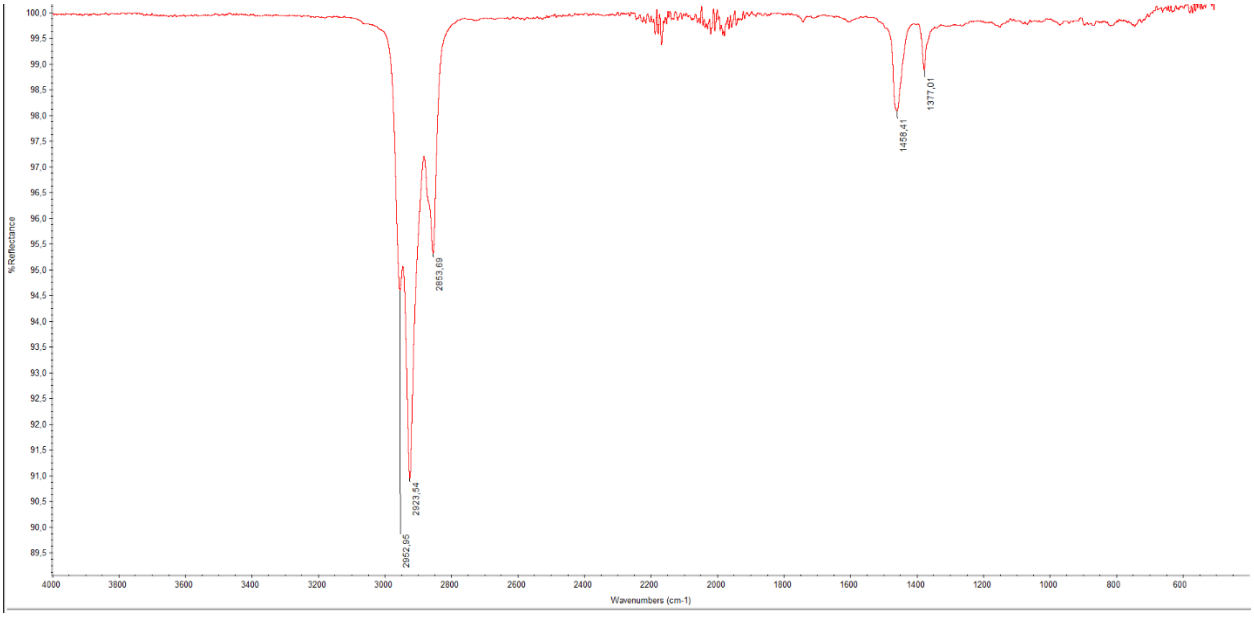

Figure A5-15: Crude oil C.

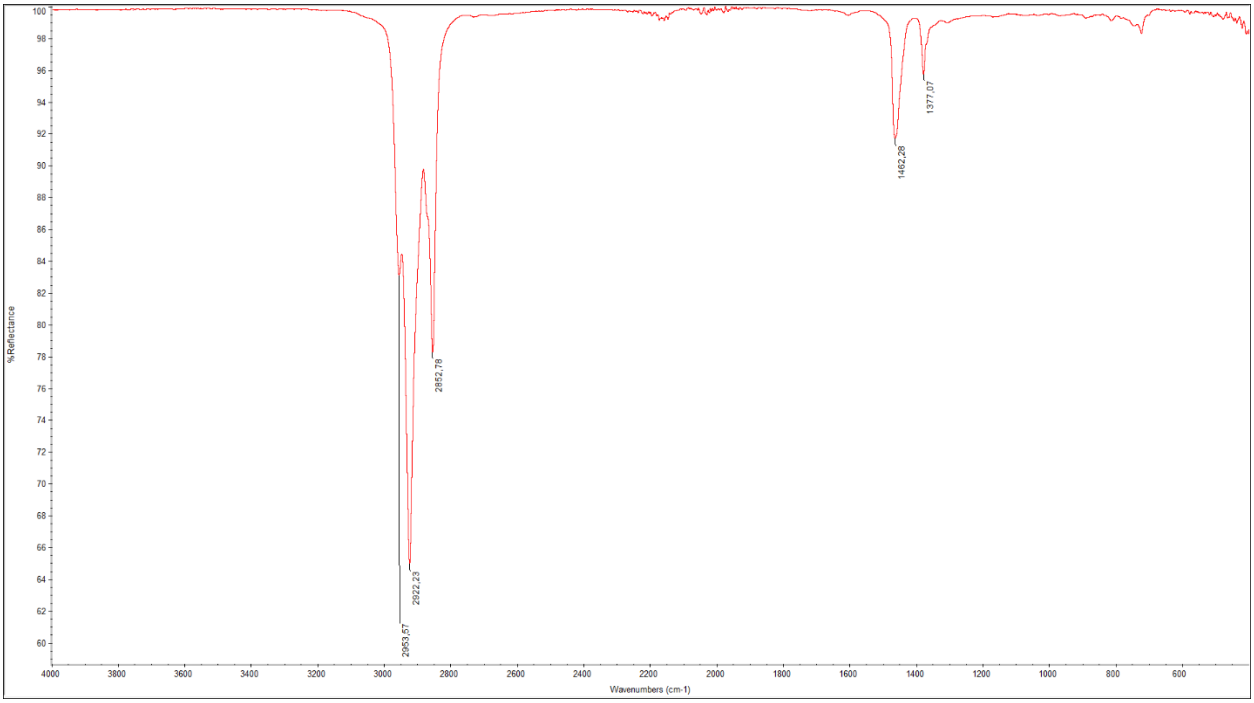

Figure A5-16: Crude oil D.

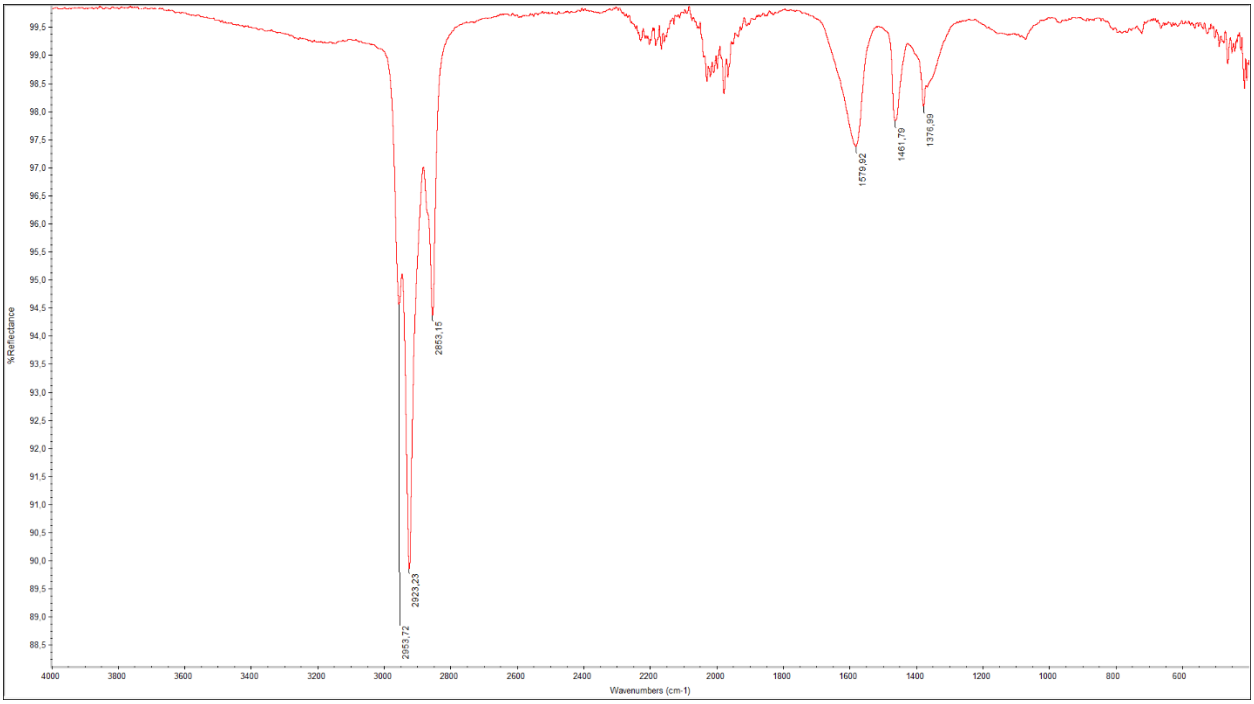

Figure A5-17: Crude oil E1.

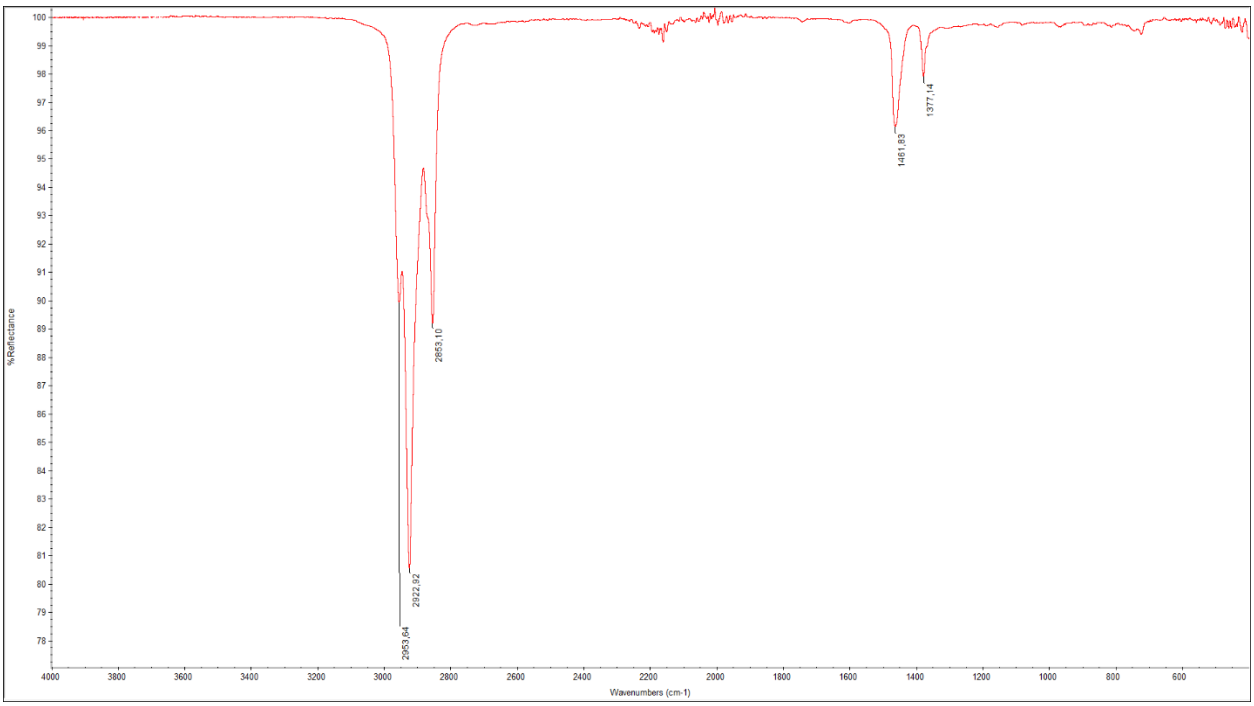

Figure A5-18: Crude oil E2.

F2

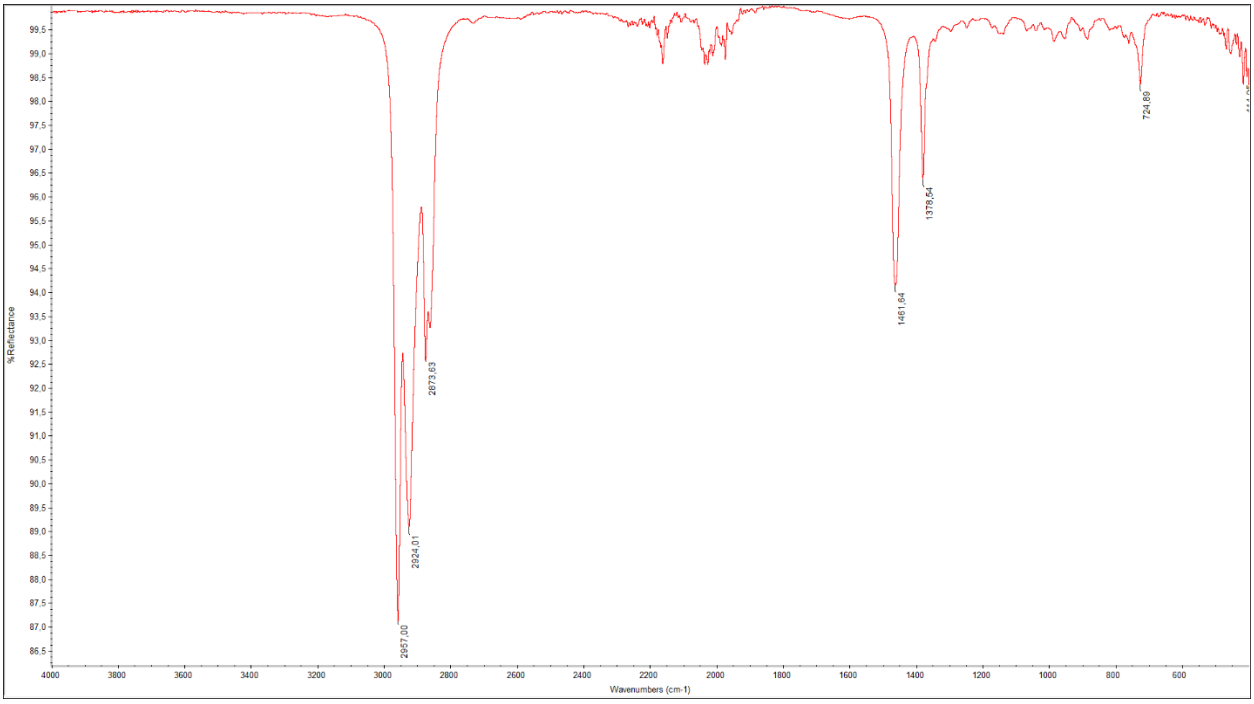

Figure A5-19: Crude oil A.

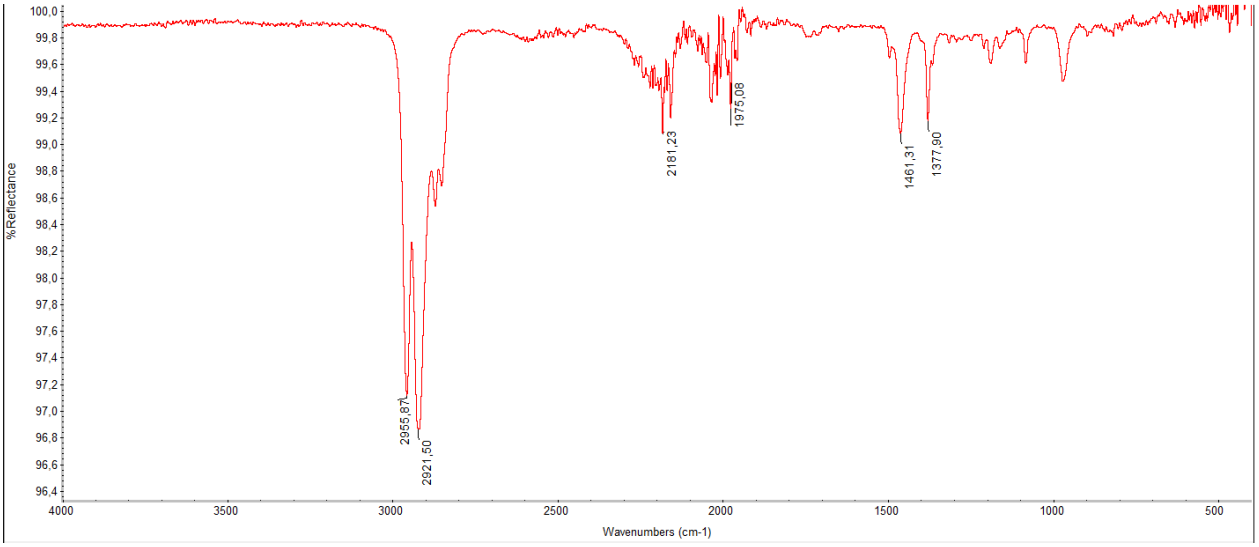

Figure A5-20: Crude oil B.

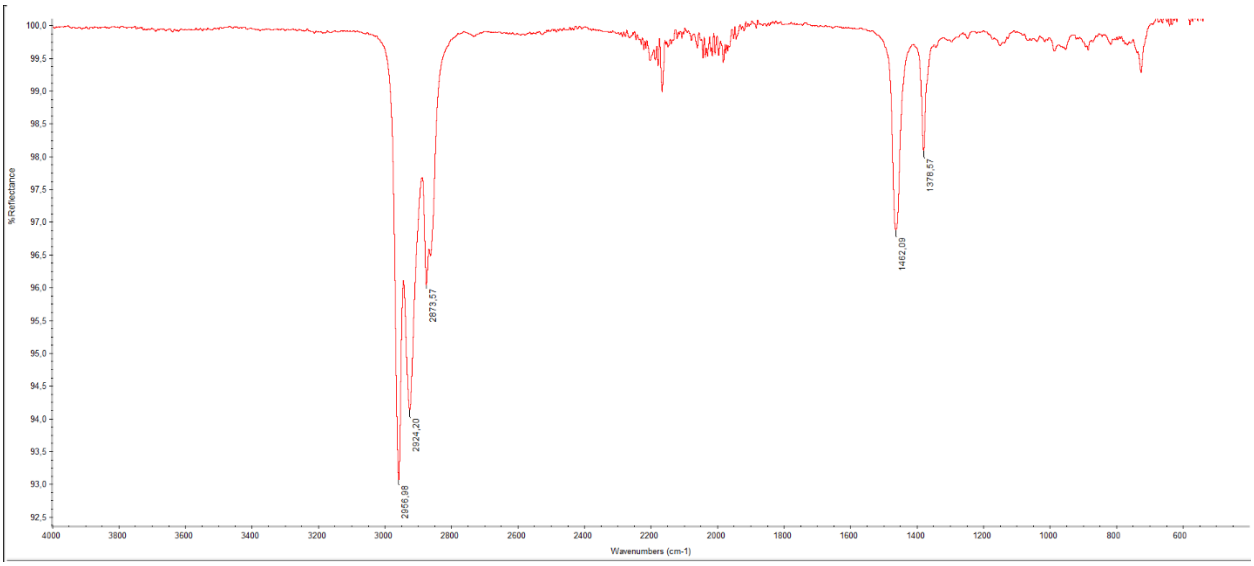

Figure A5-21: Crude oil C.

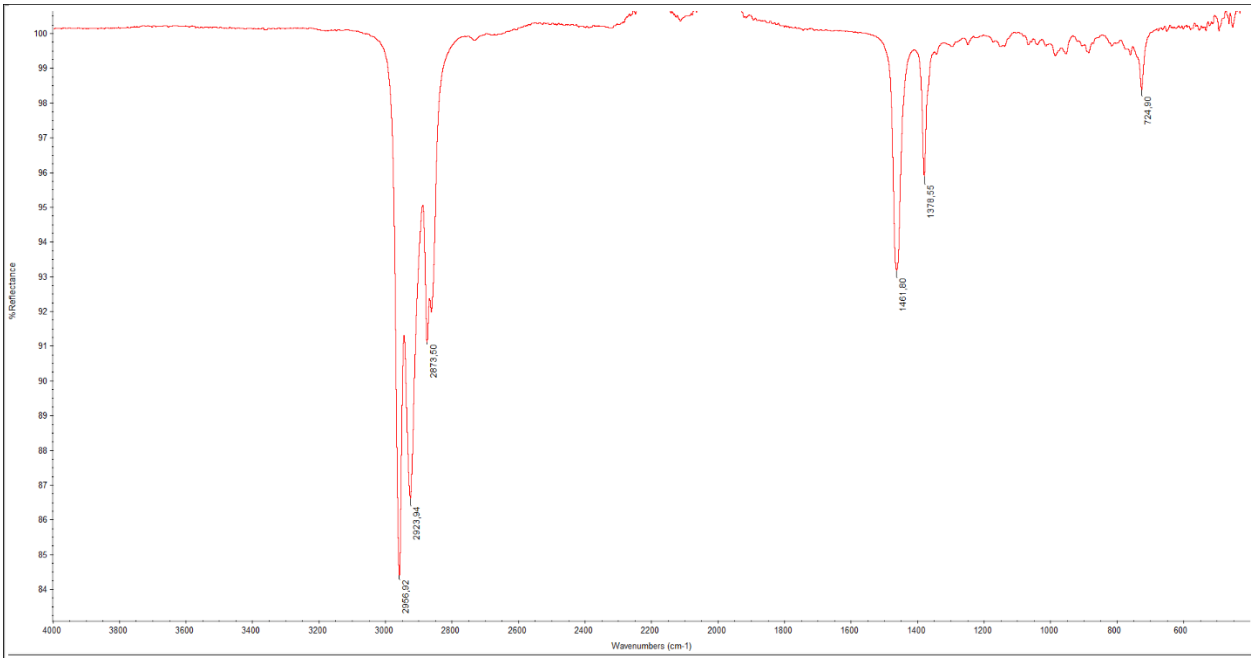

Figure A5-22: Crude oil D.

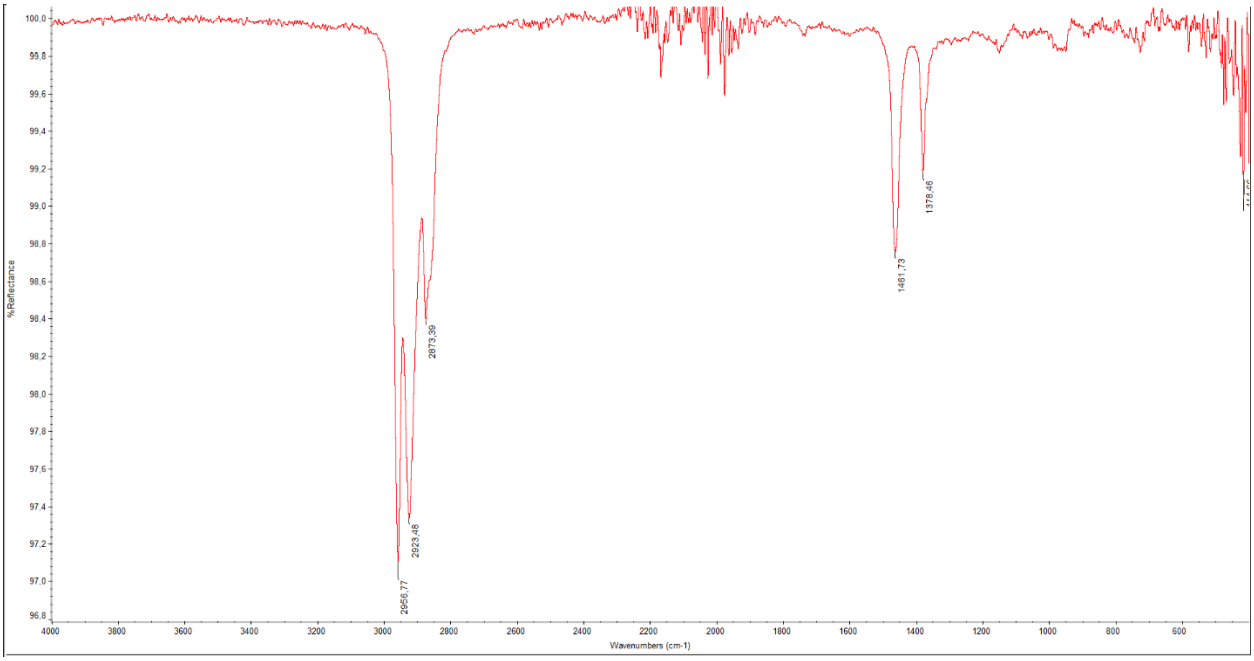

Figure A5-23: Crude oil E1.

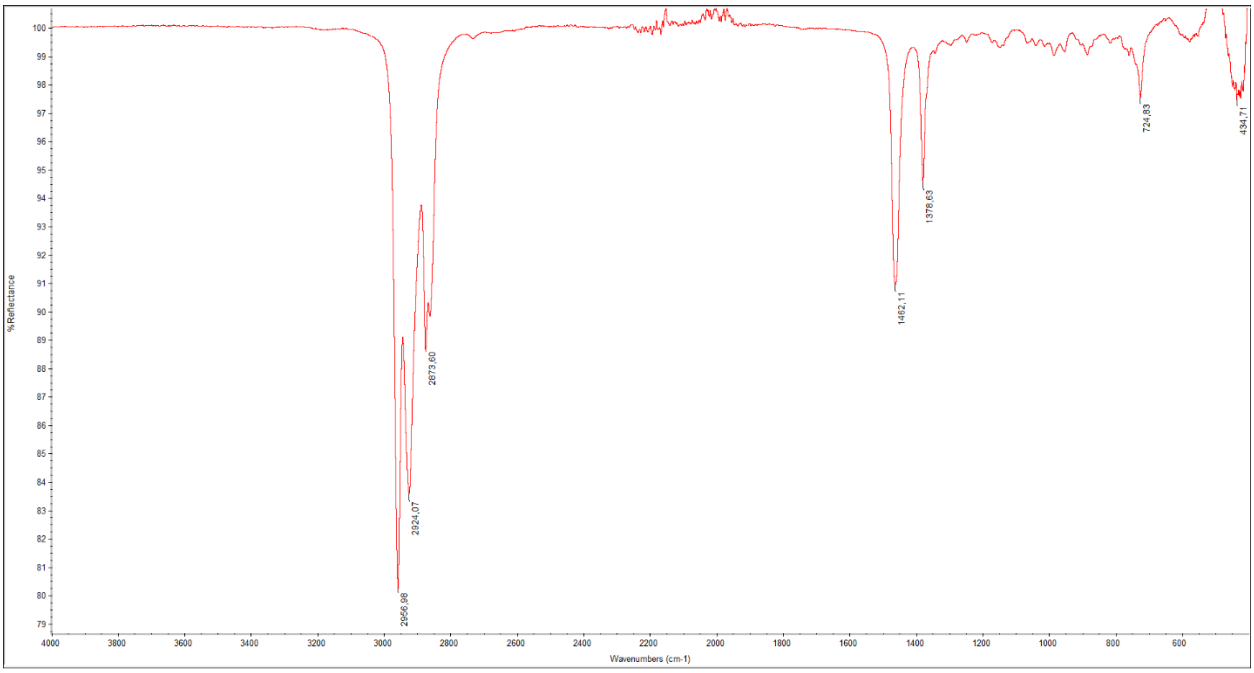

Figure A5-24: Crude oil E2.

F3

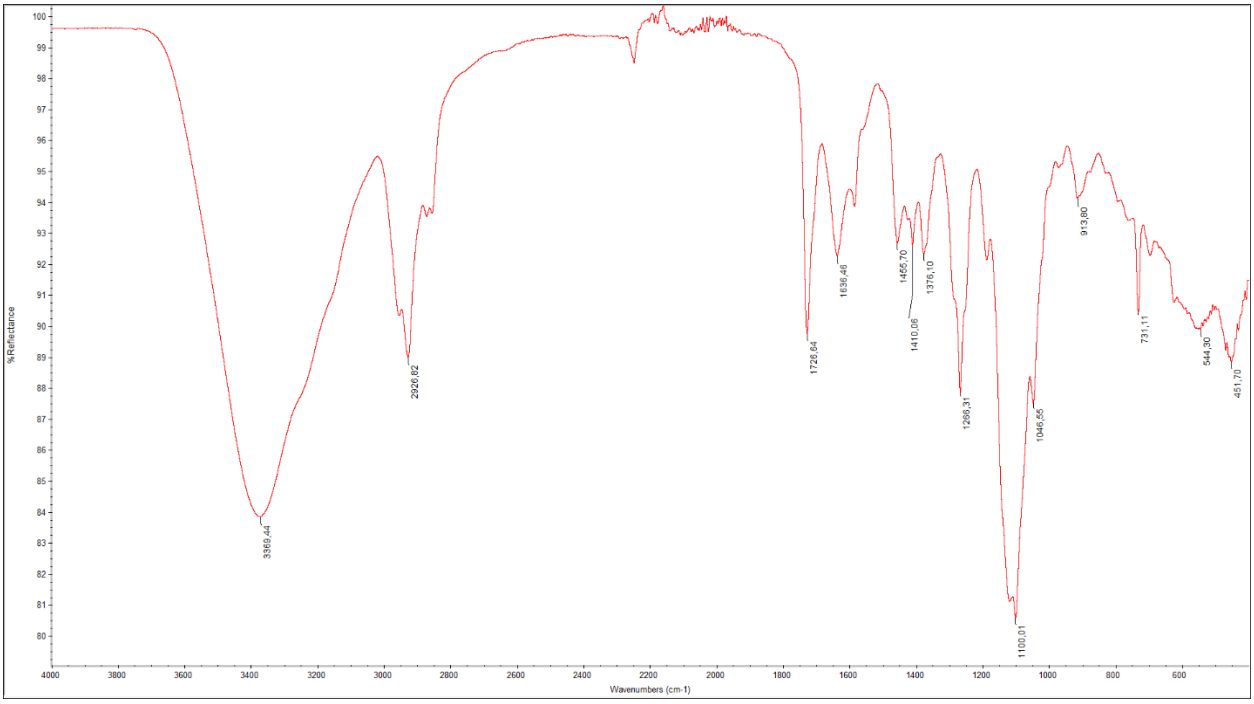

Figure A5-25: Crude oil A.

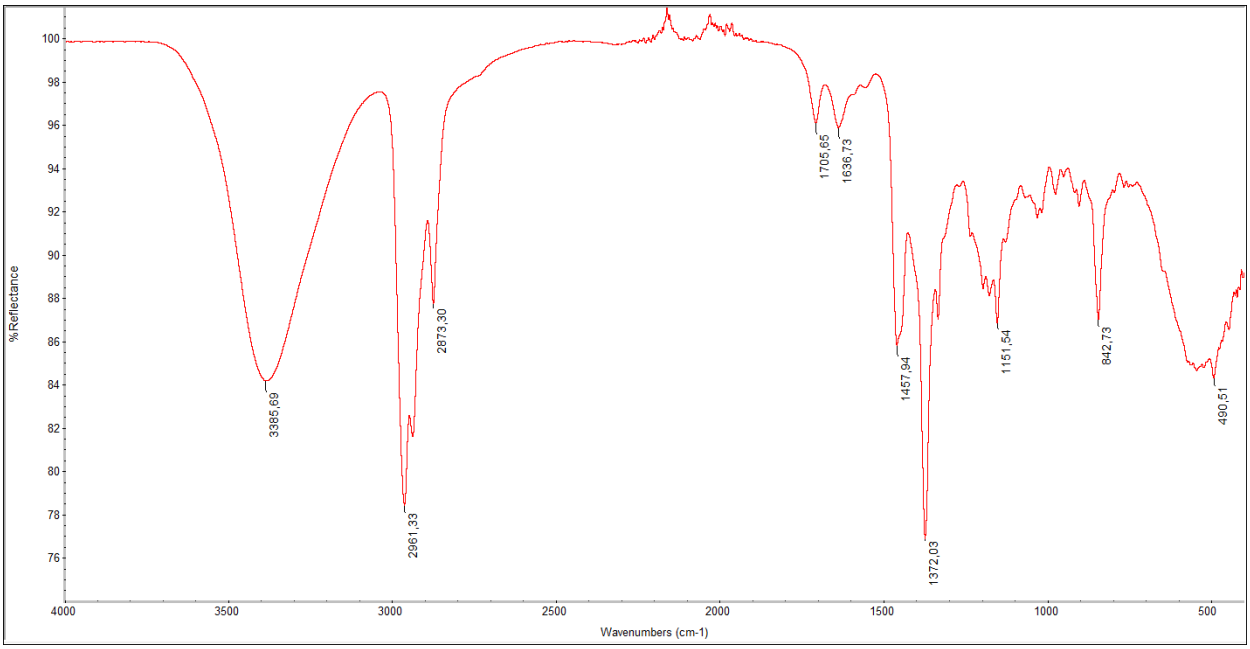

Figure A5-26: Crude oil B.

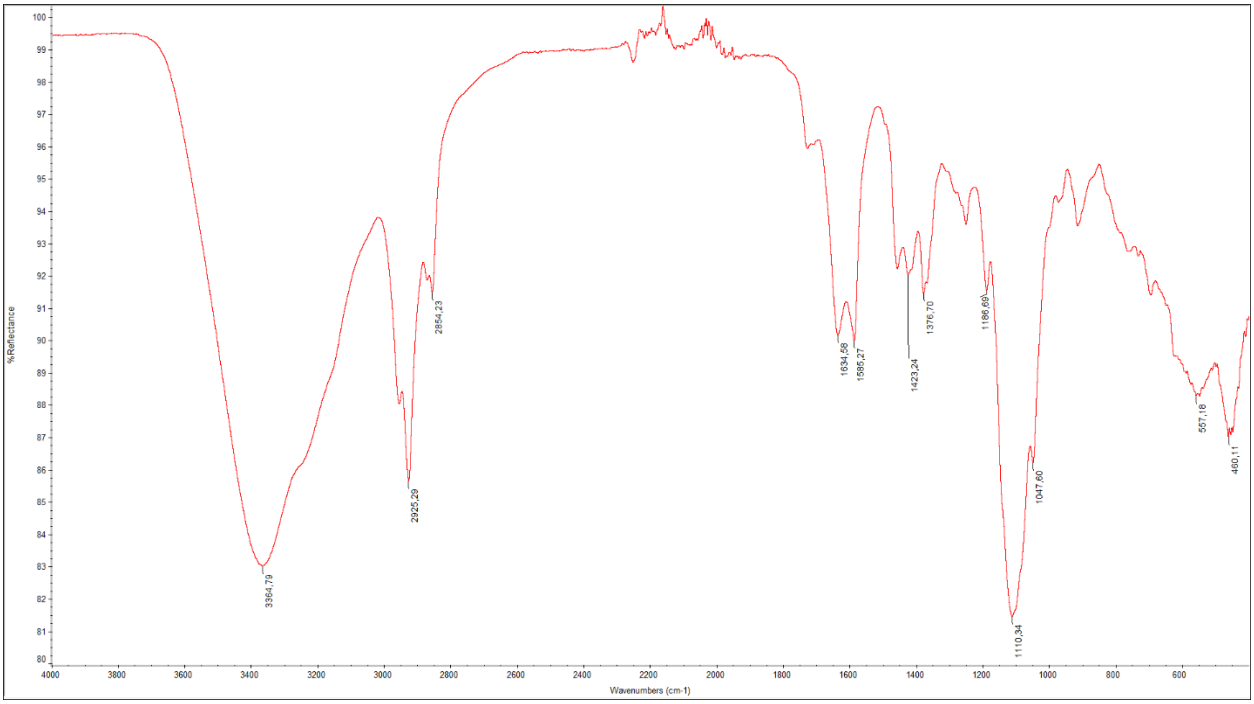

Figure A5-27: Crude oil C.

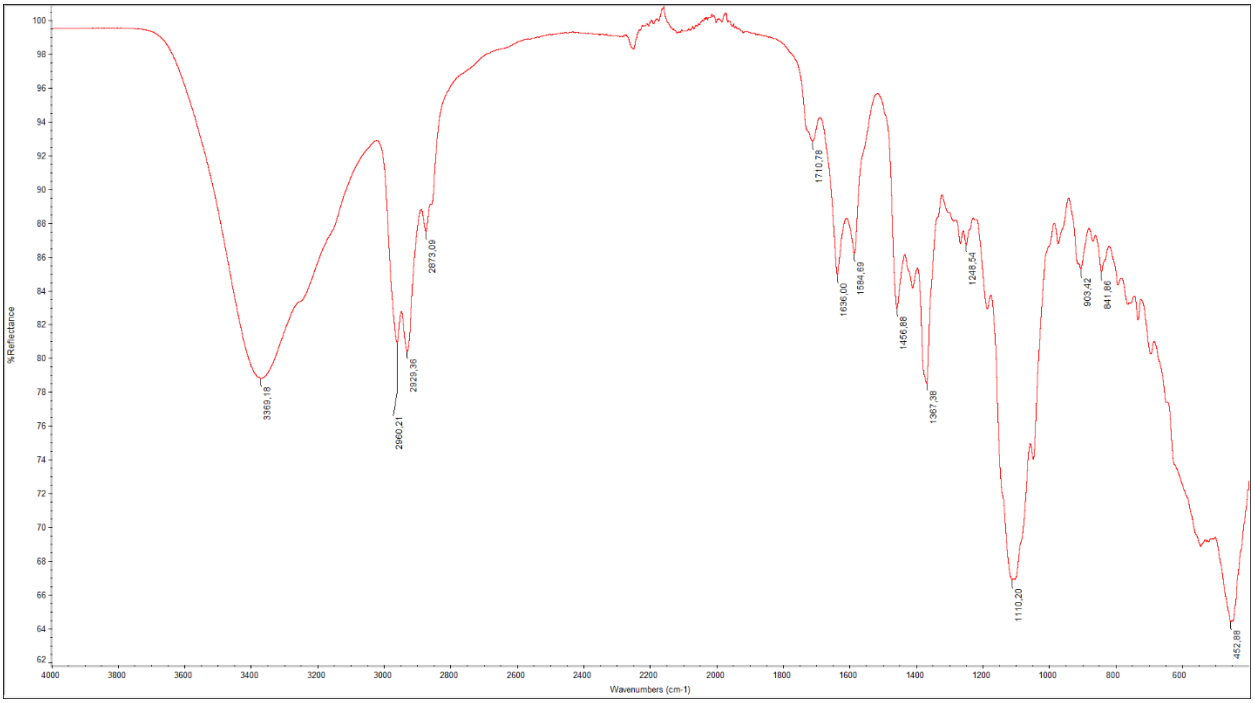

Figure A5-28: Crude oil D.

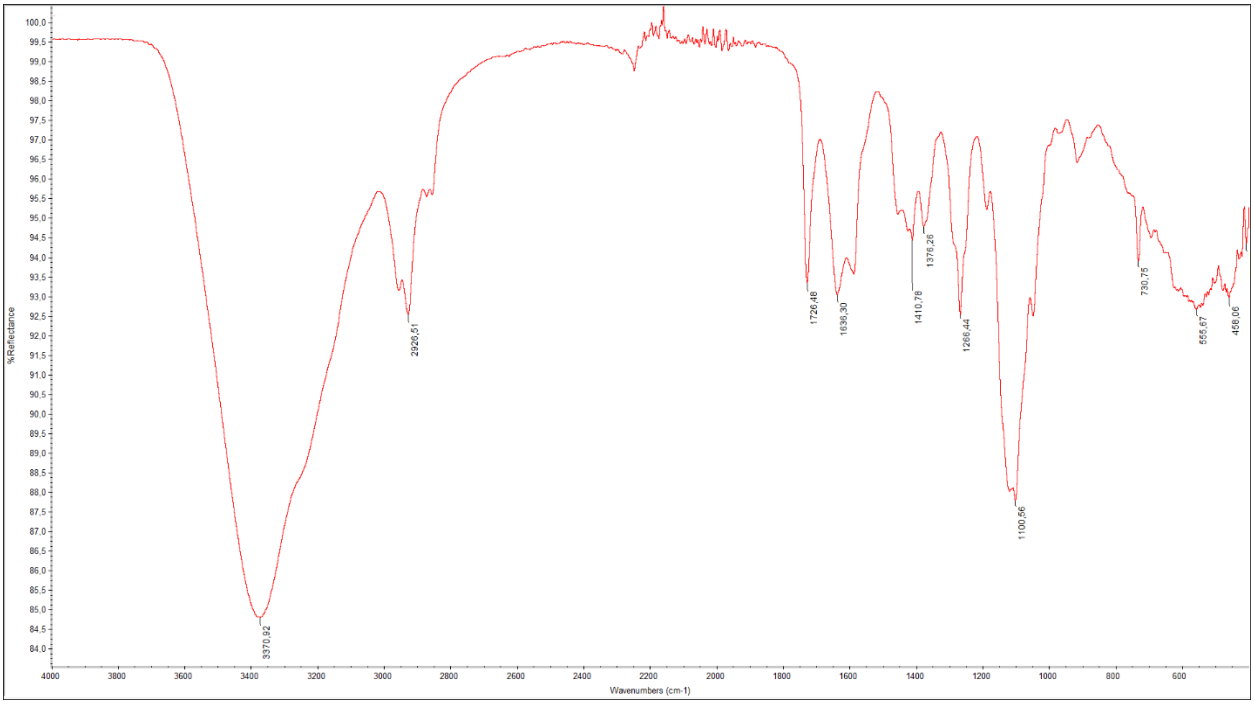

Figure A5-29: Crude oil E1.

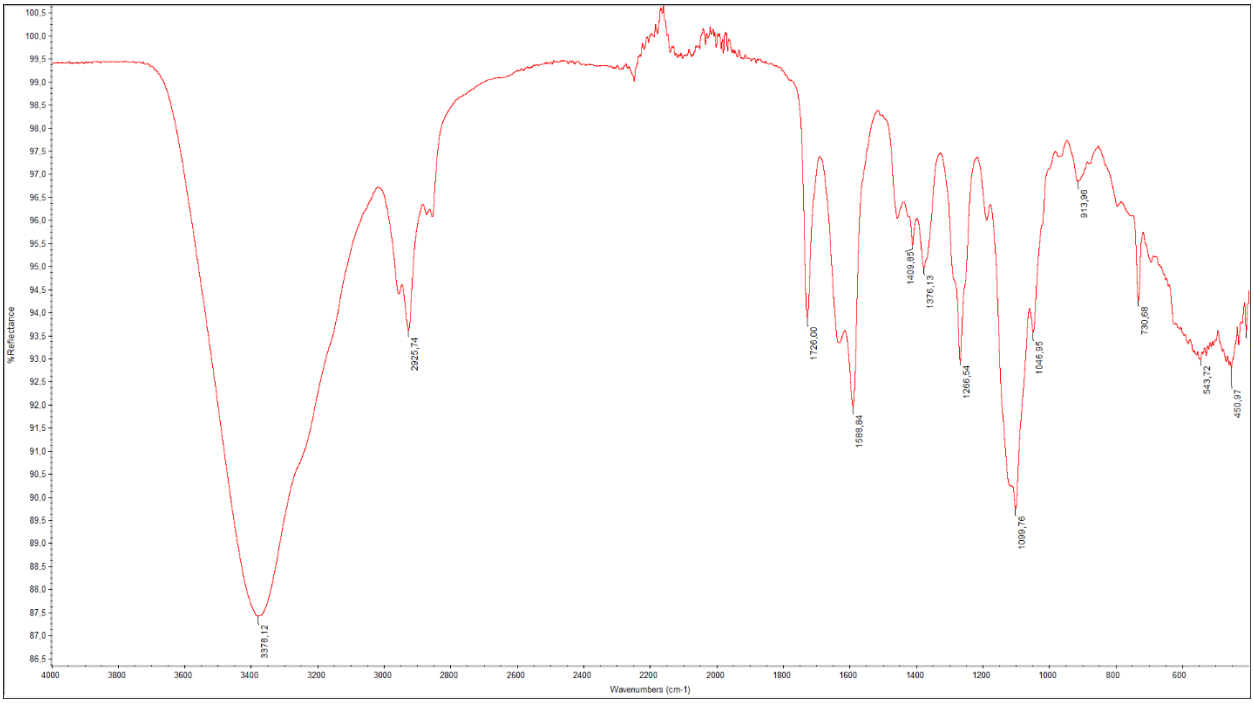

Figure A5-30: Crude oil E2.

F4

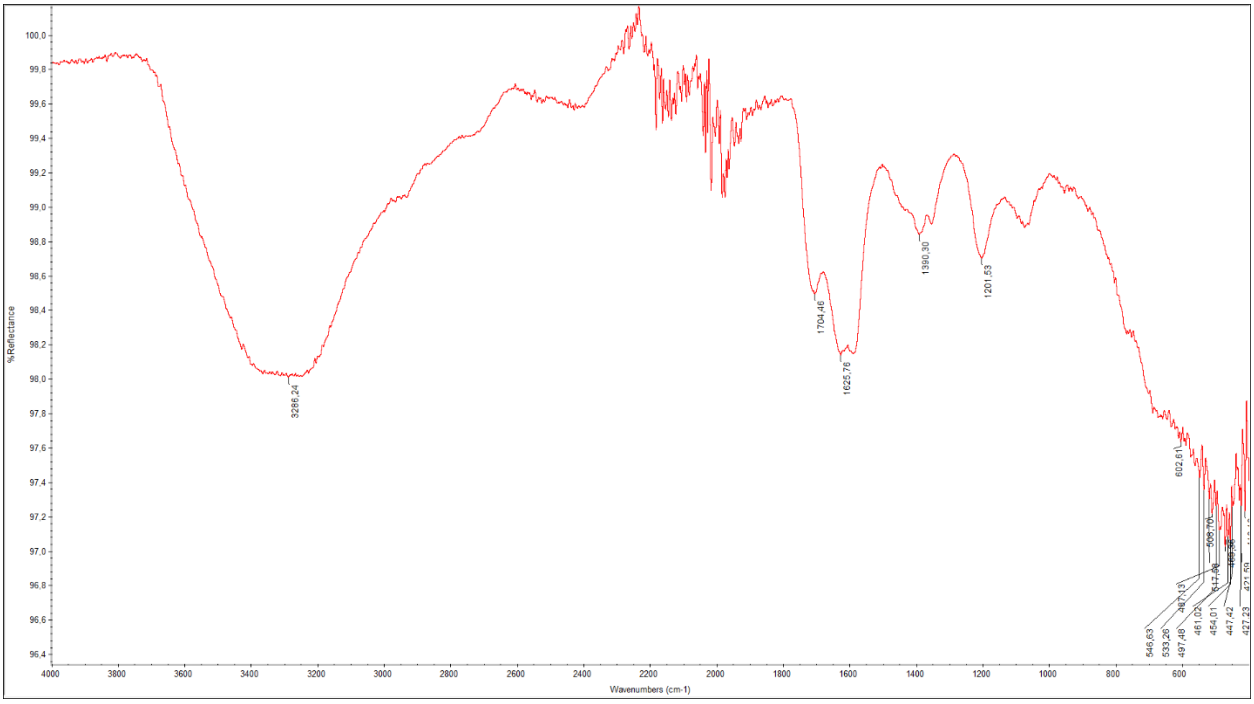

Figure A5-31: Crude oil A.

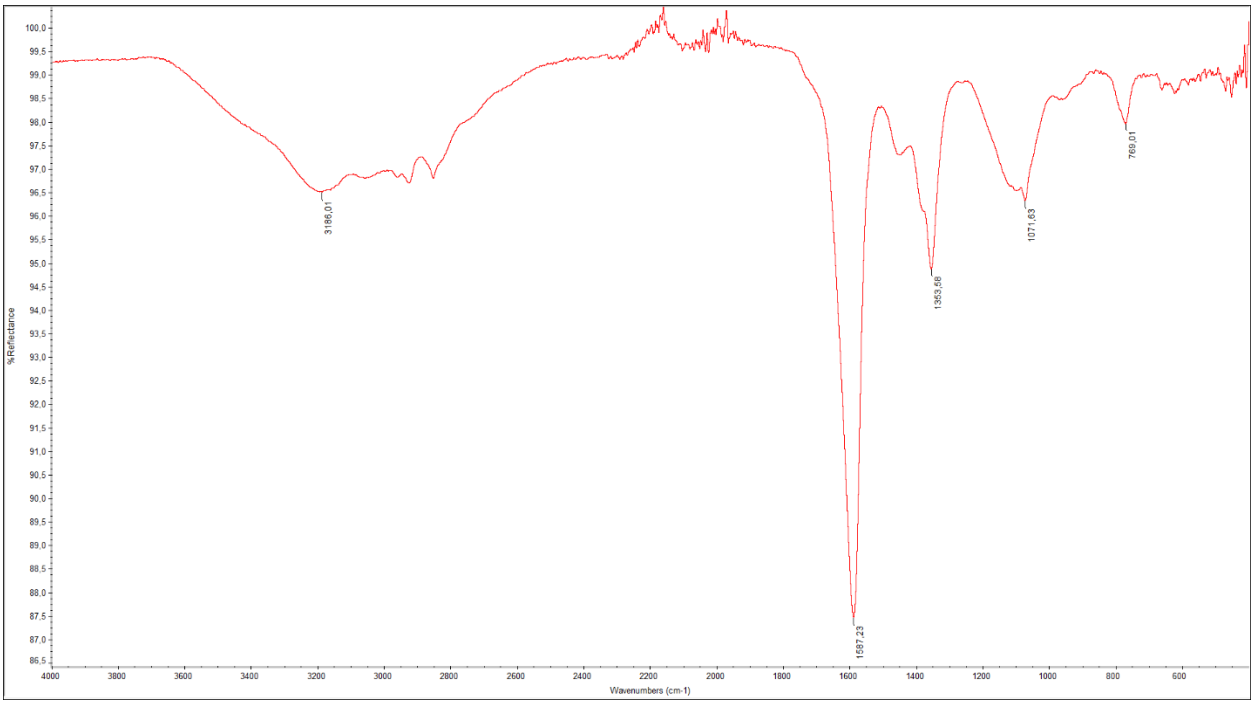

Figure A5-32: Crude oil B.

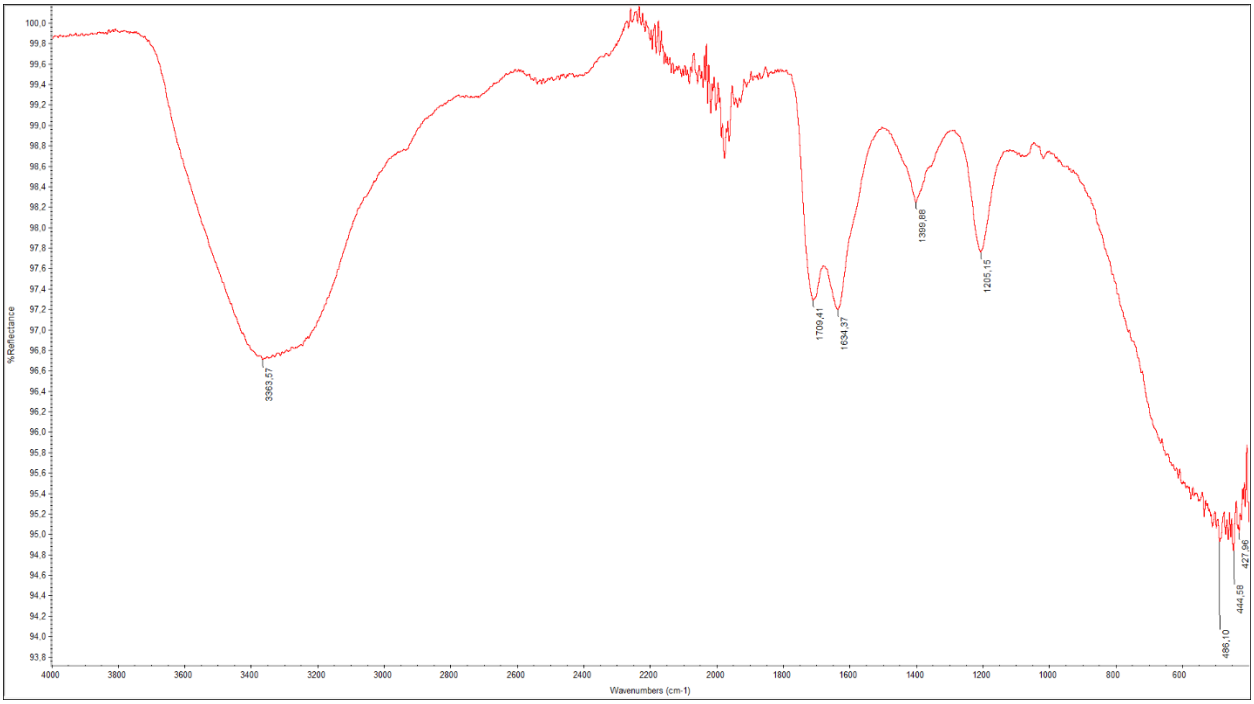

Figure A5-33: Crude oil C.

Figure A5-34: Crude oil D.

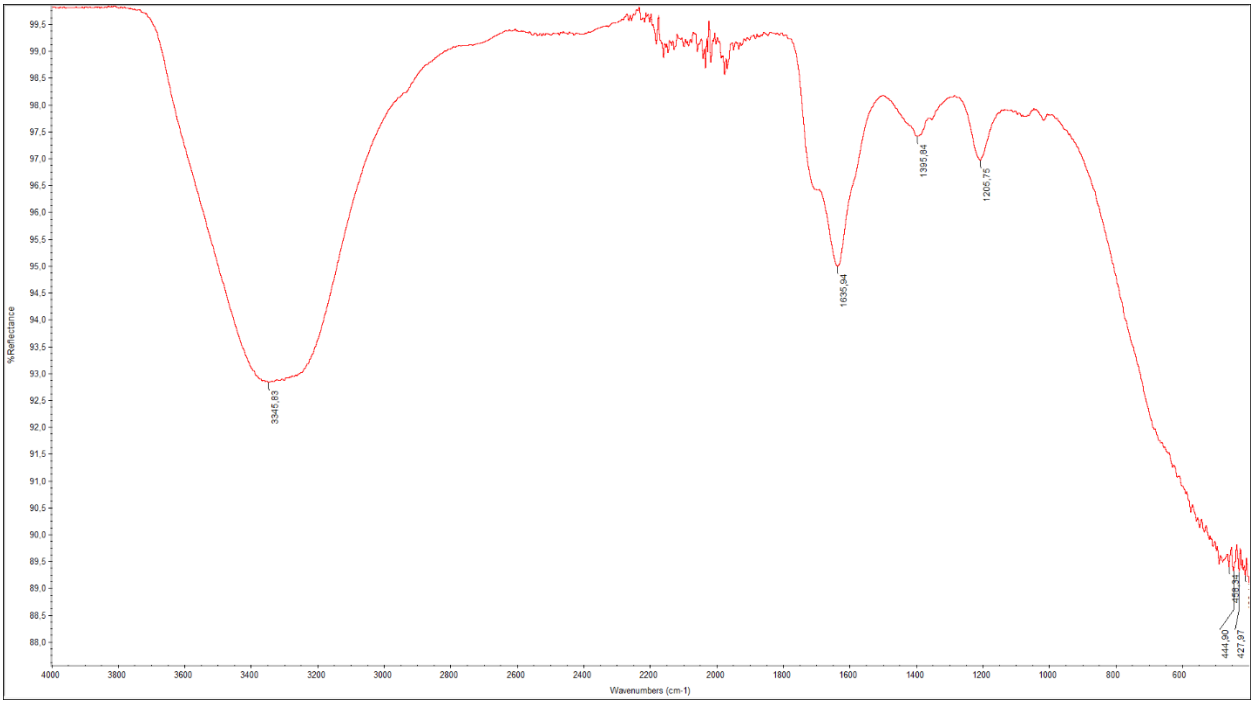

Figure A5-35: Crude oil E1.

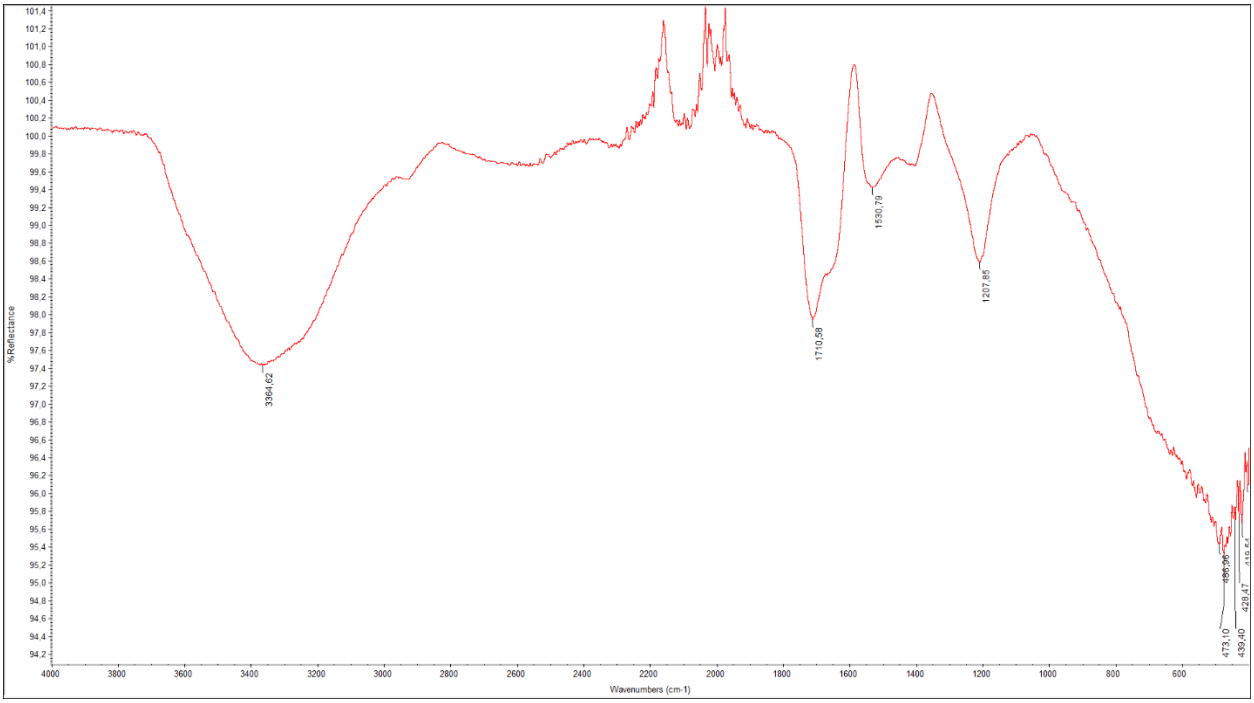

Figure A5-36: Crude oil E2.

A6 ^{31}P NMR Spectra

Maltene Fractions

F3

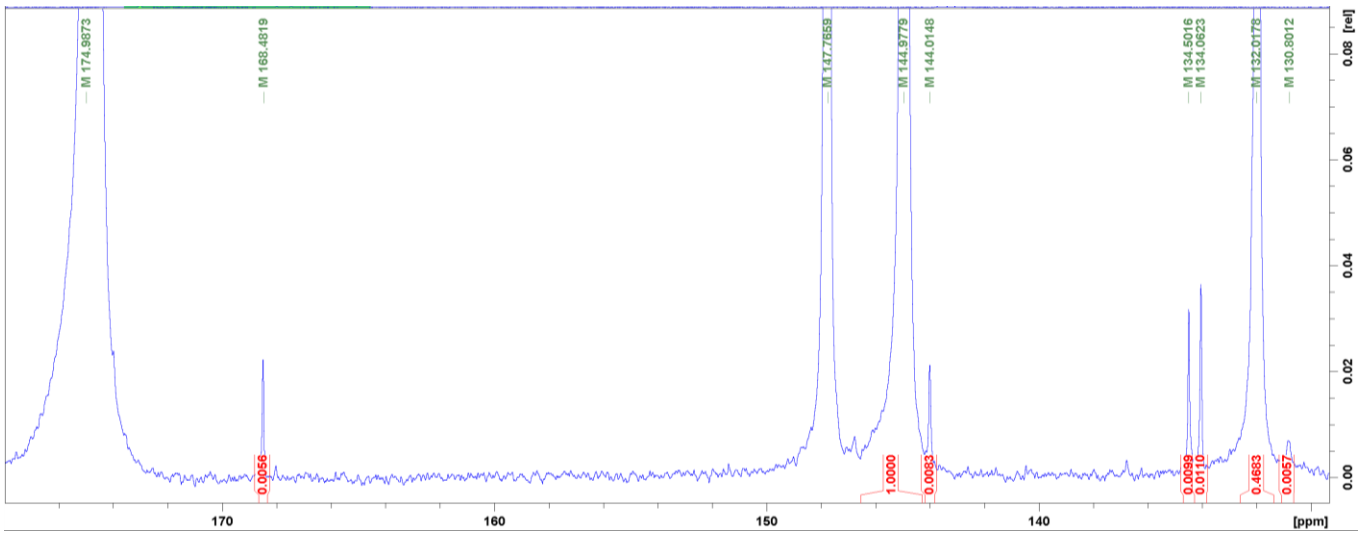

Figure A6-1: Crude oil A.

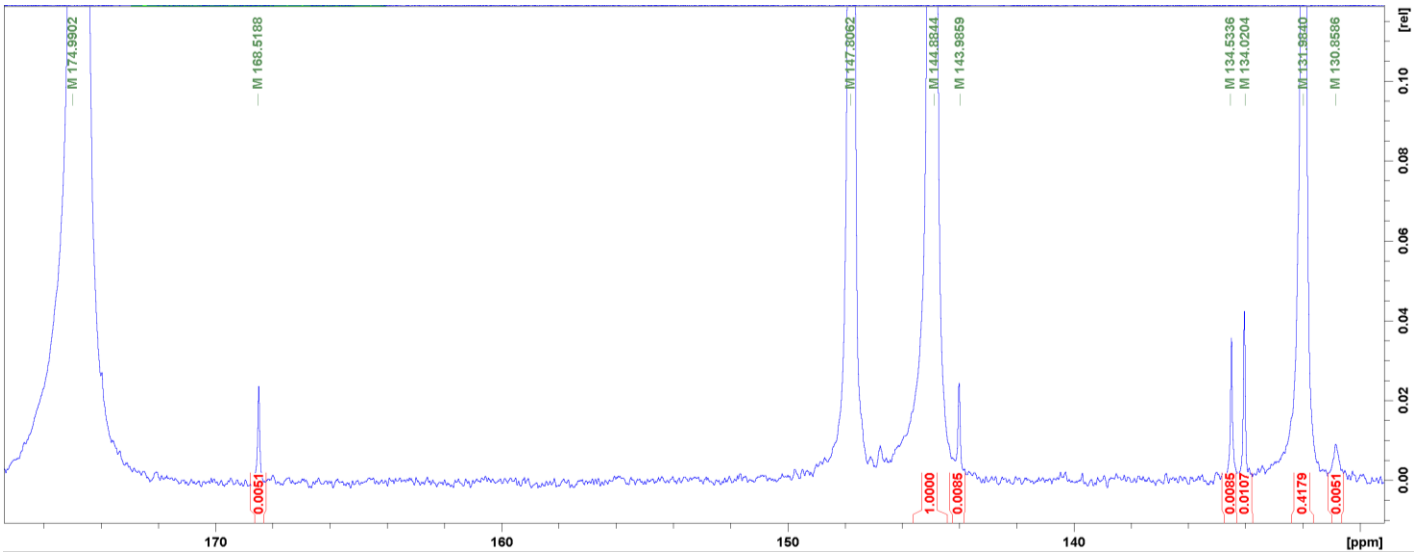

Figure A6 - 2: Crude oil B.

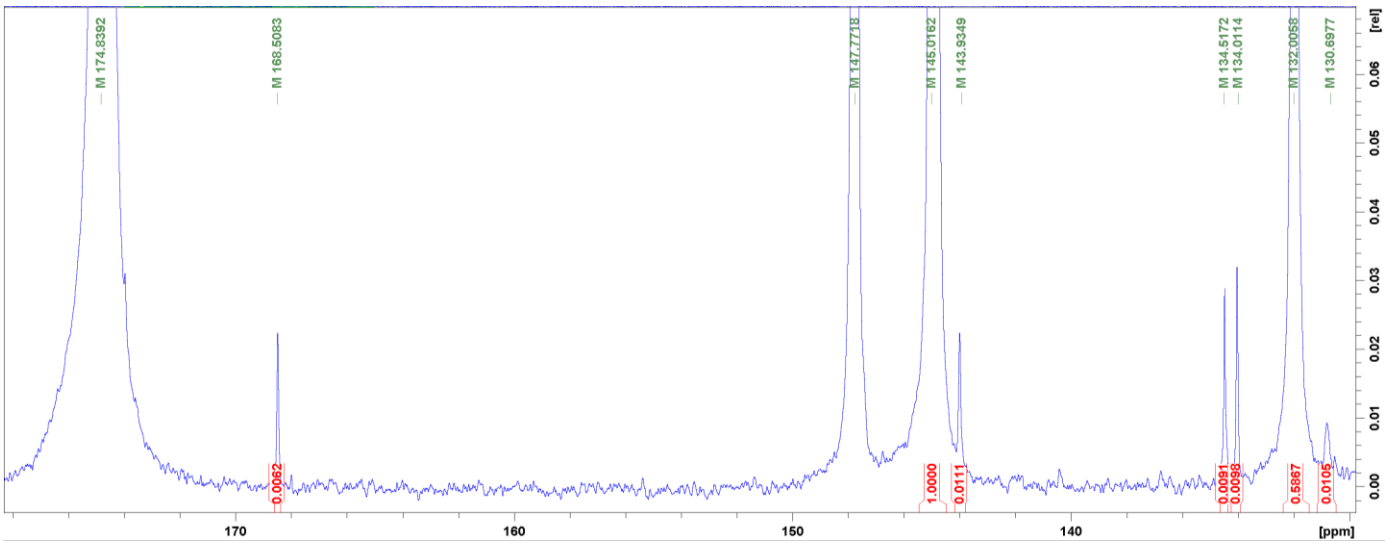

Figure A6-3: Crude oil C.

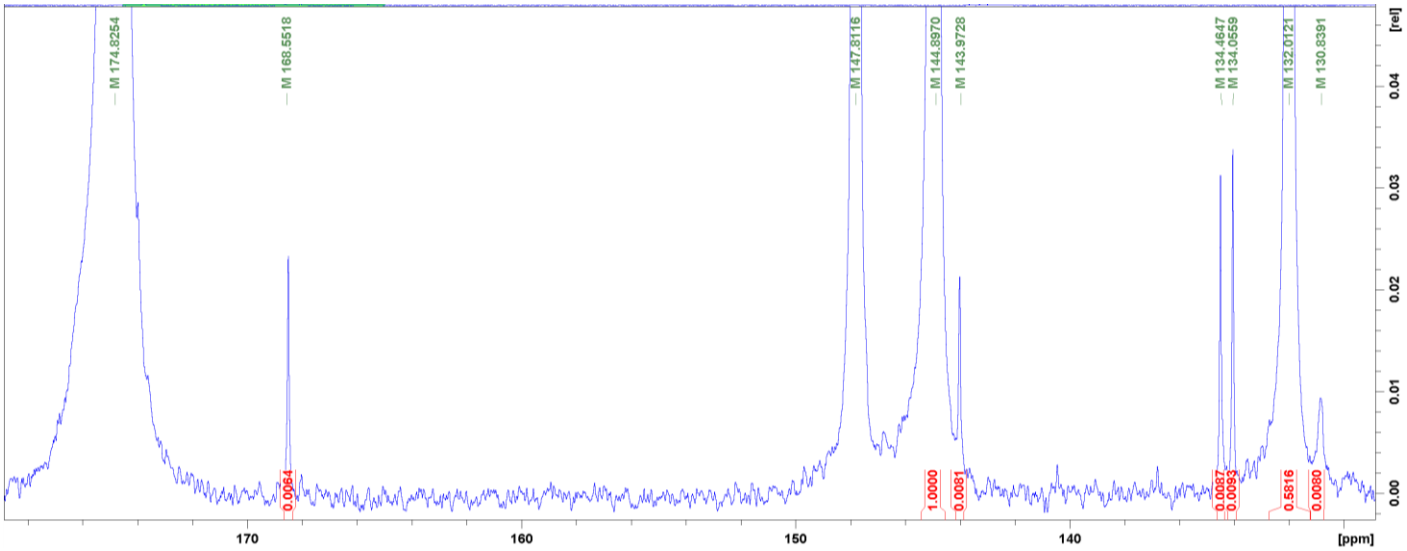

Figure A6-4: Crude oil D.

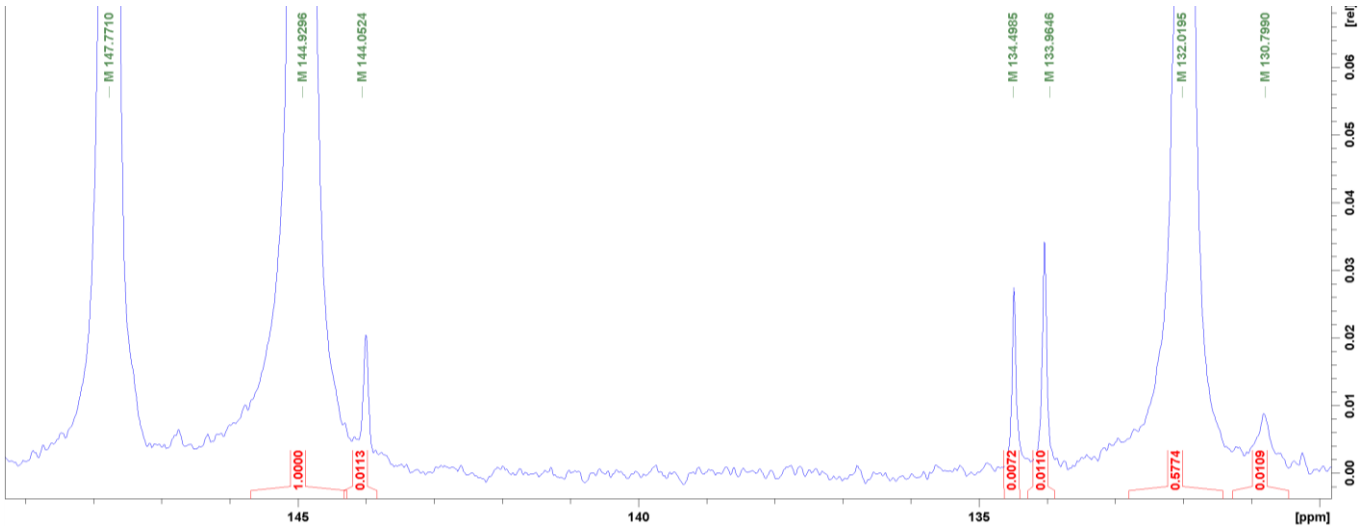

Figure A6-5: Crude oil E1.

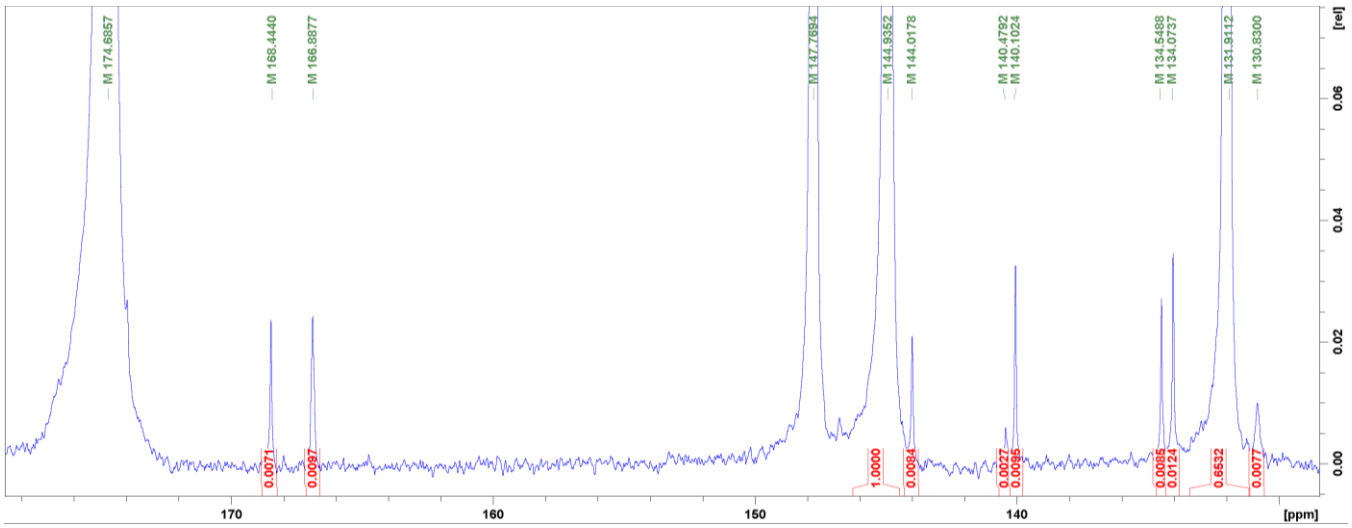

Figure A6-6: Crude oil E2.

F4

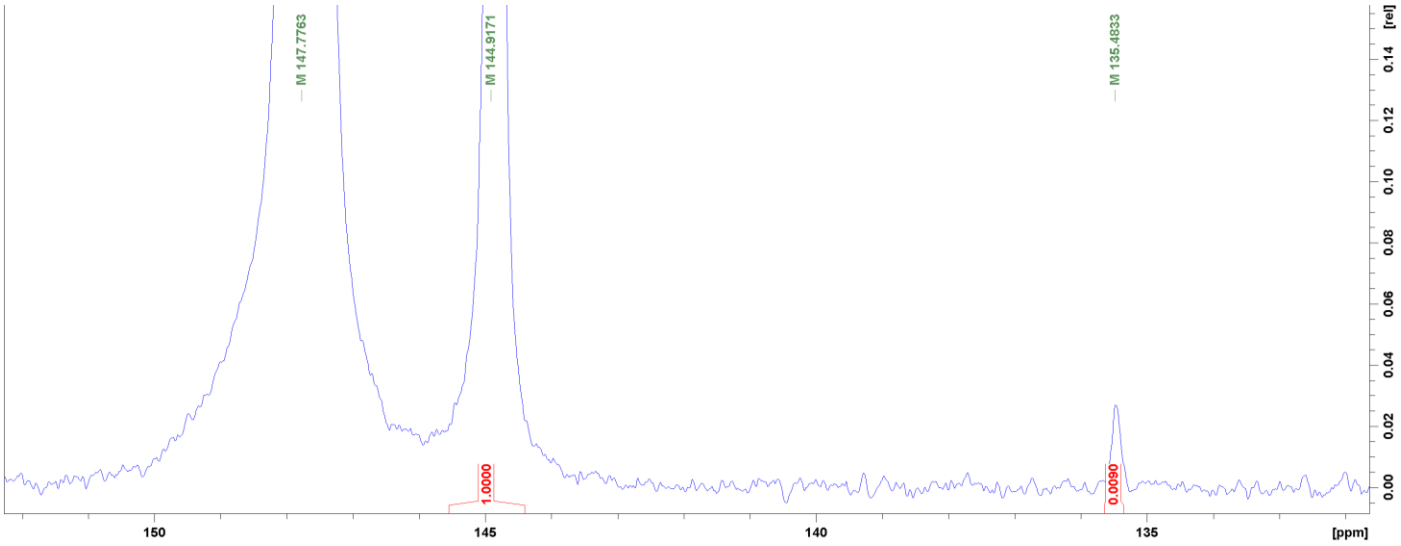

Figure A6-7: Crude oil A.

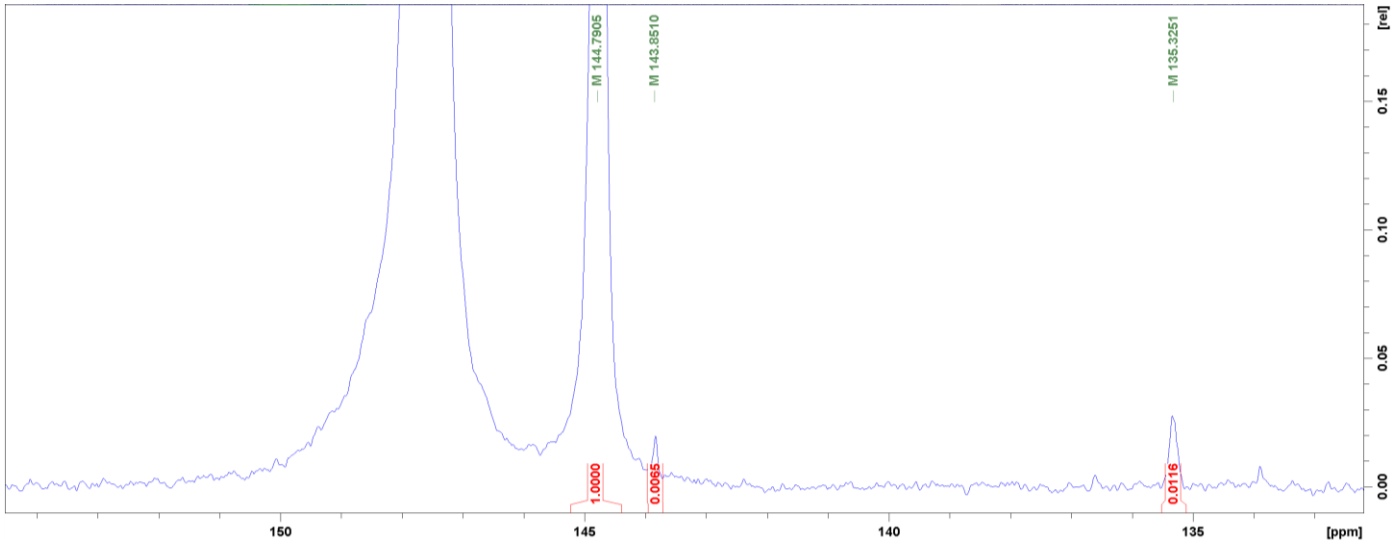

Figure A6-8: Crude oil B.

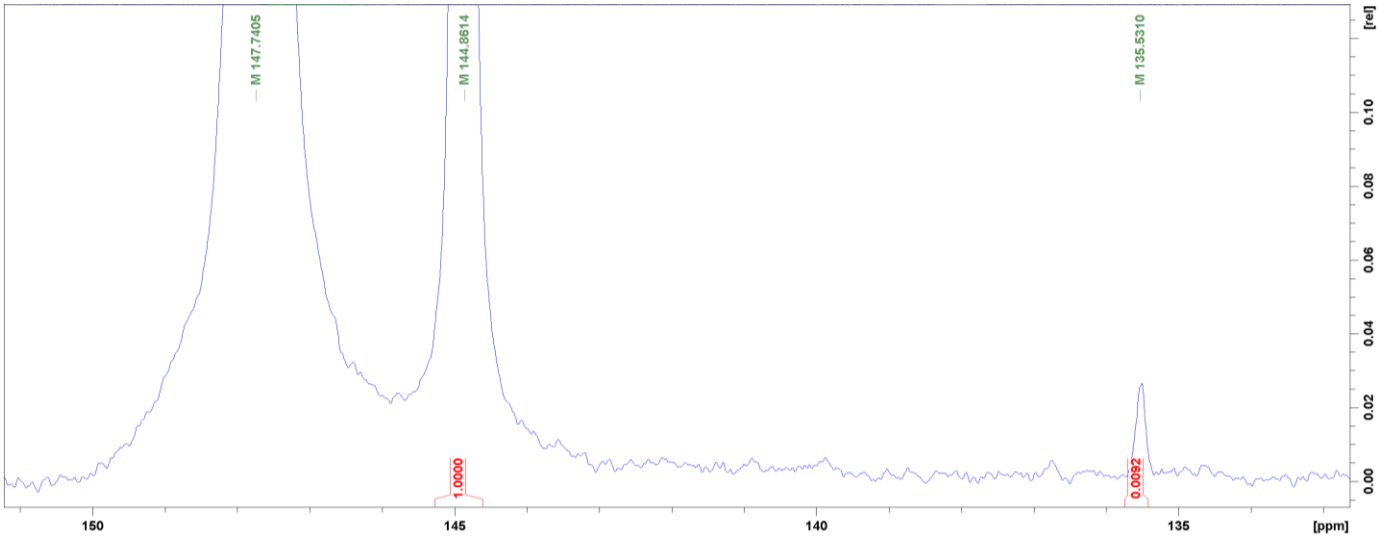

Figure A6-9: Crude oil C.

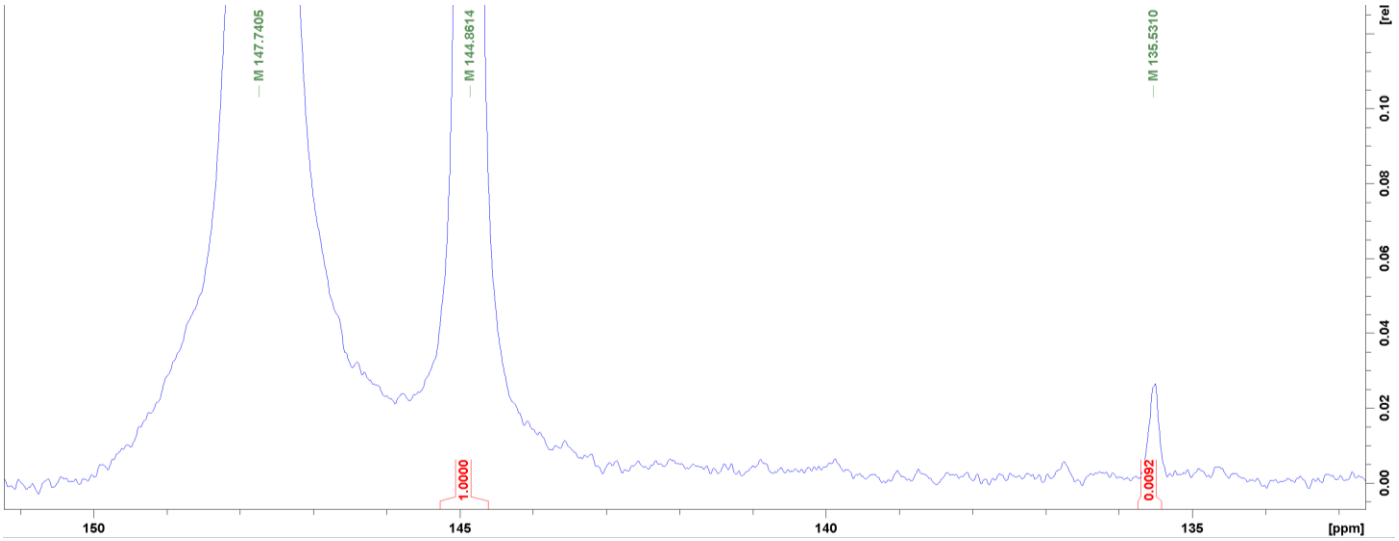

Figure A6-10: Crude oil D.

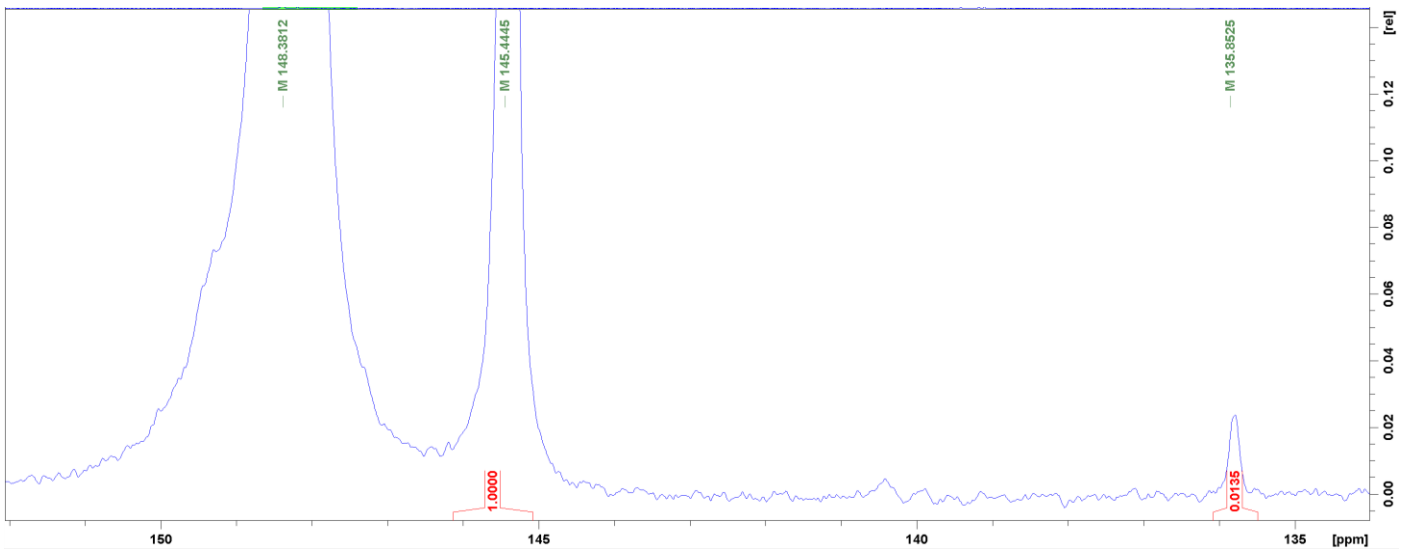

Figure A6-11: Crude oil E1

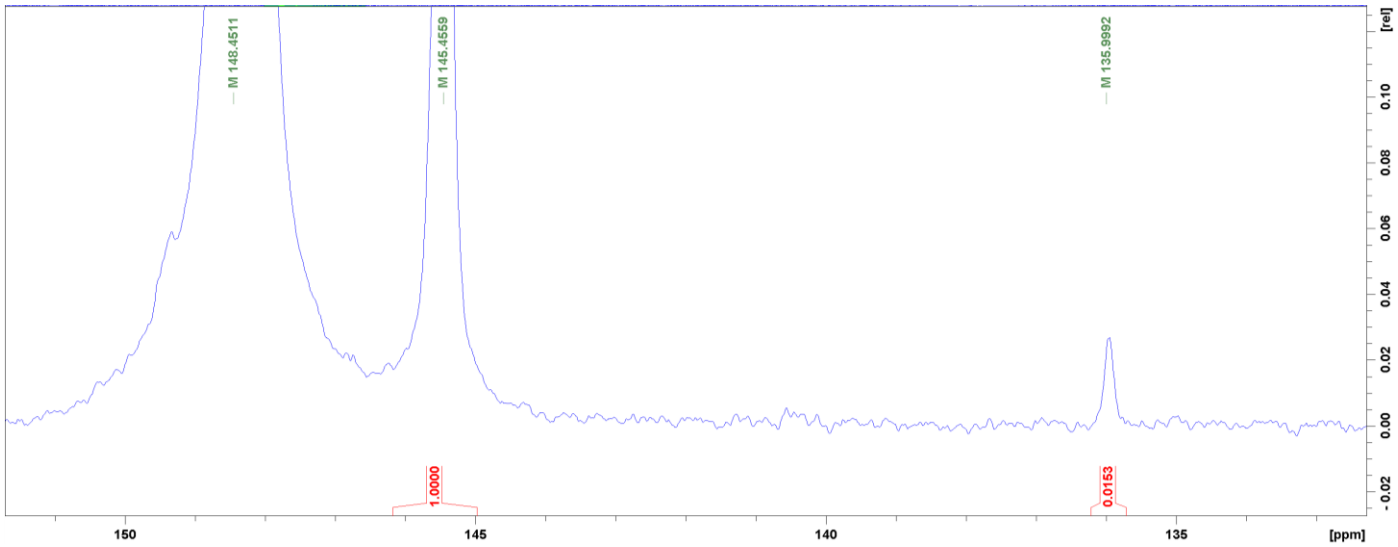

Figure A6-12: Crude oil E2

Asphaltenes

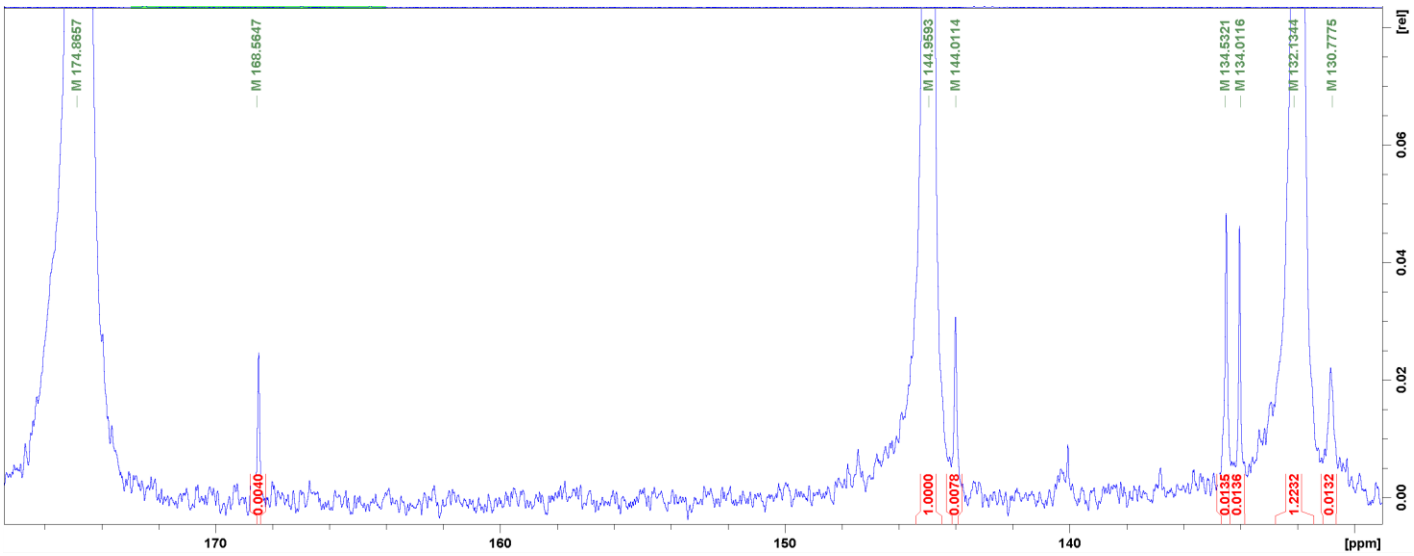

Figure A6-13: Crude oil A.

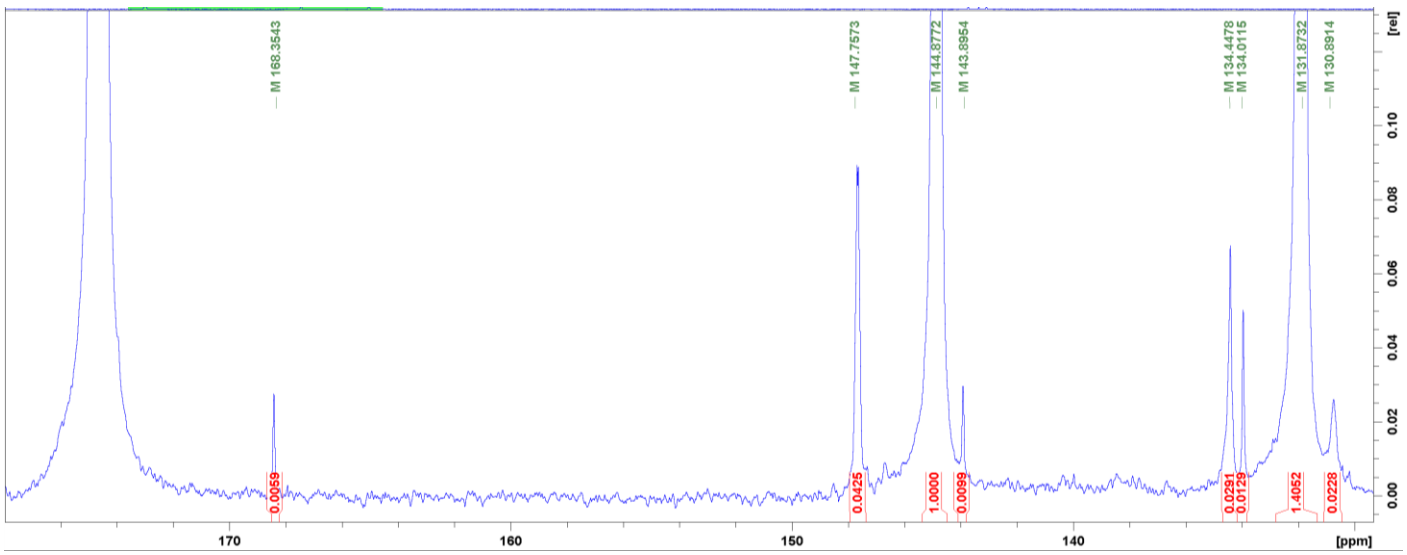

Figure A6-14: Crude oil B.

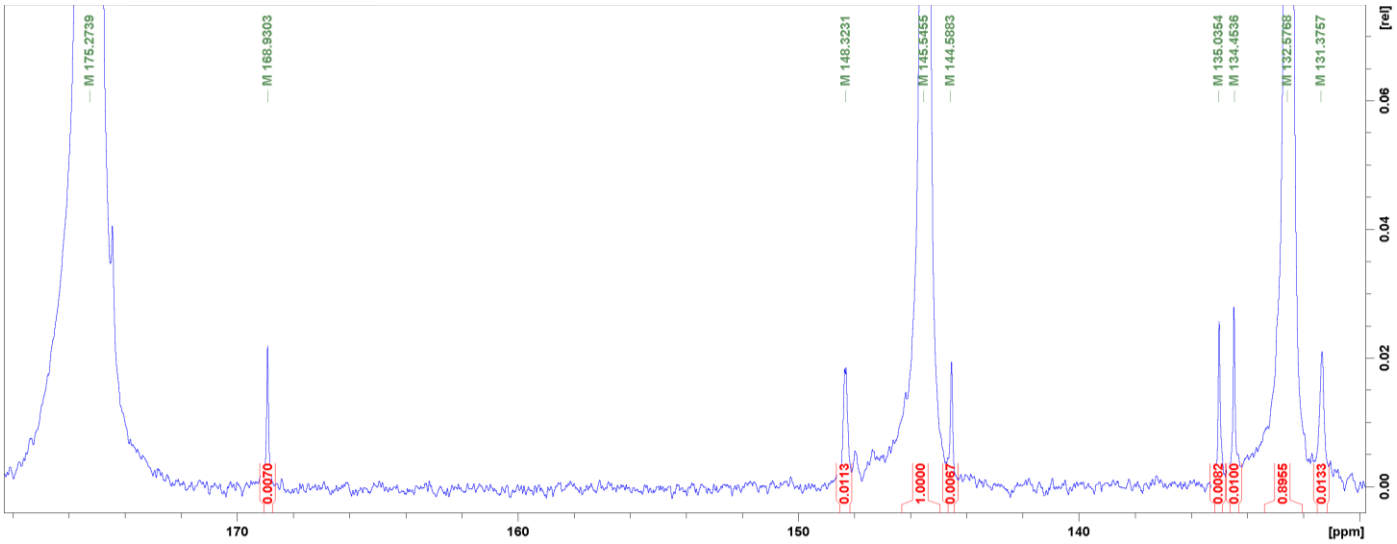

Figure A6-15: Crude oil C.

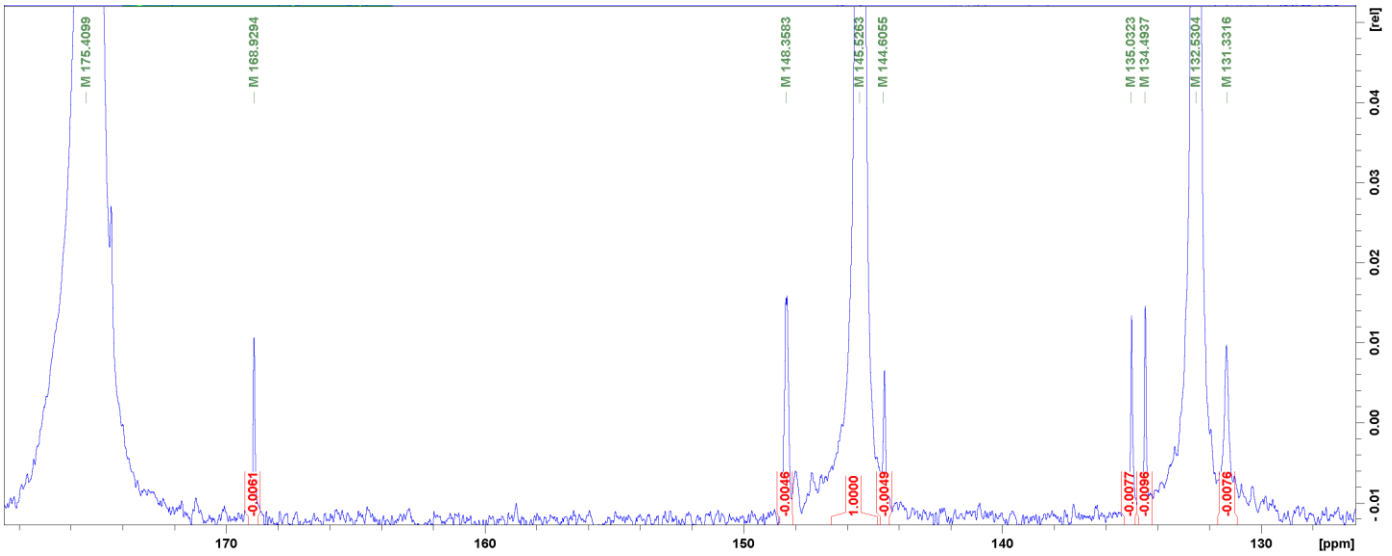

Figure A6-16: Crude oil D.

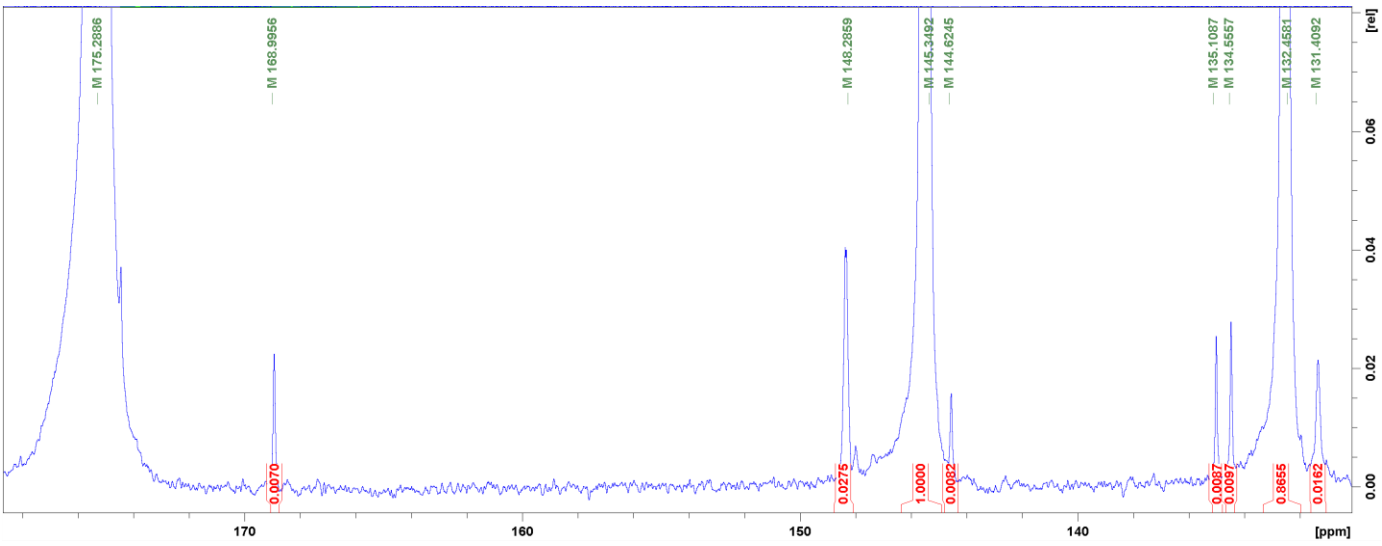

Figure A6-17: Crude oil E1.

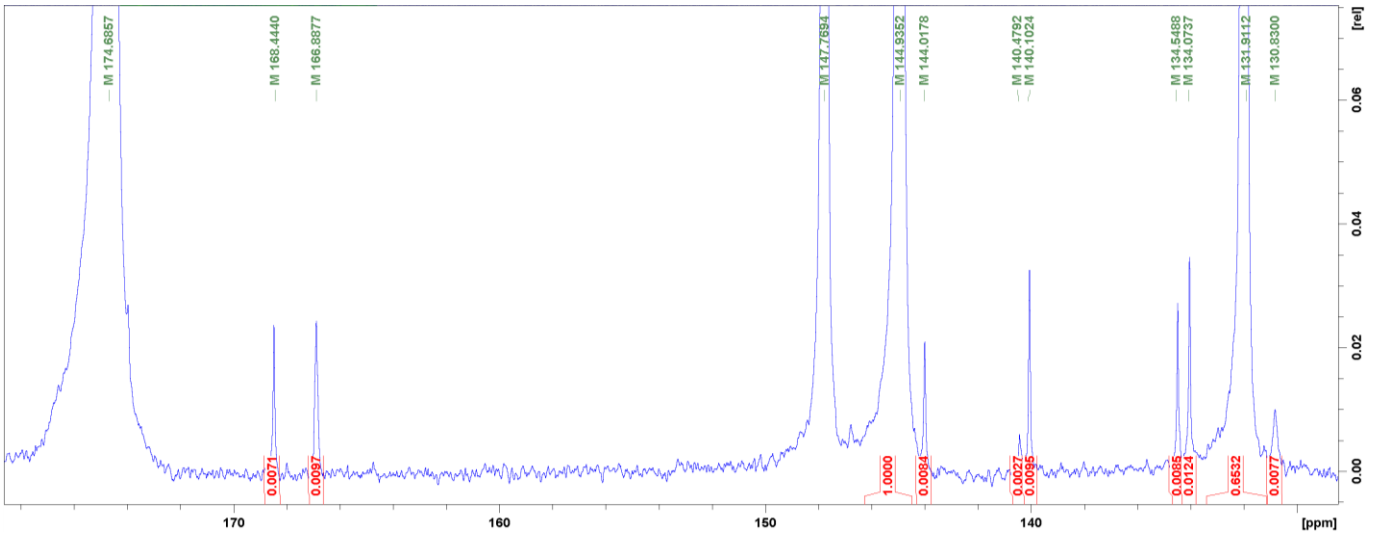

Figure A6-18: Crude oil E2.

A7 Multivariate Analysis – Experimental Setup

Table A7-1: Monovalent brine solution coding.

oil	Exp #	pH	ionic str.	Zeta	IFT	CA	Pris/C17	Pris/Phy	P&M	Asphaltenes	TAN
A	Exp1	3	0,03	26,00	26,10	-	0,88	2,07	2,50	0,25	3,01
B	Exp2	3	0,03	41,00	27,20	-	0,85	1,86	2,50	2,04	2,04
C	Exp3	3	0,03	22,00	18,50	-	3,71	1,86	4,00	0,38	0,98
A	Exp4	3	0,12	6,00	22,90	30,00	0,88	2,07	2,50	0,25	3,01
B	Exp5	3	0,12	29,00	23,80	40,00	0,85	1,86	2,50	2,04	2,04
C	Exp6	3	0,12	11,00	19,30	55,00	3,71	1,86	4,00	0,38	0,98
A	Exp7	3	2,40	-	12,30	56,00	0,88	2,07	2,50	0,25	3,01
B	Exp8	3	2,40	-	9,60	30,00	0,85	1,86	2,50	2,04	2,04
C	Exp9	3	2,40	-	11,50	97,00	3,71	1,86	4,00	0,38	0,98
A	Exp10	6	0,03	-30,00	22,90	-	0,88	2,07	2,50	0,25	3,01
B	Exp11	6	0,03	-16,00	30,10	-	0,85	1,86	2,50	2,04	2,04
C	Exp12	6	0,03	-43,00	17,50	-	3,71	1,86	4,00	0,38	0,98
A	Exp13	6	0,12	-12,00	20,50	27,00	0,88	2,07	2,50	0,25	3,01
B	Exp14	6	0,12	-16,00	25,80	31,00	0,85	1,86	2,50	2,04	2,04
C	Exp15	6	0,12	-14,00	17,60	32,00	3,71	1,86	4,00	0,38	0,98
A	Exp16	6	2,40	-	9,60	30,00	0,88	2,07	2,50	0,25	3,01
B	Exp17	6	2,40	-	10,10	55,00	0,85	1,86	2,50	2,04	2,04
C	Exp18	6	2,40	-	9,30	59,00	3,71	1,86	4,00	0,38	0,98
A	Exp19	9	0,03	-76,00	21,50	-	0,88	2,07	2,50	0,25	3,01
B	Exp20	9	0,03	-87,00	27,40	-	0,85	1,86	2,50	2,04	2,04
C	Exp21	9	0,03	-54,00	17,00	-	3,71	1,86	4,00	0,38	0,98
A	Exp22	9	0,12	-37,00	9,10	49,00	0,88	2,07	2,50	0,25	3,01
B	Exp23	9	0,12	-24,00	21,00	70,00	0,85	1,86	2,50	2,04	2,04
C	Exp24	9	0,12	-64,00	15,00	60,00	3,71	1,86	4,00	0,38	0,98
A	Exp25	9	2,40	-	0,46	62,00	0,88	2,07	2,50	0,25	3,01
B	Exp26	9	2,40	-	0,20	59,00	0,85	1,86	2,50	2,04	2,04
C	Exp27	9	2,40	-	0,90	57,00	3,71	1,86	4,00	0,38	0,98
A	Exp28	11	0,03	-102,00	-	-	0,88	2,07	2,50	0,25	3,01
B	Exp29	11	0,03	-89,00	-	-	0,85	1,86	2,50	2,04	2,04
C	Exp30	11	0,03	-101,00	-	-	3,71	1,86	4,00	0,38	0,98
A	Exp31	11	0,12	-63,00	0,00	12,30	0,88	2,07	2,50	0,25	3,01
B	Exp32	11	0,12	-39,00	0,16	9,60	0,85	1,86	2,50	2,04	2,04
C	Exp33	11	0,12	-64,00	0,10	11,50	3,71	1,86	4,00	0,38	0,98
A	Exp34	11	2,40	-	0,00	-	0,88	2,07	2,50	0,25	3,01
B	Exp35	11	2,40	-	0,20	-	0,85	1,86	2,50	2,04	2,04
C	Exp36	11	2,40	-	0,20	-	3,71	1,86	4,00	0,38	0,98

Table A7-2: Divalent brine solution coding.

oil	Exp #	pH	ionic str.	Zeta	IFT	CA	Pris/C17	Pris/Phy	P&M	Asphaltene	TAN
A	Exp1	3	0,03	25,00	25,30	24,00	0,88	2,07	2,50	0,25	3,01
B	Exp2	3	0,03	41,00	37,00	44,00	0,85	1,86	2,50	2,04	2,04
C	Exp3	3	0,03	25,00	20,60	54,00	3,71	1,86	4,00	0,38	0,98
A	Exp4	6	0,03	-37,00	23,20	28,00	0,88	2,07	2,50	0,25	3,01
B	Exp5	6	0,03	-24,00	27,90	19,00	0,85	1,86	2,50	2,04	2,04
C	Exp6	6	0,03	-28,00	18,70	51,00	3,71	1,86	4,00	0,38	0,98
A	Exp7	9	0,03	-50,00	16,20	42,00	0,88	2,07	2,50	0,25	3,01
B	Exp8	9	0,03	-59,00	15,60	37,00	0,85	1,86	2,50	2,04	2,04
C	Exp9	9	0,03	-39,00	12,60	55,00	3,71	1,86	4,00	0,38	0,98
A	Exp10	11	0,03	-96,00	14,40	-	0,88	2,07	2,50	0,25	3,01
B	Exp11	11	0,03	-91,00	6,30	-	0,85	1,86	2,50	2,04	2,04
C	Exp12	11	0,03	-83,00	11,00	-	3,71	1,86	4,00	0,38	0,98